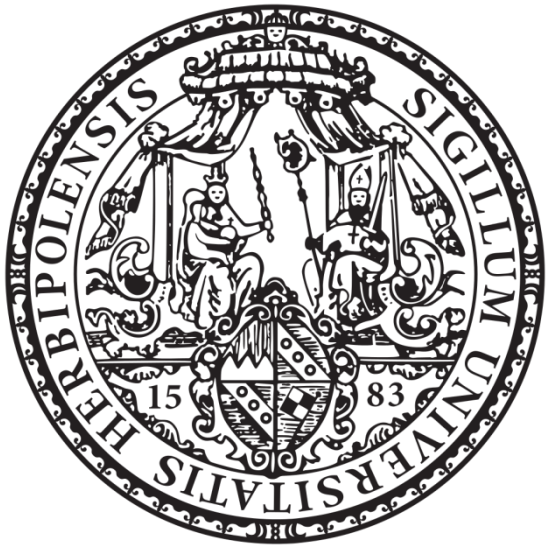


# Pharmacological control of CAR T-cells by dasatinib

# Pharmakologische Kontrolle von CAR T-Zellen durch Dasatinib

DOCTORAL THESIS

FOR A DOCTORAL DEGREE

AT THE GRADUATE SCHOOL OF LIFE SCIENCE,

JULIUS-MAXIMILIANS UNIVERSITÄT WÜRZBURG,

SECTION INFECTION AND IMMUNITY

submitted by

**Katrin Mestermann**

from

**Dortmund, Germany**

Würzburg, 2018

Submitted on: ……..……..

Office stamp

**Members of the *PhD thesis committee:***

Chairperson: Prof. Markus Sauer

Primary Supervisor: Dr. Michael Hudecek

Supervisor (Second): PD Dr. Friederike Berberich-Siebelt

Supervisor (Third): Prof. Dr. Thomas Herrmann

Supervisor (Fourth): Prof. Dr. Hermann Einsele

Date of Public Defense: ……..……

Date of Receipt of Certificates: …….....

# Table of Contents

# Summary

Cellular therapies using chimeric antigen receptor (CAR) modified T-cells to eradicate tumor cells have been a major breakthrough in the treatment of hematologic malignancies. However, there are no measures to control CAR T-cell activity after infusion, which is mostly required in cases of CAR T-cell overreaction, e.g. cytokine release syndrome, or in the case of T-cell failure, e.g. caused by exhaustion.

In our study, we identified the tyrosine kinase inhibitor (TKI) dasatinib (© Sprycel) as a suitable agent to steer CAR T-cells *in vitro* and *in vivo*. We show that single treatment of $CD4^+$ and $CD8^+$ CAR T-cells with dasatinib conferred either partial or complete inhibition, depending on the applied concentration. The blockade was immediate and encompassed specific lysis, cytokine secretion and proliferation following antigen encounter. The mechanism relied on reduced phosphorylation of key kinases in the CAR signaling cascade, which led to abrogation of nuclear factor of activated T-cells (NFAT) signaling. Importantly, inhibition was fully reversible by dasatinib-withdrawal. *In vivo*, dasatinib blocked CAR T-cell function without impairing the engraftment of CAR T-cells or their subsequent anti-tumor function once dasatinib administration was discontinued. We therefore introduce dasatinib as a new tool to efficiently block CAR T-cells *in vitro* and *in vivo*, with data suggesting that dasatinib can be used in a clinical setting to mitigate toxicity after adaptive transfer of CAR-modified T-cells and other forms of T-cell based immunotherapy.

Additionally we show that intermittent inhibition of CAR T-cells by dasatinib improves the efficacy of CAR T-cell therapy. By pausing T-cells for short periods of time *in vivo*, upregulation of programmed death protein 1 (PD-1) and subsequent induction of exhaustion was prevented, which increased the expansion of T-cells and the rate of tumor eradication. Our data therefore suggest that dasatinib can additionally be used to overcome T-cell exhaustion that is induced by massive tumor burden and upregulation of inhibitory receptors.

# Zusammenfassung

Zelluläre Therapien, die das patienteneigene Immunsystem zur Tumorbekämpfung nutzen, gehören zu den großen medizinischen Fortschritten unserer Zeit. T-Zellen, die einen chimären Antigen-Rezeptor (CAR) exprimieren, sind dabei in der Lage, entartete Zellen aufzuspüren und zu eliminieren. Trotz vielversprechender Erfolge sind zellbasierte Immuntherapien häufig von gravierenden Nebenwirkungen wie Zytokinsturm oder neurologischen Ausfallerscheinungen begleitet, und es gibt es bis heute keine Möglichkeit, die einmal injizierten Zellen zu kontrollieren. Kontrolle ist nicht nur im Falle einer Überreaktion der CAR T-Zellen nötig, sondern auch, wenn der Tumor nicht effektiv bekämpft wird. Ein Versagen der CAR T-Zellen wird oft mit T-Zell Exhaustion, einer Ermüdung der T-Zellen aufgrund von Überstimulation in Verbindung gebracht.

In der vorliegenden Studie haben wir den Tyrosinkinase Inhibitor (TKI) Dasatinib als möglichen CAR T-Zellen Inhibitor beschrieben und seine hemmenden Eigenschaften *in vitro* und *in vivo* näher charakterisiert. *In vitro* war eine einzelne Behandlung von $CD4^+$ bzw. $CD8^+$ CAR T-Zellen ausreichend, um – abhängig von der verwendeten Dosis – eine komplette oder partielle Hemmung zu bewirken. Die Blockade setzte unmittelbar ein und umfasste alle relevanten Funktionen einschließlich spezifischer Lyse, Freisetzung von Zytokinen und Proliferation nach Antigen-Kontakt. Der zugrunde liegende Mechanismus basierte auf einer reduzierten Phosphorylierung von Kinasen der CAR-Signal-Kaskade, und verhinderte im weiteren Verlauf die Freisetzung des Transkriptionsfaktors nuclear factor of activated T-cells (NFAT). Diese Blockade war ohne Einschränkungen reversibel. Auch *in vivo* konnte eine komplette Hemmung der injizierten CAR T-Zellen beobachten werden; gleichzeitig war weder das Anwachsen noch die nachfolgende Anti-Tumor Funktion nach Absetzen des Medikaments beeinträchtigt. Aufgrund der in dieser Studie gewonnenen Erkenntnisse schlagen wir Dasatinib als neues Werkzeug zur effizienten Blockade von CAR T-Zellen vor.

Des Weiteren konnten wir zeigen, dass kurzzeitige Unterbrechungen der T-Zell Aktivierung durch Dasatinib einer Ermüdung von T-Zellen entgegen wirken. Dies zeigte sich in einer verringerten Expression von programmed death protein 1 (PD-1) auf der Zelloberfläche sowie einer verbesserten Anti-Tumor Wirkung. Unsere Daten deuten daher darauf hin, dass Dasatinib zusätzlich eingesetzt werden kann, um eine Ermüdung von T-Zellen zu verhindern, die durch massive Tumorbelastung und Hochregulation entsprechender Rezeptoren hervorgerufen wird.

# 1 Introduction

Despite being a major topic in research, cancer is still the most common illness-related reason of death in the western world. For many decades, treatment options have been limited to surgery chemotherapy and radiotherapy. In the 1970s, hematopoietic stem cell based therapies were developed to treat hematologic tumors that function due to graft versus leukemia effects *(1)*. Since then, the idea to use the immune system to track down tumor cells that are distributed in the body has been tempting, and many approaches using parts of the adaptive immune system have been developed, e.g. antibody-based therapies *(2)*, and adoptive T-cell therapy *(3)*.

## 1.1 CAR T-cells for immunotherapy

Besides therapies focusing on the use of endogenously tumor specific lymphocytes, adoptive immunotherapies involving T-cells engineered to express a chimeric antigen receptor (CAR) are under preclinical and clinical investigation. This innovative and highly effective treatment gives hope to many patients suffering from advanced chemo- and radiotherapy-refractory malignancies in hematology and oncology. CARs are synthetic designer receptors, commonly comprising an extracellular antigen-binding moiety that binds to a surface molecule or structure on tumor cells, and an intracellular signaling module that activates and stimulates CAR T-cell functions after binding of respective target molecules. Initially introduced in 1989 by Eshhar et al. *(4, 5)*, this idea has been pushed forward and improved in the last 15 years (Table 1).

CAR T-cells are generated *ex vivo* after isolating the desired T-cell subset from patient's peripheral blood mononuclear cells (PBMCs), thus making the identification of a matching donor obsolete. T-cells are then genetically engineered by inserting a gene cassette encoding the

**Table 1: Timeline of CAR development**

| year | event |
|---|---|
| **1989** | First generation CARs (CD3zeta based) *(4)* |
| **2002** | Second generation CARs (containing CD28 as costimulatory domain) *(6)* |
| **2004** | Second generation CARs (containing 4-1BB as costimulatory domain) *(7)* |
| **2010** | First case report of successful CD19-CAR therapy in lymphoma *(8)* |
| **2011** | First report of successful CD19-CAR therapy in CLL *(9)* |

| | |
|---|---|
| **2013** | First report of successful CD19-CAR therapy in ALL *(10)* |
| **2017** | approval of CD19-CAR therapy for pediatric ALL and NHL in the U.S. *(11)* |
| **2018** | approval of CD19-CAR therapy in the European Union |

CAR by either lentiviral *(12)* or non-viral gene-transfer resulting in stable genomic integration *(13)*. Afterwards, CAR expressing T-cells are enriched and expanded *in vitro* and eventually re-infused to the patient (Figure 1). Clinical proof-of-concept for the efficacy of CAR T-cell immunotherapy has been accomplished in hematologic malignancies with CAR T-cells targeting CD19 (CD19-CAR T-cells), an antigen expressed on healthy and malignant B-cell in leukemia and lymphoma *(14)*, and recently also with CAR T-cells specific for the B-cell maturation antigen (BCMA) expressed in multiple myeloma (MM) *(15)*. Adoptive transfer of CD19-CAR T-cells has induced partial and durable complete responses in patients with acute lymphoblastic leukemia (ALL) *(16, 17)*, chronic lymphocytic leukemia (CLL) *(18, 19)*, non-Hodgkin lymphoma (NHL) *(20)*, and others *(21)* . In 2017, two CD19-CAR T-cell products named Kymriah (©Novartis) and Yescarta (©Gilead) have been approved by the American Food and Drug Administration (FDA) for the treatment of relapsed/refractory ALL and NHL *(11)* in the United States, and was approved by the European Medicines Agency (EMA) in June 2018 *(22)*. At present, numerous clinical trials with CAR T-cells targeting CD19, BCMA and other antigens are ongoing at cancer centers world-wide *(23)*.

## 1.2 Pharmacokinetics of CAR T-cell products

CAR T-cells are administered as a single-shot 'living drug' treatment. Following intravenous (i.v.) administration, CAR T-cells accumulate in target expressing tissues, or home into lymphoid organs. They expand upon antigen encounter, and concentration of CAR T-cells in blood and tumor bearing compartments rises until peak levels are reached in the second week after infusion *(19, 24, 25)*. Afterwards, CAR T-cell concentrations slowly decrease over a period of several weeks. As T-cells are capable of developing a memory phenotype, they are able to per-

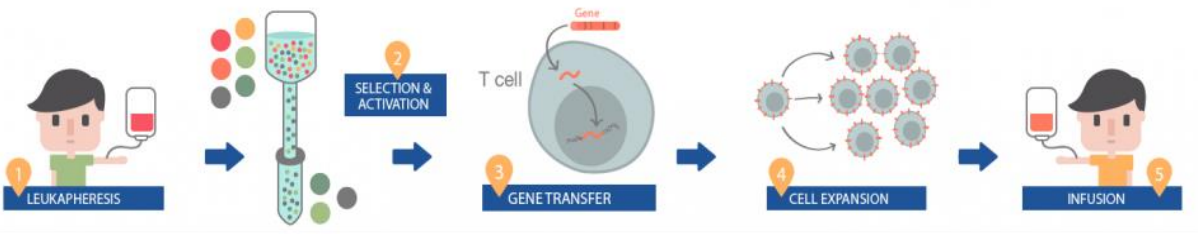


**Figure 1**: **The manufacturing procedure to generate CAR T-cells.**

To generate patient specific CAR T-cells, the patient undergoes leukapheresis (1). Afterwards, distinct T-cell subsets are isolated and activated (2), genetically engineered by either viral or non-viral genetransfer (3) and expanded (4), before being re-infused into the same patient (5).

sist for several months to years in patient and can undergo sequential expansion, contraction and re-expansion *in vivo* upon (re-)exposure to their antigen *(20, 26–28)*. With these attributes, CAR T-cells are fundamentally different from conventional pharmacologic drugs that decay with predictable half-life and have to be administered repeatedly in order to sustain the therapeutic effect.

In order to create a niche and make space for the CAR T-cells, endogenous lymphocytes in the patient are depleted by preparative chemotherapy (lymphodepletion) prior to CAR T-cell infusion, which improves engraftment and persistence of CAR T-cells. A study evaluating the impact of preconditioning chemotherapy was performed by Turtle et al. in 2016, and showed that the peak level of CAR T-cells was reached seven days after injection following lymphodepletion with fludarabine (Flu) and cyclophosphamide (Cy), whereas peak concentration was much lower and delayed in patients receiving Cy only *(20)*. Recent studies furthermore indicate that the efficacy of CAR T-cells is determined by a complex network of immune-players, and modification of tumor environment and other compartments of the immune system might further interact with CAR T-cell efficacy.

In contrast to conventional drugs, there is no clear dose-response relationship in most studies on clinical CAR T-cell efficacy *(29)*. Instead, efficacy of tumor eradication corresponds with persistence, which is directly affected by high peak levels of CAR T-cells following expansion *(19, 30)*. Single reports further indicate that in some patients, single CAR T-cell clones mediate the response, and it thus seems likely to be not the sheer number of CAR T-cells at time of injection, but the expansion of responsive clones after stimulation in the patient *(31)*.

In general, the CAR design itself and especially the type of co-stimulation of the CAR plays a major role for engraftment and persistence: CAR T-cells harboring a CD28 co-stimulatory domain showed limited persistence of a few months, whereas CAR T-cells containing tumor necrosis factor receptor superfamily member 9 (4-1BB) as co-stimulation-domain are able to persist for several years *(19, 28, 32)*. The pharmacokinetic of CAR T-cells furthermore depends on several intrinsic and extrinsic factors *(19, 26, 33–36)*: Parameters that favor good expansion and long persistence include the use of $CD8^+$ T-cells with naïve or central memory instead of effector phenotype, and high CAR expression. Using

a defined 1:1 ratio of $CD4^+$ and $CD8^+$ CAR T-cells can help to predict the pharmacokinetics and to increase engraftment and persistence after infusion *(20)*. Additionally, the dosing is fixed in some trials but adapted to body weight in others. Therefore, CAR T-cell pharmacokinetics vary significantly between patients, and defining dosing regimens that lead to consistent efficacy with acceptable toxicity has been challenging *(37)*. So far, control of pharmacokinetics is only possible by dose adjustment during dose escalation trials, but is not existent for individual patients.

## 1.3 Acute and chronic side effects of immunotherapies

Even though CAR T-cell therapy is being appraised as a remarkably potent and highly effective novel anticancer treatment, there are remaining challenges related to safety. The clinical use of CAR T-cells (including CD19-CAR T-cells and BCMA-CAR T-cells) has disclosed a number of acute and chronic, potentially life-threatening and in some cases fatal toxicity. Thus, the clinical use of CAR T-cells is still limited and restricted to medically fit patients at highly specialized cancer centers with in-depth experience in bone marrow transplantation and immunotherapy *(38–42)*.

A common side effect of CAR T-cell therapy is cytokine release syndrome (CRS), which is caused by strong activation of CAR T- and bystander immune-cells and subsequent cytokine release. Especially in presence of a large number of tumor cells expressing the respective target antigen, CRS can be overwhelming. In ongoing studies, CRS has been the major cause of morbidity and mortality in CAR T-cell therapy. The symptoms are predominantly caused by elevated levels of pro-inflammatory cytokines including interferon γ (IFNγ), interleukin 1 (IL-1), interleukin 2 (IL-2) and interleukin 6 (IL-6) *(32, 43)* and commonly start with development of high fever, often within hours to a few days after CAR T-cell transfer. Symptoms also include tachycardia/hypotension, hypoxia malaise, fatigue, myalgia, nausea, anorexia and capillary leak and may result in multi-organ failure *(42)*. As control over established CRS is difficult, many efforts have been made to predict and prevent the development of CRS in patients. Risk factors include a high total dose of CAR T-cells and large tumor burden prior to CAR T-cell therapy *(32, 35)*. Additionally, early onset of symptoms during the first three days of CAR T-cell therapy can be an indicator for subsequent development of high grade CRS *(28, 44)*. A panel of predictive biomarkers including elevated serum levels of IL-6, IFNγ and macrophage inflammatory protein 1 (MIP-1) even before visible onset of symptoms may help to anticipate the severity of upcoming CRS and thus reduce the morbidity among patients

if effective counter measures can be taken *(20, 45)*. This counter measures include supportive care, administration of antibodies interfering with the IL-6/IL-6 receptor (IL-6R) interaction and corticosteroids.

CAR T-cell related encephalopathy syndrome (CRES) is also observed during CAR T-cell therapy. The severity of CRES can range from mild symptoms including diminished attention, language disturbance, and impaired handwriting to more severe ones such as raised intracranial pressure, seizures and motor weakness, unconsciousness and cerebral edema. Blockade of the IL-6/IL-6R interaction and administration of corticosteroids can be indicated; however, these pharmaceuticals are not always able to improve severe CRES, and fatal cases have been reported despite treatment *(38, 41)*.

Besides, on-target recognition and elimination of healthy cells in the patient's body that express the respective target antigen is reported, especially when targeting $CD19^+$ healthy B-cells are depleted, and B-cell aplasia is induced. Depletion of healthy B-cells and thus B-cell aplasia is an expected toxicity, and presence of B-cells during therapy is a strong indicator for therapy failure. The lack of B-cells, which will be absent as long as CD19-CAR T-cells persist, is counteracted by supplementing γ globulin as replacement therapy in the case of infections *(46)*.

As novel CARs with altered signaling domains, designs and specificities are continuously being developed, unexpected toxicities may arise. While clinically evaluating new targets, on-target/off tumor recognition of healthy cells in the patient's body that also express the respective target antigen of the CAR needs to be considered. This is highlighted by a published case report describing the death of a patient after receiving ERBB2 specific CAR T-cells getting highly activated by target expression in the lung *(47)*. Additionally, tonic signaling and activation of CAR T-cells independent from stimulation with antigen could lead to permanent activation of T-cells, and thus may increase the risk of side effects. Especially for these cases, the development of effective control mechanisms is of utmost importance.

## 1.4 Current pharmaceutical strategies to manage side effects

So far, the mechanisms at hand to deal with upcoming side effects are limited and focus on symptomatic treatment and supportive care, e.g. using antipyretics that control fever. Especially for the treatment of low grade CRS (defined as ≤ grade 2 using the grading system defined by Neelapu et al. *(41)*), the administration of i.v. fluids or low dose vasopressors is indicated to stabilize the systolic blood pressure. Patients facing CRS ≥ grade 3 need specific

monitoring and care at an intensive care unit, and often require substitution of oxygen and treatment of upcoming organ toxicities *(41, 42)*. Additionally, there are mainly two strategies to manage severe side effects including CRS and CRES, that are applied universally even of it is unclear whether they interfere with the respective pathomechanisms. The first one focuses on the antibody mediated blockade of the IL-6/IL-6R interaction. IL-6 plays a critical role in the development and progression of CRS, and it has been shown that blocking the IL-6/IL-6R interaction by antibodies such as Tocilizumab or Siltuximab mitigates CRS in a significant proportion of patients *(38, 41, 48)*. However, this intervention does not directly affect CAR T-cells as IL-6 itself is predominantly produced by bystander immune cells including monocytes and macrophages getting activated by IFNγ and by tumor cell debris *(49–51)*. In general, blockade of the IL-6/IL-6R pathway efficiently improves symptoms of CRS without influencing efficacy of CAR T-cells. Importantly, CAR T-cell activity itself is not controlled by these measures, which is insufficient in many cases.

Therefore, as a second option, it is commonly attempted to mitigate CRS or other CAR T-cell-mediated side effects through administration of steroids, e.g. dexamethasone, with the intention to directly affect T-cell activation. Because steroids are known to be immunosuppressive and can induce apoptosis in T-cells, their use in the context of CAR T-cell therapy is controversial, as they may negatively influence the therapeutic effect of CAR T-cells. Steroids have been commonly known to affect the gene-expression following T-cell activation, and are thus expected to also modulate CAR T-cell effector functions. Additionally, direct effects of glucocorticoids towards early events of signal transduction have been described *(52)*. By binding to a membrane bound glucocorticoid receptor, dexamethasone changes the submembrane localization of key signaling molecules including the lymphocyte-specific protein tyrosine kinase (Lck), thus impairing the early phosphorylation events following stimulation of the endogenous T-cell receptor (TCR) *(52)*. Thus far, it is not known whether this mode of action also plays a role in CAR mediated signaling. Fatal side effects that occurred despite administration of IL-6 blockade and steroids further highlight the necessity of additional and more efficient strategies to improve the safety of CAR T-cell therapy.

## 1.5 Controlling CAR T-cells by design

### 1.5.1 CAR design and mode of action

Clinical activity has been confirmed for a variety of CARs that share a common general structure containing an antigen-binding domain, a CD3zeta derived signaling domain and a cost-

imulatory domain, which defines these CARs as second generation in contrast to first generation CARs using CD3zeta only for signaling *(37)*. Usually, the antigen-binding domain is derived from a monoclonal antibody (mAb) specifically binding the desired antigen, which should be tumor specific or limited in its expression to malignant and non-essential healthy tissues; e.g. most of CARs targeting CD19 including the ones in clinical application are derived from mAb FMC63 *(53)*. The antigen-recognizing domain is connected to the transmembrane domain by a spacer which is highly variable between CARs and depends on accessibility of epitope *(32)*. All CARs that are currently under evaluation utilize CD3zeta as part of their signaling module to induce T-cell activation. This copies the endogenous T-cell receptor that uses CD3zeta to induce activation of T-cells after antigen encounter. The downstream signaling cascade upon CAR engagement is thus expected to be highly similar to the signaling induced by the endogenous TCR. It involves phosphorylation of the kinases Lck, that mediates phosphorylation of CD3zeta and zeta-chain-associated protein kinase 70 (Zap70) and thus eventually induces the expression of transcription factors such as NFAT and the nuclear factor kappa-light-chain-enhancer of activated B-cells (NF-κB) *(55, 56)*. First generation CARs containing only CD3zeta for signaling effectively targeted tumor cells *in vitro*, but showed low engraftment abilities and persistence in patients *(57, 58)*. Thus, co-stimulatory domains have been included to promote adequate signaling and function *(6, 7)*. Being second generation CARs, the constructs used in the following study additionally contain either 4-1BB or CD28 as a co-stimulatory domain. Both co-stimulatory moieties are well described and used in clinically approved CAR T-cell products. While 4-1BB promotes an oxidative metabolism that favors persistence due to a memory cell phenotype of T-cells, CD28 emphasizes the differentiation towards highly functional but short lived effector T-cells *(59–61)*. In contrast to endogenous T-cell receptors requiring antigen-induced stimulation and an additional costimulatory signal, second generation CARs combine these two signals in one receptor. Thus, full activation of CAR T-cells is induced by antigen-recognition alone and is intended to not require engagement of additional receptors. Additionally, the CARs used in the following study contain a truncated, non-signaling epidermal growth factor receptor (EGFRt) that is separately expressed on the cell surface due to a ribosomal skip sequence. By this, it serves as a transduction marker and can be used for detection, enrichment and purification of CAR T-cells.

### 1.5.2 Eradication of CAR T-cells as a safety strategy

As T-cells have the potential to cause severe damage and side effects, one effort to increase safety of CAR T-cell therapy is the inclusion of mechanism that enable quick eradication of T-cells if needed. Transduction markers like EGFRt or truncated CD20 (CD20t) can not only be used for detection and enrichment, but can also be targeted by antibodies that induce antibody-dependent cellular cytotoxicity (ADCC) or complement-dependent cytotoxicity (CDC) to remove CAR T-cells, and thus can serve as depletion markers *(62–64)*. Importantly, depletion markers relying on ADCC or CDC are more effective if the patient's immune system is still functional which is often not the case after intensive chemotherapy that depletes compartments of the immune system needed for ADCC or CDC. Alternatively, some CAR T-cell products are equipped with suicide genes like inducible caspase 9 (iCasp9) or herpes simplex virus thymidine kinase (HSV-TK) that can be triggered to induce apoptosis in CAR T-cells independently of the patient's remaining immune system *(65–68)*. Unfortunately, iCasp9 works best in CAR T-cells that express high levels of this suicide gene, but is less effective in low expressers *(69)*. The use of HSV-TK is also limited, as it has been shown to be immunogenic itself and thus causes recognition of modified T-cells by endogenous immune-cells *(70)*.

So far, both of the CAR T-cell products that gained clinical approval are not equipped with suicide genes or depletion markers. Even though some products in advanced clinical development contain EGFRt, physicians hesitate to eliminate CAR T-cells, as they try to avoid termination of the therapeutic effect. Complete eradication of CAR T-cells is of particular concern because it terminates the anti-tumor effects. Additionally, multiple infusions of CAR T-cells are not possible in some patients: Due to the immunogenicity of current CAR constructs, patients may develop an immune response and reject CAR T-cells at the time of second infusion. Therefore, ongoing preclinical studies try to gain control over CAR T-cells by titrating iCasp9 induced depletion of T-cells, thus reducing the amount of active T-cells without complete depletion in order to treat severe side effects such as CRS *(69)*. However, there is at present no reported clinical case where iCasp9 or EGFRt have been triggered in the context of CAR T-cell immunotherapy.

### 1.5.3 ON/OFF switch strategies to control CAR T-cell function

Due to the lack of precise control over CAR T-cell function after infusion, great efforts have been made to improve safety and controllability of CAR T-cells by structural modifications of the receptor. Many of these altered designs aim at splitting the signals needed for activation of CAR T-cells to two separate molecules. The so called "ON-switch CAR" (Figure 2) does not

only rely on the presence of a specific tumor antigen to become activated, but additionally requires the presence of a small molecule (Rapamvcin analog AP21957, or Rapalog) that is provided externally via injection. Rapalog induces the hetero-dimerization of antigen binding and signaling domain, which are expressed by the T-cells as independent molecules *(71)*. Titration of rapalog controls the function of CAR T-cells, thus it not only regulates killing of target cells,

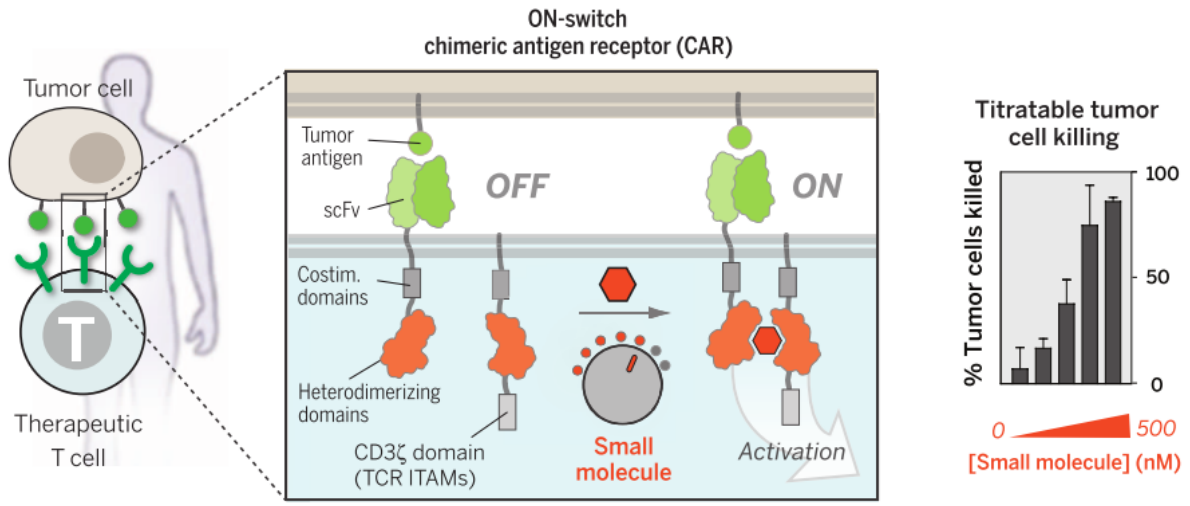


**Figure 2: The "ON-switch CAR" introduced by Wu et al.** *(71)*.

The function of "ON-switch" CAR T-cells can be steered by titrating a small molecule needed for activation. The single chain variable fragment (scFv) is connected to the costimulatory domain, whereas the CD3zeta signaling domain is seperately expressed. The two independently expressed molecules contain heterodimerizing domains, that dimerize in the presence of a small molecule, resulting in dose-dependend function of CAR T-cells.

but also cytokine secretion and proliferation. As withdrawal of rapalog leads to inactivation of T-cells, dynamics of activation are mostly determined by the half-life of rapalog.

The split, universal and programmable (SUPRA) CAR offers additional features to provide control over CAR T–cell function *(72)*. The SUPRA platform is based on leucine zippers, which bind to each other by direct interaction (Figure 3). T-cells are engineered to express the so called zipCAR, which contains all signaling domains. The extracellular domain of the zipCAR provides a leucine zipper, but no antigen-binding domain. The scFv required for target recognition, called zipFv, needs to be administered to the patient by injection. Thus, the system offers great flexibility, as the amplitude of T-cell activation can be steered by I) changing the affinity of the zipFv-leucine zipper, II) using a scFv with an altered affinity for the target antigen, or III) using titrated amounts of zipFv. Additionally, the system can be switched off by the administration of competitive zipFv. By binding the activating zipFv with

higher affinity, the competitive zipFv neutralizes the activating zipFv and thus prevents further T-cell activation. Both SUPRA and ON-Switch CAR T-cells have been successfully tested in mouse models, but remain to be evaluated in patients regarding efficiency and their contribution towards safety. Thus, both of these systems are not available for clinical application.

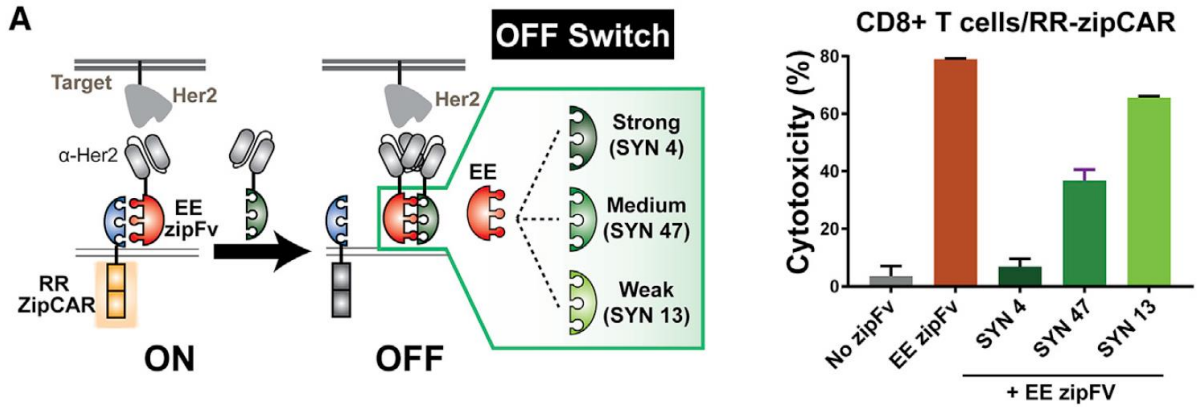


**Figure 3: SUPRA CAR platform introduced by Cho et al.** *(72).*
The signaling part of CAR (RR ZipCAR) ,expressed by the T-cell, is seperated from the antigen binding domain (EE zipFv), which is provided externally and forms a heterodimer with the CAR's signaling domain by interaction of leucing zippers. T-cell function can be titrated or completely switched OFF by injecting competive inhibitory scFv binding the activating zipFv with strong, medium or weak affinity.

## 1.6 The influence of dasatinib on unmodified, non-malignant T-cells

In malignant and healthy cells, signals are transmitted by phosphorylation of kinases that can be influenced by TKIs. TKIs are small molecules developed to treat cancer by influencing kinase based signal pathways that are vital for many tumors. The TKI dasatinib functions as an antagonist of the fusion protein BCR-ABL commonly expressed in Philadelphia-chromosome positive (Ph+) chronic myeloid leukemia (CML) and in about 20% of cases in ALL *(73, 74)*. Since 2010, dasatinib is approved as first-line treatment of Ph+ ALL and CML. Besides BCR-ABL, dasatinib has been shown to inhibit members of Src-family kinases that are essential for signal transduction in T-cells, and thus can influence activation and exertion of effector function of T-cells, including proliferation, cytokine secretion and degranulation at a clinically relevant dose between 1 and 100 nM *(75–77)*. By binding and blocking the adenosine triphosphate (ATP) binding sites of the Src family kinase Lck, dasatinib prevents the subsequent phosphorylation of the T-cell receptor CD3zeta-chain *(77)*. Indeed, immunosuppression and atypical infections have been observed during dasatinib treatment in one ALL *(78)* and a

subset of CML patients *(79)*, suggesting that interference of dasatinib with T-cell functions is possible in patients.

## 1.7 Study objectives and specific aims

Adoptive immunotherapy with gene-engineered CAR-expressing T-cells is currently causing a revolution in cancer medicine. CD19-specific CAR T-cells have recently been clinically approved for the treatment of B-cell malignancies in children and adults, and numerous CAR T-cell products targeting alternative antigens in hematologic and solid tumors are under investigation. As CAR T-cells are 'living drugs' that can undergo substantial amplification *in vivo*, they can confer activity for several months to years after single administration, and patients receiving cellular immunotherapies require special monitoring and care. At present, the lack of technologies that allow controlling the activation state and function of CAR T-cells after infusion causes considerable challenges for the clinical management of patients. As the majority of CAR T-cell products currently employed in clinical trials, including both FDA-approved CD19-CAR T-cell products, is not equipped with any safety technology, there is a high incidence of clinically relevant toxicities resulting from strong CAR T-cell activation *in vivo* and inability to turn their function OFF if indicated.

Thus, the aim of the presented study was to find a tool to exert control over activation and effector functions of CAR T-cells *in vitro* and *in vivo*. Since T-cell activation involves kinase-dependent protein phosphorylation, we hypothesized that the use of kinase inhibitors would provide an elegant option to control CAR T-cells. As the TKI dasatinib is known to block the phosphorylation of Lck − a key player in the CAR-dependent signaling cascade − we focused on dasatinib as the lead candidate to achieve control over CAR T-cell activation and, ensuing, effector functions. From this hypothesis we generated the following objectives of the study:

(1) To examine if dasatinib prevents effector functions in resting and activated CAR T-cells
(2) To evaluate molecular consequences of dasatinib-exposure on CAR signaling events.
(3) To analyze the kinetics of dasatinib-mediated CAR T-cell control
(4) To validate the suitability of dasatinib as a pharmaceutical safety switch *in vivo*.

To experimentally approach the objectives, we analyzed the effector functions of CAR T-cells by assessing elimination of tumor cells, cytokine secretion and proliferation of CAR T-cells following antigen encounter in the presence or absence of dasatinib. Initially, experiments were performed using a CD19-CAR as it is currently under clinical investigation *(80)*.To compare dasatinib-mediated effects between CAR T-cells, we performed dose titration experiments with CAR T-cells derived from $CD4^+$ and $CD8^+$ T-cells. To confirm the dosing, we tested the effect of dasatinib on CAR T-cells targeting the receptor tyrosine kinase-like orphan receptor 1 (ROR1), and evaluated the influence of the costimulatory domain by exchanging 4-1BB against CD28. To elucidate the molecular mechanism underlying the observed dasatinib-mediated effects on CAR T-cell activation and functions we studied the phosphorylation status of Lck, CD3zeta and Zap70, which are the three major players involved in the signal transduction early after CAR engagement. Additionally, we generated an NFAT-responsive reporter gene to trace the consequences of dasatinib treatment on a genomic level. We recorded the kinetics of re-activation after dasatinib removal and following stimulation and assessed fitness and functionality of CAR T-cells after short and long term exposure to dasatinib. To ensure the clinical impact of this work, we validated the characteristics and kinetics of dasatinib-mediated control *in vivo* by performing studies in tumor bearing, CAR T-cell treated mice. Here, we analyzed tumor pro- and regression and serum levels of human cytokines, as well as presence, proliferation, and activation of CAR T-cells before, during and after dasatinib treatment.

# 2 Materials

## 2.1 Equipment and consumables

| Name | Manufacturer |
|---|---|
| 25, 75 $cm^2$ surface area cell culture flasks | Corning, Kaiserslautern |
| 96 well half-area plates, Corning® Costar® | Corning, Kaiserslautern |
| 96 well plate ,white, flat bottom, Corning® Costar® | Corning, Kaiserslautern |
| 96 well plates, Corning® Costar® U bottom | Corning, Kaiserslautern |
| 48, 12, 24 well plates, Corning® Costar®flat bottom | Corning, Kaiserslautern |
| Biocoll separating solution | Merck, Darmstadt |
| Biological safety cabinets, Herasafe™ KS | Thermo Fisher, Waltham, MA, USA |
| Centrifuge tubes, 10, 15, 50 mL | Greiner Bio-One, Frickenhausen |
| Centrifuge 5415D | Eppendorf, Hamburg |
| Centrifuge, Heraeus Megafuge 40R | Thermo Fisher, Darmstadt |
| ChemiDoc MP imaging system | BioRad, Munich |
| $CO^2$ Incubators, Heracell™ 150i and 240i | Thermo Fisher, Darmstadt |
| Flow cytometer, BD FACSCantoTM II | BD Biosciences, Heidelberg |
| Flow cytometery tubes, Röhre 5 mL | Sarstedt, Nümbrecht |
| Gel electrophoresis system, Owl™ Minigel | Thermo Fisher, Darmstadt |
| Heraeus Fresco17 Centrifuge | Thermo Fisher, Darmstadt |
| Heraeus Multifuge 3SR+ Centrifuge | Thermo Fisher, Darmstadt |
| Heat block, neoBlock1 | neoLab, Heidelberg |
| Hydrospeed, Platewasher | TECAN, Männedorf, Switzerland |
| Ice maker | Scotsman, Vernon Hills, IL, USA |
| Incubator | Memmert, Schwabach |
| Leucosep tubes | Greiner Bio-One, Frickenhausen |
| MACS separation columns, 25 LS | Miltenyi, Bergisch Gladbach |
| MAGPIX-Luminex | Luminex Corporation, Hertogen-bosch, The Netherlands |
| Microscope, Primo Vert | ZEISS, Jena |
| MiniPROTEAN™ Tetra System | BioRad, Munich |
| Multimode multiplate reader, Infinite 200 PRO | TECAN, Männedorf, Switzerland |
| PCR thermal cycler, Mastercycler, Personal | Eppendorf, Hamburg |

| | |
|---|---|
| Refrigerator, -4 and -20 °C | Liebherr, Bulle, Switzerland |
| Rnase free Biosphere plus SafeSeal microtube, 1.5 mL | Sarstedt, Nümbrecht |
| Shaker Incubator | INFORS HT, Basel, Switzerland |
| Trans-Blot® Turbo Transfer System | Bio-Rad, Munich |
| Ultracentrifuge, Sorvall WX80 | Thermo Fisher, Darmstadt |
| Ultra-low temperature freezer, -80 °C FORMA 900 | Thermo Fisher, Darmstadt |
| UV transilluminator | neoLab, Heidelberg |
| Water bath | Memmert, Schwabach |

## 2.2 Software

| **Software** | **Application** | **manufacturer** |
|---|---|---|
| FACSDiva (version 6.1.3) | Flow cytometry | BD Bioscience, Heidelberg |
| FlowJo software (version 10.2) | Flow cytometry | TreeStar Inc., Ashland, OR, USA |
| Prism 6 (version 6.01) | Graphical/ statistical analysis | Graphpad Software, La Jolla, CA, USA |
| ImageLab (version 5.1) | Westernblot analysis | BioRad, Munich |
| Living Image (version 4.4) | Mouse imaging | Caliper LifeScience |
| i-control (version 3.8.2.0) | Absorption, luminescence | TECAN, Männedorf, Switzerland |
| xPONENT (version 4.2) | Cytokine multiplex | Luminex Corporation, Hertogenbosch, The Netherlands |

## 2.3 Chemicals and reagents

### 2.3.1 Molecular biology

| Name | **Manufacturer** |
|---|---|
| BSA | AppliChem, Darmstadt |
| ClarityTM Western ECL Subtrate | BioRad, Munich |
| DCTM Protein Assay Reagent A | BioRad, Munich |
| DCTM Protein Assay Reagent B | BioRad, Munich |
| DCTM Protein Assay Reagent S | BioRad, Munich |

| | |
|---|---|
| LB AGAR Plates with Carbenicillin -100 | TEKnova, Hollister, CA, USA |
| LB AGAR Plates with Kanamycin | TEKnova, Hollister, CA, USA |
| LDS Sample Buffer Non Reducing | Thermo Fisher, Darmstadt |
| Skimmed milk powder | Sucofin, Zeven |
| NuPAGE Sample Buffer | Invitrogen, Carlsbad, CA, USA |
| NuPAGE Sample Reducing Agent | Invitrogen, Carlsbad, CA, USA |
| PBS-Tween tablets | Millipore, Billerica, MA, USA |
| Precision Plus Protein Kaleidoscope | BioRad, Munich |
| RIPA buffer | Sigma Life Science, Darmstadt |
| TEMED | BioRad, Munich |
| Trans-Blot Turbo 5X Transferbuffer | BioRad, Munich |
| Tris/Glycine/SDS buffer, 10X | BioRad, Munich |

### 2.3.2 Cellular biology and immunology

| **Name** | **Manufacturer** |
|---|---|
| 2-Mercaptoethanol | Life Technologies, Darmstadt |
| 7-AAD | BioLegend, Fell |
| Anti-biotin MicroBeads | Miltenyi, Bergisch Gladbach |
| Anti-CD62L MicroBeads | Miltenyi, Bergisch Gladbach |
| Anti-PE MicroBeads | Miltenyi, Bergisch Gladbach |
| Biocoll separating solution | Biochrom, Berlin |
| Cell trace CFSE | Life Technologies, Darmstadt |
| Dimethyl sulfoxide (DMSO) | Sigma-Aldrich, Steinheim |
| D-Luciferin firefly, Potassium Salt | Biosynth, Staad, Switzerland |
| Dulbecco's Modified Eagle Medium (DMEM) | Life Technologies, Darmstadt |
| Dulbecco's Phosphate-Buffered Saline (DPBS) | Life Technologies, Darmstadt |
| Dynabeads® Human T-Activator CD3/CD28 | Life Technologies, Darmstadt |
| Ethylenediaminetetraacetic acid (EDTA ) 0.5 M | Life Technologies, Darmstadt |
| Fetal calf serum (FCS) | Life Technologies, Darmstadt |
| GlutaMax-I 100X | Life Technologies, Darmstadt |
| Glutamine 200 mM | Life Technologies, Darmstadt |
| HEPES 1M | Life Technologies, Darmstadt |
| Human AB Serum | Bayerisches Rotes Kreuz |

| | |
|---|---|
| Ionomycin | Sigma-Aldrich, Steinheim |
| Poly-Ethylon Glycol (PEG300) | Sigma-Aldrich, Steinheim |
| PE Streptavidin 0.2 mg/mL | BioLegend, Fell |
| Penicillin/Streptomycin 10,000 U/mL | Life Technologies, Darmstadt |
| Phorbol 12-myristate 13-acetate (PMA) | Sigma-Aldrich, Steinheim |
| Polybrene (Millipore, 10 mg/mL) | Merck, Darmstadt |
| Purified Anti-human CD3 (OKT3) | Life Technologies, Darmstadt |
| Recombinant human IL-2 (PROLEUKIN ® S) | Novartis, Basel, Switzerland |
| RPMI 1640, GlutaMAX™ Supplement, HEPES | Life Technologies, Darmstadt |
| Trypan blue | Life Technologies, Darmstadt |

## 2.4 Kits from commercial vendors

| **Name** | **Manufacturer** |
|---|---|
| $CD4^+$ T-cell isolation Kit, human | Miltenyi, Bergisch Gladbach |
| $CD8^+$ Memory T-cell Isolation Kit, human | Miltenyi, Bergisch Gladbach |
| Cytokine Human Magnetic 10-Plex Panel | Invitrogen, Carlsbad, CA, USA |
| ELISA MAX™ Deluxe Set, human IFNγ | BioLegend, San Diego, CA, USA |
| ELISA MAX™ Deluxe Set, human IL-2 | BioLegend, San Diego, CA, USA |
| MAGPIX ® Calibration Kit | Luminex Corporation, Hertogenbosch, The Netherlands |
| MAGPIX ® Performance verification Kit | Luminex Corporation, Hertogenbosch, The Netherlands |
| Nucleobind ® Xtra Maxi EF | Macherey-Nagel, Düren |
| TGX-Stainfree™ Fast Cast™ Acrylamid, 10% | BioRad, Munich |
| Trans-Blot ® Turbo™ RTA Transferkit LF PVDF | BioRad, Munich |

## 2.5 FACS antibodies

| **Ligand** | **Clone** | **Conjugation** | **species** | **Manufacturer** |
|---|---|---|---|---|
| CD3 | UCHT1 | Pacific blue | mouse | BD, Heidelberg |
| CD4 | M-T466 | APC | mouse | Miltenyi, Bergisch Gladbach |
| CD4 | VIT4 | PE-Vio770 | mouse | Miltenyi, Bergisch Gladbach |
| CD8 | BW135/80 | FITC | mouse | Miltenyi, Bergisch Gladbach |

| | | | | |
|---|---|---|---|---|
| CD8a | RPA-T8 | PE/cy7 | mouse | BioLegend, San Diego, USA |
| CD19 | HIB19 | PE/Cy7 | mouse | BioLegend, San Diego, USA |
| CD45 | HI30 | APC/Cy7 | mouse | BioLegend, San Diego, USA |
| CD45RA | HI100 | APC | mouse | BioLegend, San Diego, USA |
| CD45RO | UCHL1 | FITC | mouse | BioLegend, San Diego, USA |
| CD62L | DREG-56 | PE | mouse | BioLegend, San Diego, USA |
| ROR1 | 2A2 | PE | mouse | Miltenyi, Bergisch Gladbach |
| EGFR | C225 | unconjugated | humanized | Merck KGaA, Darmstadt |
| EGFR | C225 | Biotinylated | Humanized | In-house |
| EGFR | C225 | AlexaFlour | Humanized | In-house |
| Her2/new | 4D5-8 | unconjugated | humanized | Roche, Mannheim |
| Her2/new | 4D5-8 | biotinylated | humanized | In-house |

## 2.6 Westernblot antibodies

| **Ligand** | **Clone** | **species** | **Manufacturer** |
|---|---|---|---|
| pSrc fam Y416/Y394 | polyclonal | rabbit | cell signaling, Cambridge, Great Britain |
| Lck | polyclonal | rabbit | cell signaling, Cambridge, Great Britain |
| pCD247 Y142 | K25-407.69 | mouse | BD, Heidelberg |
| CD247 | polyclonal | rabbit | Sigma Aldrich, St. Louis, MO; USA |
| pZap70 Y319 | 65E4 | rabbit | cell signaling, Cambridge, Great Britain |
| Zap70 | D1C10 | rabbit | cell signaling, Cambridge, Great Britain |
| b-actin | AC-74 | mouse | Sigma-Aldrich, St. Louis, MO; USA |
| anti-mouse-HRP | polyclonal | goat | BioRad, Munich |
| anti-rabbit-HRP | polyclonal | goat | BioRad, Munich |

## 2.7 Media

**T-cell medium (TC medium)**

| | |
|---|---|
| RPMI 1640 medium with 25 mM HEPES and L-Glutamine | 500 ml |
| Human Serum (heat inactivated at 56 °C 30 min) | 50 ml (9%) |
| Penicillin/Streptomycin (10,000 U/ml) | 5 ml (90 U/ml) |
| GlutaMAX Supplement (100x) | 5 ml (0.9x) |
| 2-Mercaptoethanol (50 mM) | 0.5 ml (45 µM) |

All ingredients were mixed and sterilized with filter (0.22 µm PES-membrane)

**Suspension tumor cell medium (STC medium)**

| | |
|---|---|
| RPMI 1640 medium with 25 mM HEPES and L-Glutamine | 500 ml |
| Fetal Calf Serum (heat inactivated) | 50 ml (9%) |
| Penicillin/Streptomycin (10,000 U/ml) | 5 ml (90 U/ml) |
| GlutaMAX Supplement (100x) | 5 ml (0.9x) |

All ingredients were mixed and sterilized with filter (0.22 µm PES-membrane)

**Freezing medium**

| | |
|---|---|
| T-cell medium | 25 ml (50%) |
| Fetal Calf Serum (heat inactivated) | 20 ml (40%) |
| DMSO | 5 ml (10%) |

## 2.8 Buffer

**MACS buffer**

| | |
|---|---|
| DPBS | 500 ml |
| Fetal Calf Serum (heat inactivated) | 2.5 ml (0.5%) |
| EDTA (0.5 M) | 2 ml (2 mM) |

**FACS buffer**

| | |
|---|---|
| DPBS | 500 ml |
| Fetal Calf Serum (heat inactivated) | 2.5 ml (0.5%) |
| EDTA (0.5 M) | 2 ml (2 mM) |
| Sodium azide (1.5 M) | 0.5 ml (1.5 mM) |

**PBS/EDTA buffer**

| | |
|---|---|
| DPBS | 500 ml |
| EDTA (0.5 M) | 2 ml (2 mM) |

**TBS-T buffer**

| | |
|---|---|
| TRIS Ultra Pure | 20 mM |
| NaCl | 150 mM |
| Tween-20 | 0.1% (v/v) |

Dissolved in $dH_2O$ and adjusted to pH 7.4 with HCL

**Blocking Buffer (milk based)**

| | |
|---|---|
| Skimmed milk powder (Sucofin) | 5% (w/v) |
| Dissolved in TBS-T | |

**Blocking Buffer (BSA based)**

| | |
|---|---|
| Bovine serum albumin | 5% (w/v) |
| Dissolved in TBS-T | |

**Antibody incubation Buffer (I)**

| | |
|---|---|
| BSA | 5% (w/v) |
| Dissolved in TBS-T | |

**Antibody incubation Buffer (II)**

| | |
|---|---|
| Skimmed milk powder | 5% (w/v) |
| Dissolved in TBS-T | |

**SDS Running Buffer**

| | |
|---|---|
| Tris/Glycine/SDS Buffer 10x | 100 ml (1x) |
| Mixed with 900 ml $dH_2O$ | |

**Blotting Buffer**

| | |
|---|---|
| Transfer Buffer 5x concentrate | 200 ml (1x) |
| Ethanol absolute | 200 ml (20%) |
| Mixed with 600 ml $dH_2O$ | |

**TAE Buffer**

| | |
|---|---|
| TRIS-acetate-EDTA (TAE) 50x | 20 ml (1x) |
| Mixed with 980 ml $dH_2O$ | |

## 2.9 Pharmaceuticals

| TKI | Reconstituted in | concentration | company |
|---|---|---|---|
| Bosutinib | DMSO | 10 mM | Selleckchem, Munich |
| Dasatinib (5 mg) | DMSO | 10 mM | cell signaling, Cambridge, |

| | | | |
|---|---|---|---|
| | | | Great Britain |
| Dasatinib (100mg) | DMSO | 75 mg/ml | Selleckchem, Munich |
| Dexamethasone | DMSO | 100 mM | Sigma Aldrich, St. Louis, USA |
| Lapatinib | DMSO | 10 mM | cell signaling, Cambridge, Great Britain |
| PP-1 inhibitor | DMSO | 10 mM | Selleckchem, Munich |
| Saracatinib | DMSO | 10 mM | Selleckchem, Munich |

## 2.10 Cell lines

The 293T, K562, Raji and RCH-ACV cell lines were obtained from the German Collection of Microorganisms and Cell Cultures (DSMZ, Braunschweig, Germany). K562/ROR1 cells were generated by lentiviral transduction with the full-length human ROR1-gene. K562/CD19 cells were generated by lentiviral transduction with the full-length human CD19-gene. Each of the K562, Raji and RCH-ACV cell lines were transduced with a lentiviral vector encoding a fire-fly luciferase (ffluc) enhanced green fluorescent protein (GFP) transgene to enable detection by flow cytometry (GFP), bioluminescence-based cytotoxicity assays (ffluc), and bioluminescence imaging (ffluc) in mice. Each of the cell lines was cultured in Dulbecco's modified Eagle's medium supplemented with 10 % fetal calf serum and 100 U/ml penicillin/streptomycin.

## 2.11 Primary T-cells

Blood samples were obtained from healthy donors who provided written informed consent to participate in research protocols approved by the Institutional Review Board of the Universitätsklinikum Würzburg, Germany (UKW). PBMC were isolated by centrifugation over Ficoll-Hypaque (Sigma, St. Louis, MO) and further processed as described in the methods.

## 2.12 Mice

The Institutional Animal Care and Use Committee of UKW approved all mouse experiments. NOD.Cg-Prkdc$^{scid}$ IL-2rg$^{tm1Wjl}$/SzJ (NSG) mice (female, 6–8 week old) were purchased from Charles River.

# 3 Methods

## 3.1 Generation of CAR T-cells

### 3.1.1 Isolation of T-cell subsets

PBMC were isolated from peripheral blood of healthy donors using Ficoll density centrifugation, followed by immunomagnetic bead selection to further select specific T-cell subsets. To isolate $CD8^+$ central memory T-cells ($T_{CM}$), a two-step protocol was used: first, untouched $CD8^+$ $CD45RA^-$ $CD45RO^+$ memory T-cells (that contain both $CD62L^+$ central and $CD62L^-$ effector memory fractions) were isolated by depletion of non-$CD8^+$ T-cells and $CD8^+$ $CD45RA^+$ T-cells (Miltenyi, $CD8^+$ Memory T-cell isolation kit). Second, central memory T cells were enriched by using beads binding central memory marker CD62L (Miltenyi, anti-CD62L-beads). $CD4^+$ bulk T-cells were isolated using a single step isolation protocol (Miltenyi, $CD4^+$ T-cell isolation kit, human) based on negative selection, thus by depleting all cells which are not $CD4^+$ T-cells. The purity and yield of all cell fractions was analyzed by flow cytometry and cell counting. T-cells were cultured in RPMI-1640 supplemented with 10% human AB pool serum, 1 % Glutamax, 1 % Penicillin-Streptomycin and 0.1 % β-Mercaptoethanol (T-cell medium).

### 3.1.2 Vector construction

The construction of epHIV7 lentiviral vectors containing ROR1- or CD19-specific CARs with 4-1BB or CD28 costimulatory domain has been described elsewhere *(81)*. All CAR encoding vectors contain an antigenspecific scFv, an immunoglobulin G4 (IgG4) hinge region and a transmembrane domain which is derived from CD28. Additionally, the vectors comprise EGFRt, encoded in the transgene cassette downstream of the CAR, which can be used for enrichment and tracking *(62)*. The CAR and EGFRt transgenes are separated by a T2A ribosomal skip element, which leads to the expression of two independent proteins during the process of translation (Figure 4).

A reporter gene vector (Figure 5) was developed out of the epHIV7 lentiviral vector, containing wildtype green fluorescent protein (NFAT/GFP(wt)) or a GFP-variant destabilized by a mutated version of the residues 422 to 461 of mouse ornithine decarboxylase with an *in vivo* half-life of approximately four hours (NFAT/GFP(d4)). As the GFP is under control of a minimal promotor (minP) that gets activated only when NFAT binds to the NFAT response elements (-RE), the gene functions as a marker for T-cell activation. A truncated hu-

man epidermal growth factor receptor 2 (Her2t) was included to enable the enrichment of transduced cells.

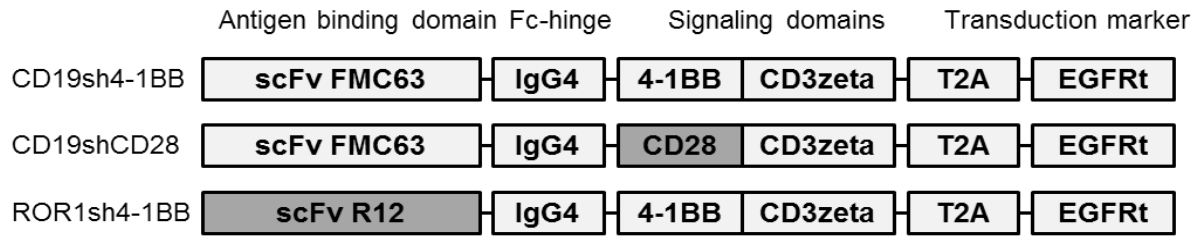


**Figure 4: Design of CAR constructs.**

Schematic display of CAR-constructs used in the study. All constructs are second generation CARs containing a short IgG4 spacer domain of twelve amino acids, a CD3zeta signaling domain and EGFRt as a marker for transduction and for enrichment.

### 3.1.3 Production of lentivirus

CAR/EGFRt, ffluc/GFP and NFAT/GFP-encoding lentivirus supernatants were produced in 293T cells co-transfected with the respective lentiviral vector plasmids and the packaging vectors pCHGP-2, pCMV-Rev2 and pCMV-G. In detail, Lenti-X cells were plated at a density of $5x10^6$ in 10 cm petri dishes and incubated for six hours to allow the cells to settle. Transfection with the lentiviral and helper plasmids was performed using a calcium phosphate-based method (Clontech, Mountain View, CA): The plasmids were diluted in $CaCl_2$ solution, an equal volume of 2x Hepes-buffered saline (HBS) was added, and the mixture incubated for 20 minutes at room temperature, then distributed drop-wise to the Lenti-X plates and the plates incubated at 37 °C overnight. The following morning, the cells were washed twice with pre-warmed phosphate buffered saline (PBS), and fresh culture medium was added that contained 0.6 M sodium butyrate, which has been shown to augment the titer of epHIV7 in this system *(81, 82)*. At 24, 48 and 72 hours after transfection, the culture medium (lentivirus supernatant) was collected, centrifuged at 2.000 rpm for ten minutes and filtered through a 0.45 µm low-protein adherence vacuum filter to remove any cellular debris.

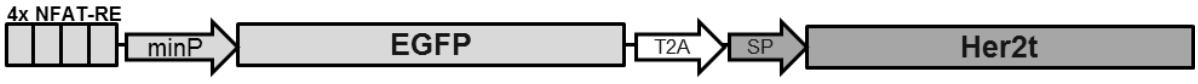


**Figure 5: Design of an activation reporter gene.**

Schematic display of NFAT/GFP: GFP is under control of a minimal Promotor (minP), which is induced upon binding of NFAT to the NFAT response element (NFAT-RE).

After the final collection, all supernatant was pooled, and the lentivirus precipitated with polyethylenglycol (PEG) (ratio of supernatant and PEG = 3:1) during overnight incubation on a rocking shaker at 4 °C. The following day, the lentivirus-PEG precipitate was pelleted by centrifugation for 20 minutes at 3000 rpm and 4 °C, re-suspended in serum-free DMEM and an ultracentrifugation performed at 24,500 rpm for 90 minutes to yield purified lentivirus. The final lentivirus preparation was diluted in 400 µl DMEM, aliquoted and stored at -80 °C for titrating and T-cell transductions.

### 3.1.4 Titration of lentivirus

For titration, Jurkat cells were plated in a 48-well plate at $2.5x10^5$ cells per well in 250 µl STC medium with 5 µg/ml Polybrene that facilitates viral entry into cells. Serial dilutions of lentivirus prep (0.5, 1, 2, 5 or 10 µl) were added to consecutive wells and incubated for four hours at 37 °C. Following incubation, the culture medium in each well was brought up to 1 ml, the cells cultured for another 48 hours, and expression of the transgene analyzed by flow cytometry using the EGFRt transduction marker encoded within the lentiviral vector *(62)*. The lentivirus titer in transforming units (TU) per µl from data obtained in the linear range of vector expression (20 % - 80 %) was calculated using the following equation:

$$\text{Titer (TU/µl)} = \frac{\text{Cell count at time of transduction x (\% positive cells/100)}}{\text{Volume of virus added [µl]}}$$

### 3.1.5 Lentiviral transduction of T-cells

Purified $CD8^+$ central memory and $CD4^+$ bulk T-cells were activated with anti-CD3/CD28 beads according to the bead manufacturer's instructions (Life Technologies), and transduced with lentiviral supernatant at a moiety of infection (MOI) of 5. In some experiments, T-cells were co-transduced with CAR/EGFRt and NFAT/GFP-encoding lentiviral supernatant. Lentiviral transduction was performed on day 1 after bead stimulation by spinoculation. T-cells were propagated and maintained in RPMI-1640 with 10 % human serum, GlutaminMAX (Life technologies), 100 U/mL penicillin-streptomycin and 50 U/mL IL-2. Trypan blue staining was performed to quantify viable T-cells. Beads were removed on day 6 and T-cells were expanded for 10 to 14 days.

### 3.1.6 Enrichment of CAR transduced T-cells

Prior to enrichment, transduction efficiency was confirmed by flow cytometry. Flow analysis was done on a FACS Canto (Becton Dickinson) and data was analyzed using FlowJo software (Treestar). Staining for EGFRt transduction marker was performed with biotinylated anti-EGFR mAb (©Erbitux, BMS) for CAR- expression and anti-Her2t for staining of iCasp or NFAT/GFP. Secondary staining was performed with labeled Streptavidin. To purify $EGFRt^+$ T-cells, we used biotinylated anti-EGFR mAb and anti-Biotin microbeads (Miltenyi) for immunomagnetic selection.

### 3.1.7 Antigen dependent expansion

Following enrichment, the CD19-CAR transduced, i.e. $EGFRt^+$ T-cell subset was expanded by stimulation with irradiated (8,000 rad) $CD19^+$ transformed B-lymphoblastoid tumor cells (TM-LCL) at a T-cell: tumor cell ratio of 1:7. T-cells were cultured in T-cell medium supplemented with 50 U/mL recombinant human IL-2 (rhIL-2) on day 1, and then every 48 hours. At the end of a 7-10 day expansion cycle, the phenotype of the expanded T-cell line was confirmed and functional assays performed as described below.

### 3.1.8 Antigen independent expansion

Following enrichment, ROR1-CAR transduced, i.e. $EGFRt^+$ T-cells were expanded by stimulation with anti-CD3 mAb (OKT3) and irradiated feeder cells as described in the rapid expansion protocol *(83)*. In brief, OKT3 was used at a final concentration of 30 ng/ml, and irradiated TM-LCL (8,000 rad) were added at a T-cell: TM-LCL ratio of 1:100 and irradiated PBMC (3,500 rad) at a T-cell: PBMC ratio of 1:600. Cell cultures were supplemented with 50 U/ml of rhIL-2 on day 1. A complete medium change was performed on day 4, and cell cultures received fresh medium and 50 U/ml rhIL-2 every 72 hours. The phenotype of expanded T-cells was analyzed between day 10 and 14 and functional assays performed as described below.

## 3.2 Immunophenotyping

PBMC and T-cell lines were stained with one or more of the following conjugated mAb: CD3, CD4, CD8, CD45RA, CD45RO, CD62L, PD-1 and matched isotype controls (BD Biosciences, San Jose, CA). CAR Transduced (i.e. $EGFRt^{+}$) T-cells were detected by staining with anti-EGFR antibody (ImClone Systems Inc.) that had been biotinylated in-house (EZ-Link™Sulfo-NHS-SS-Biotin, ThermoFisher Scientific, IL; according to the manufacturer's instructions) and streptavidin-PE (BD Biosciences). Staining with 7-AAD (BD Biosciences) was performed for live/dead cell discrimination as directed by the manufacturer. Flow analyses were done on a FACS Canto and data analyzed using FlowJo software (Treestar, Ashland, OR).

## 3.3 Functional analysis

### 3.3.1 Cytotoxicity assay

Target cells were stably transduced with ffluc_GFP and incubated in triplicate wells at $1\times10^4$ cells/well with effector T-cells at an effector to target (E:T) ratio of 5:1. D-luciferin substrate (Biosynth, Staad, Switzerland) was added to the co-culture to a final concentration of 0.15 mg/ml and the decrease in luminescence signal in wells that contained target cells and T-cells was measured using a luminometer (Tecan, Männedorf, Switzerland). Specific lysis was calculated using the standard formula.

### 3.3.2 Cytokine secretion assay

$5\times10^4$ T-cells were plated in duplicate or triplicate wells with target cells at an E:T ratio of 4:1 (K562/ROR1, K562/CD19, RCH-ACV), and IFN-γ and IL-2 were measured by enzyme-linked immunosorbent assay (ELISA), or cytokine panels were measured by multiplex cytokine immunoassay (Luminex) in supernatant removed after 20 hours of incubation. Dasatinib was added at concentrations and time points as indicated in the figure legends. Specific cytokine production was calculated by subtracting the amount of cytokines released by unstimulated CAR T-cells from the amount of cytokines released after antigen-specific stimulation. The remaining cytokine secretion in % as shown in the diagrams was normalized to CAR T-cells in the absence of dasatinib-treatment (100 %).

### 3.3.3 CFSE proliferation assay

T-cells were labeled with 0.2 μM carboxyfluorescein succinimidyl ester (CFSE, Invitrogen), washed and plated in duplicate or triplicate wells with irradiated (80 Gy) stimulator cells at an E:T ratio of 4:1 (K562/ROR1, K562/CD19 or RCH-ACV). No exogenous cytokines were added to the culture medium. Dasatinib was added at concentrations and time points as indicated in the figure legends. After a 72-hour incubation, cells were labeled with anti-CD3 mAb, and analyzed by flow cytometry to assess cell division of T-cells. The proliferation index was calculated using FlowJo Software (FlowJo, LLC, Ashland, Oregon, USA), and used to determine the "remaining proliferation", i.e. normalized to the proliferation of CAR T-cells in the absence of dasatinib (100 %).

### 3.3.4 Western blot analysis

After expansion, T-cells were washed and cultured in absence of exogenous IL-2 for two days. Protein was isolated after a 30-minute stimulation of T-cells with RCH-ACV (E:T ratio of 4:1) in the absence or presence of 100 nM dasatinib. Western blots were performed under reducing conditions using the following antibodies according to the manufacturer's instructions: anti-pSrc family Y416 (cell signaling #2101S), anti-Lck (cell signaling #2752S), anti-pCD247 Y142 (CD3zeta, BD #558402), anti-CD247 (Sigma Life science #HPA008750), anti-pZap70 Y319 (cell signaling #2717S) and anti-Zap70 (cell signaling #3165S). Staining against β-actin (Sigma Aldrich #A5316) was used as a loading control and for normalization. Western blots were developed using the ChemiDoc MP imaging system (Biorad, Munich, Germany); quantitative analysis of western blots was performed using Image Lab Software (Biorad, Munich, Germany).

### 3.3.5 NFAT reporter assay

T-cells (co-)expressing the NFAT/ GFP(wt) reporter gene were co-cultured in the presence of 10 U IL-2 with irradiated (80 Gy) Raji or K562 tumor cells at an E:T ratio of 5:1 or without target cells. T-cells and target cells were co-cultured in the absence or in the presence of 100 nM dasatinib. After 24 hours of co-culture, cells were labeled with anti-CD3 mAb, and analyzed by flow cytometry to assess GFP expression in T-cells.

### 3.3.6 Apoptosis assay

$CD8^+$ CD19-CAR T-cells were cultured in the presence of 50 U IL-2 either alone or with irradiated (80 Gy) K562/CD19 tumor cells at an E:T ratio of 4:1. Dasatinib was added to a final concentration of 100 nM either at the start of the assay or two hours after the start of the assay. After 24 hours, co-cultures were labeled with anti-CD8 mAb, 7-AAD and Annexin V according to the manufacturer's instructions (BD Biosciences, Heidelberg, Germany), and analyzed by flow cytometry to evaluate the amount of apoptotic and dead T-cells.

## 3.4 Preclinical *in vivo* experiments

NOD.Cg-Prkdc$^{scid}$ Il2rg$^{tm1Wjl}$/SzJ (NSG) mice (female, 6–8 week old) were inoculated with $1\times10^6$ Raji/ffluc_GFP tumor cells via tail vein injection (i.v.). Mice were treated with $5\times10^6$ CAR-modified or control untransduced T-cells (CD4:CD8 ratio = 1:1) via tail vein injection (i.v.). Tumor burden and distribution was analyzed by serial bioluminescence imaging on an IVIS Lumina imager (Perkin Elmer, Baesweiler, Germany): mice received intraperitoneal (i.p.) injections of 0.3 mg/g luciferin and images were acquired 10 min after luciferin injection in small binning mode at an acquisition time of 1 s to 1 min to obtain unsaturated images. Data were analyzed using LivingImage Software (Caliper) and the average radiance (or photon flux) analyzed in regions of interest that encompassed the entire body of each individual mouse. Mice were sacrificed at the end of the experiment and human T-cells in bone marrow, peripheral blood and spleen were analyzed by flow cytometry. The presence of human cytokines in serum was measured using multiplex cytokine analysis.

### 3.4.1 Serial injection

Mice were inoculated with $1\times10^6$ Raji/ffluc_GFP tumor cells (i.v.) on day 0. Mice were treated with either CAR T-cells or control T-cells on day 0. All T-cells expressed the NFAT/GFP reporter gene to allow rapid read-outs of their activation state by flow cytometry. In each cohort, a subgroup of mice received 0.2 mg dasatinib in 13.3 % DMSO/ 26.6 % PEG/ 60 % PBS to create a function OFF phase in T-cells for the indicated period of time. $5x10^6$ T-cells (CD4:CD8 1:1) were administered i.v. either three hours after the first injection of dasatinib or 72 hours before the first injection of dasatinib, with dasatinib being injected every six hours for a total of six to eight dosages. Thereafter, dasatinib administration was discontinued and T-cells were allowed to enter a function ON phase. All animals were imaged on indicated days to evaluate the development of tumor burden during the OFF and ON phase, and serum cytokines were measured frequently.

### 3.4.2 Osmotic pumps

Mice were inoculated with $1x10^6$ ffluc$^+$/GFP$^+$ Raji cells on day 0. All animals were imaged on day 7 and immediately implanted with osmotic pumps (Alzet, Model 1007d). Pumps were loaded with 3.75 mg dasatinib in 50 % DMSO/50 % Glycerol or DMSO/Glycerol only as control and primed overnight in 15 ml 0.9 M NaCl at room temperature. The pumps were implanted s.c. in the neck of each animal, and mice were additionally treated with rimadyl to reduce pain after surgery and observed daily. $5x10^6$ T-cells (CD4:CD8 1:1, CAR or control T-cells) were injected on day 8 via tail vain injection. Mice were imaged on day 10, 12, 14, 17 and 21 to closely control the development of tumor burden during dasatinib administration and shortly after withdrawal. Subsequently, mice were imaged once weekly. To analyze the level of human cytokines in the serum, blood was drawn on day 10, 12, 17 and 21.

### 3.4.3 Intermittent injection

Mice were inoculated with $1x10^6$ ffluc$^+$/GFP$^+$ Raji cells on day 0. Dasatinib was administered by i.p. injection at a dose of 0.1 mg/mouse in 10 %DMSO/90 % DPBS. For analysis of T-cell persistence, dasatinib was injected every 24 hours from day 7 until day 11 followed by i.p. injection every 36 hours on day 12 and 14 (total seven doses). Serial bioluminescence imaging was performed to determine tumor burden on day 7, 9 and 15, and mice were sacrificed on day 15 to analyze the presence of T-cells in bone marrow and spleen. To evaluate the PD-1 expression on T-cells, mice were treated as described, but received dasatinib on seven consecutive days, from day 7 to day 13, and mice were sacrificed on day 14.

## 3.5 Statistical analysis

All *in vitro* experiments were repeated three times with CAR T-cells generated from individual donors unless indicated elsewise. Specific lysis was analyzed using two-way analysis of variance (ANOVA) with Sidak's multiple comparison test. Cytokine secretion was analyzed using ordinary one way ANOVA with Holm-Sidak's multiple comparison test or Kruskal-Wallis test with Dunn's multiple comparison test as indicated in the figure legends. Proliferation, quantification of western blot and apoptosis were analyzed by Kruskal-Wallis test

with Dunn's multiple comparison test. GFP expression following stimulation was analyzed by ordinary one-way ANOVA with Holm-Sidak's multiple comparison test.

*In vivo* experiments were repeated once with similar results. Percentages of human T-cells and GFP expression were analyzed by two-way ANOVA with Sidak's multiple comparison test, and the change in tumor burden and *in vivo* cytokine secretion was analyzed by Kruskal-Wallis test with Dunn's multiple comparison test. Data were plotted and analyzed in Prism (GraphPad).

# 4 Results

## 4.1 Characterization of dasatinib-induced effects on CD19-CAR T-cells

### 4.1.1 Dasatinib dose-dependently prevents activation of resting CAR T-cells

To evaluate the effect of dasatinib on the function of resting $CD8^+$ CAR-T-cells, we employed a CD19-CAR with 4-1BB co-stimulation (CD19-CAR/4-1BB, Figure 4) that conferred high rates of complete remissions in recent clinical trials *(26, 54)*. We enriched CAR-expressing T-cells to > 90% purity (Figure 6a) and performed co-culture assays with $CD19^+$ target cells (K562/CD19) in the presence or absence of dasatinib. To evaluate the influence of dasatinib on resting CAR T-cell effector function, we analyzed cytokine secretion, proliferation and target cell lysis by CAR T-cells after antigen encounter. Dasatinib was added simultaneously with target cells at the beginning of co-culture, with concentrations ranging from 3.125 to 100 nM. We observed inhibition of specific target cell lysis by CAR T-cells correlating with the concentration of dasatinib, and complete blockade of specific lysis was achieved at concentrations ≥ 50 nM (Figure 6b). Treatment with 25 nM dasatinib led to partial inhibition with delayed and reduced lysis of target cells as compared to untreated CAR T-cells, whereas no significant reduction of target cell lysis was observed at concentrations ≤ 12.5 nM.

We then analyzed the ability of CAR T-cells to secret cytokines. T-cells treated with concentrations above 50 nM showed completely inhibited secretion of both IFNγ (Figure 6c) and IL-2 (Figure 6d) when stimulated with K562/CD19. Lower levels of dasatinib (6.25 nM- 25 nM) in the assay medium dose-dependently reduced the secretion of IFNγ and IL-2 by CAR T-cells compared to controls without dasatinib. These results correlate with the level of proliferation of CAR T-cells, which was significantly blocked by treatment with 50 or 100 nM (Figure 6e). In summary, the data show that dasatinib retains resting $CD8^+$ CD19-CAR/4-1BB T-cells in a function OFF state and prevents the execution of effector functions in the presence of antigen.

### 4.1.2 Dasatinib blocks the function of activated CAR T-cells

In a clinical situation when control over CAR T-cells is desired, a proportion of T-cells would not be in a resting but already in an activated state. We therefore sought to determine whether dasatinib could block the function of CAR T-cells that were already activated and in the process of executing effector functions. To assess this, we activated CAR T-cells with target cells

to turn them ON, and then added dasatinib to turn them OFF. CD8$^+$ CAR T-cells rapidly started

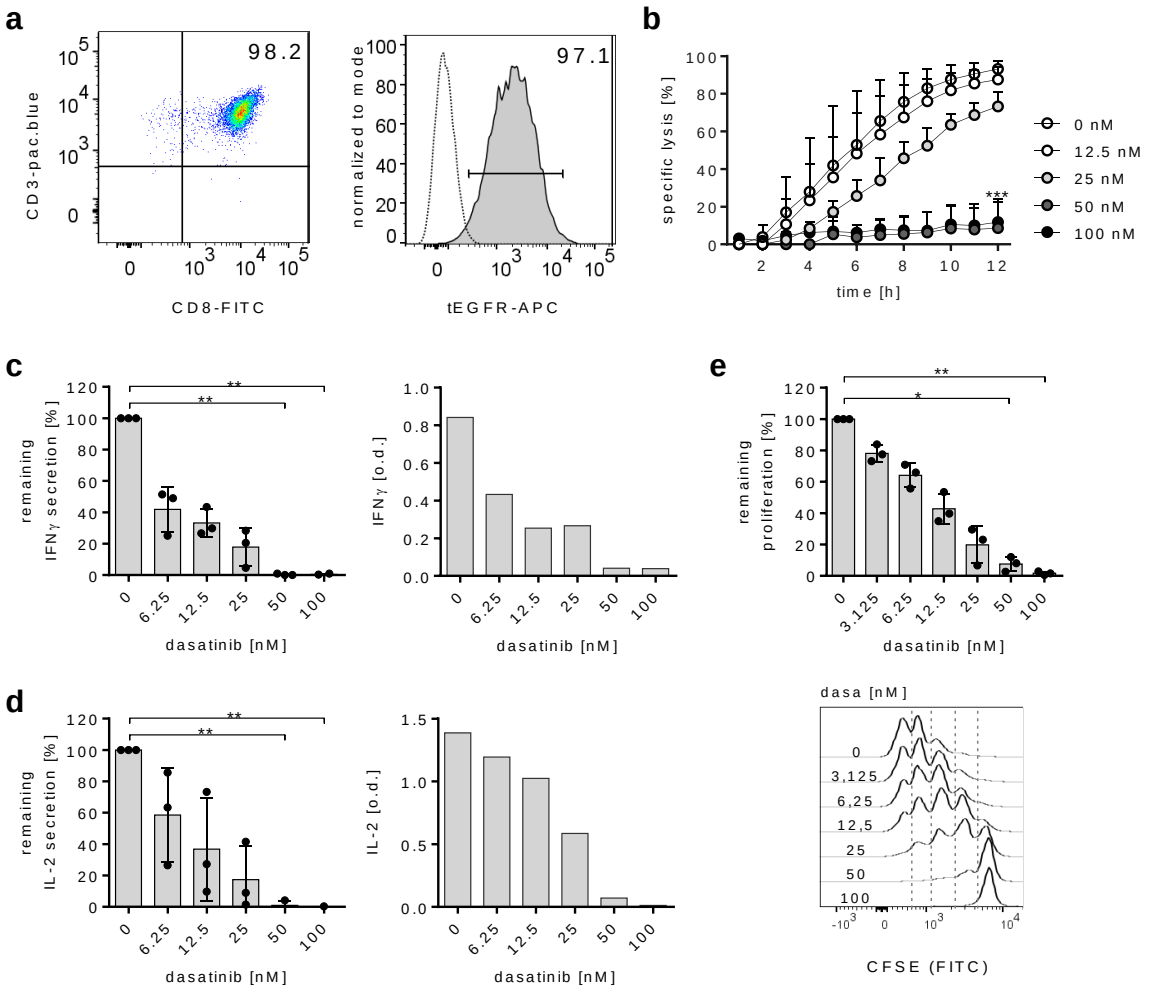


**Figure 6: Dasatinib retains resting CD8$^+$ CAR T-cells in a function 'OFF' state.**

(a) Phenotype of CD8$^+$ CD19-CAR/4-1BB T-cells, tEGFR is the transduction marker encoded with the CAR transgene. (b-e) CAR T-cells were co-cultured with K562/CD19 in the presence of titrated amounts of dasatinib (dasa), which was added at assay start. (b) The percentage of lysed target cells was determined in 1-hour intervals over a period of 12 hours (E:T ratio 5:1). (c, d) ELISA for IFNγ (c) and IL-2 (d). Left diagrams show data obtained in n = 3 experiments with T-cells from different donors, normalized to the amount of cytokines obtained by CAR T-cells in the absence of dasatinib (100 %). Right diagrams show optical densitiy (o.d.) values of one representative experiment. (e) Proliferation of CAR T-cells 72 hours after stimulation with K562/CD19 target cells. Diagram shows data from quantitative analysis of n = 3 independent experiments. Histograms show data from one representative experiment. The remaining proliferation was calculated using the proliferation index and normalized to the proliferation of CAR T-cells in the absence of dasatinib. Data shown are mean values + SD obtained in n = 3 experiments with CD8$^+$ T-cells from different healthy donors with * $P \leq 0.05$, ** $P \leq 0.005$ by two-way (b) or one-way ANOVA (c-e, Kruskal-Wallis test).

lysing target cells in the ON phase. As soon as dasatinib was added to the culture (t = +1 hour) target cell lysis stagnated and did not progress further, indicating that the OFF state had been induced (Figure 7a). Similarly, addition of dasatinib to activated $CD8^+$ CAR T-cells interfered with subsequent cytokine secretion and proliferation (Figure 7b, c). Consistent with the mechanism of action revealed earlier, the inhibitory effect of dasatinib began to cease once CAR T-cells had progressed beyond a certain point of activation, e.g. if added later than three hours after turning CAR T-cells ON, the effect of dasatinib on proliferation was low (Figure 7d).

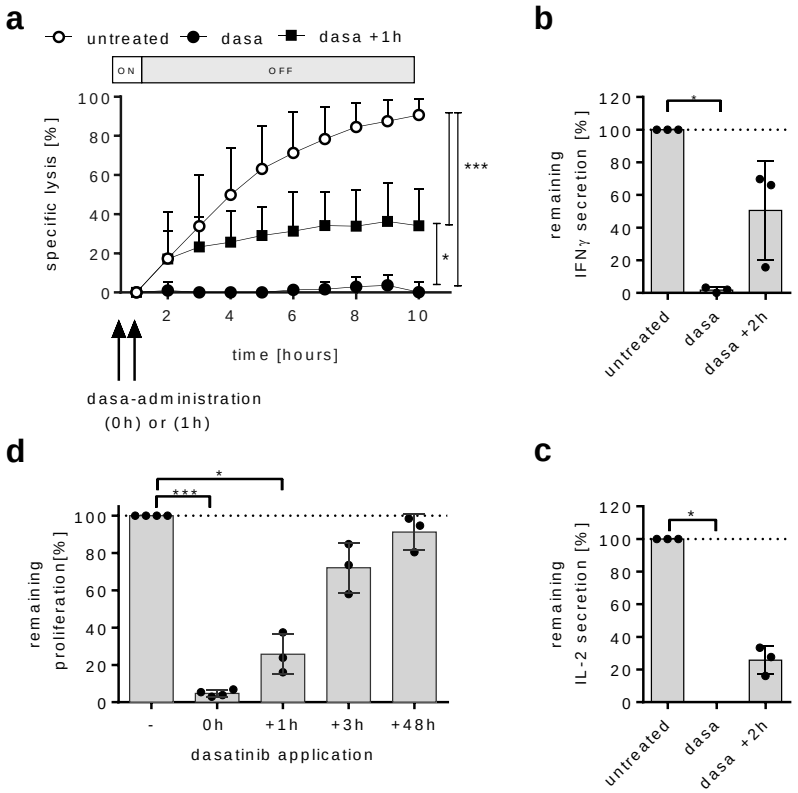


**Figure 7: Dasatinib pauses activated CAR T cells in a function OFF state.**

CAR T-cells were treated with 100 nM dasatinib, added either at assay set up, or one, two, three or 48 hours after stimulation with K562/CD19. (a) Lysis of target cells measured in 1-hour intervals over a 10-hour period. Dasatinib (100 nM) was added one hour after assay setup (black squares), in order to switch CAR T-cells OFF after the initial ON-phase. For comparison, the diagram shows lysis of target cells by untreated CAR T-cells (white circles) and by T-cells that were treated with dasatinib at assay set up (black circles). (b,c) Diagram shows the levels of IFNγ (b) and IL-2 (c). Data was normalized to the amount of cytokines produced by untreated CAR T-cells (-). CAR T-cells were treated either at the beginning (0) or two hours (2) after assay set up. (d) Proliferation was calculated based on the cell proliferation-index and normalized to proliferation of untreated CAR T-cells (-). Data shown are mean

values ± SD obtained in n = 3 experiments with $CD8^+$ T-cells from different healthy donors with * $P \leq 0.05$, ** $P \leq 0.005$ by two-way (a) or one-way ANOVA (b-d, Kruskal-Wallis test).

### 4.1.3 Direct effects of dasatinib on target cells

To exclude that the observed loss of function was caused by dasatinib-mediated eradication of target cells, we analyzed the direct effect of dasatinib on the tumor cells lines K562, K562/CD19 and Raji. We cultured luciferase expressing tumor cells in the presence and absence of 100 nM dasatinib and analyzed the change in luminescence over a 20-hour period. Treatment with dasatinib did not influence the proliferation and survival of Raji cells, as the luminescence signal increased equally in treated and untreated cells over time (Figure 8a). In contrast, the luminescence signal of K562 cells decreased over time in the presence of dasatinib, indicating direct toxic effects of dasatinib towards K562 based cell lines that became even more obvious when the survival of tumor cells was calculated in reference to untreated -cells (Figure 8b). The reduced survival of K562 in the presence of dasatinib can be explained as, in contrast to Raji cells, K562 cells endogenously express the BCR-ABL fusion protein, which is the main target of dasatinib. BCR-ABL provides essential survival signals to K562 derived cells, thus, upon blockade, they undergo apoptosis. However, this dasatinib-mediated effects were much slower than cytolytic effects mediated by CAR T-cells. With respect to this observation, specific lysis mediated by CAR T-cells was calculated in reference to equally treated untransduced T-cells in all displayed figures.

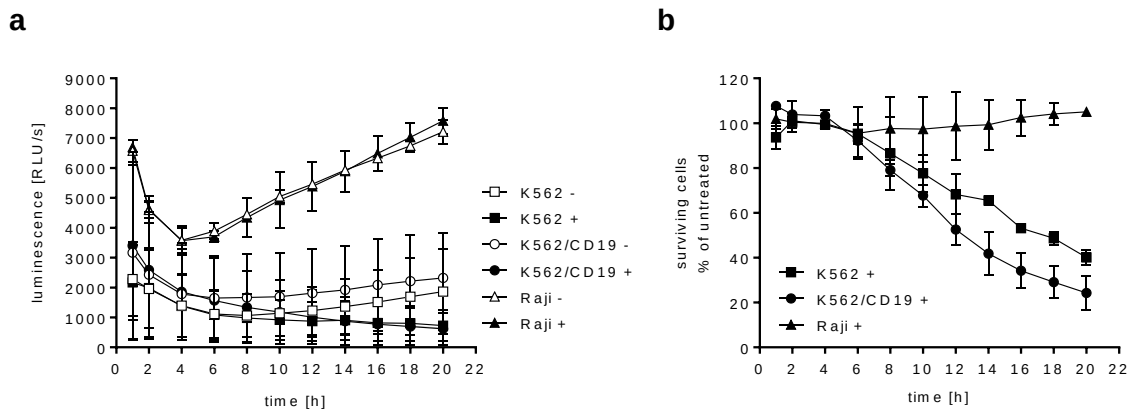


**Figure 8: The effects of dasatinib on target cell lines.**

Indicated cell lines were treated with 100 nM dasatinib (+) or not treated (-). (a) The viability of tumor cells was assessed every two hours over a 20-hour period by bioluminscence imaging. (b) Survival of tumor cells, normalized to BLI of untreated tumor cells. Data shown are mean values ± SD obtained in n = 2 independent experiments.

### 4.1.4 TCR stimulation does not bypass the dasatinib induced function OFF state

In most applications, CAR T-cells retain expression of their endogenous TCR which may bypass the dasatinib-induced blockade of the CAR. From human leukocyte antigen type A2 positive (HLA-A2$^+$) donors, we generated CD8$^+$ CD19-CAR/4-1BB T-cells that recognize the cytomegalovirus (CMV) pp65/A2-NLV epitope through their endogenous TCR. We confirmed uniform expression of CD19-CAR and CMV-specific TCR by flow cytometry (Figure 9a). Then, we stimulated T-cells with target cells that expressed either CD19 (K562/CD19) or HLA-A2 (pulsed with pp65-NLV peptide, K562/pp65) and assessed cytolytic activity over time. In both cases, the addition of dasatinib to the assay medium (concentration $\geq$ 50 nM) completely blocked target cell lysis. In particular, the addition of dasatinib at 50 nM completely blocked target cell lysis through both CD19-CAR and CMV-specific TCR, even when both receptors were engaged concomitantly (Figure 9b-d). Encouragingly, these data show that dasatinib is able to confer complete blockade of CAR T-cell function at the dose of 50 nM, which is similarly effective in preventing CAR and TCR signaling.

### 4.1.5 Influence of other Src kinase inhibitors on CAR T-cell function

Tyrosine kinase inhibitors have gained importance for the targeted therapy of a variety of hematologic and solid cancers. Many of these inhibitors focusing on the treatment of hematologic malignancies target Src family kinases essential for the signaling of healthy immunecells. To study if Src kinase inhibitors in general are capable to mediate immune-suppressive effects as observed with dasatinib, we chose the two newly approved Src kinase inhibitors saracatinib and bosutinib and evaluated their ability to inhibit CAR T-cell function. To confirm that selectively blocking Src kinases would be sufficient to mediate T-cell inhibition, we included PP1, a highly selective Src kinase inhibitor without clinical approval, to the panel. We analyzed cytolytic activity of CD8$^+$ CD19-CAR/4-1BB T-cells in a 4-hour bioluminescence-based cytotoxicity assay against K562/CD19. Src kinase inhibitors were added to the assay medium at the beginning of the assay over a 4-log concentration range.

The data show that of the three newly tested Src kinase inhibitors, two inhibitors were capable of blocking the cytolytic activity of CAR T-cells (Figure 10a): The inhibition of spe-

cific lysis mediated by PP1 was similar to the one mediated by dasatinib, confirming that selective inhibition of Src kinases is sufficient to induce blockade of CAR T-cell function. At a concentration of 10 nM of PP1 in the assay medium, there was a partial inhibition of cytolytic

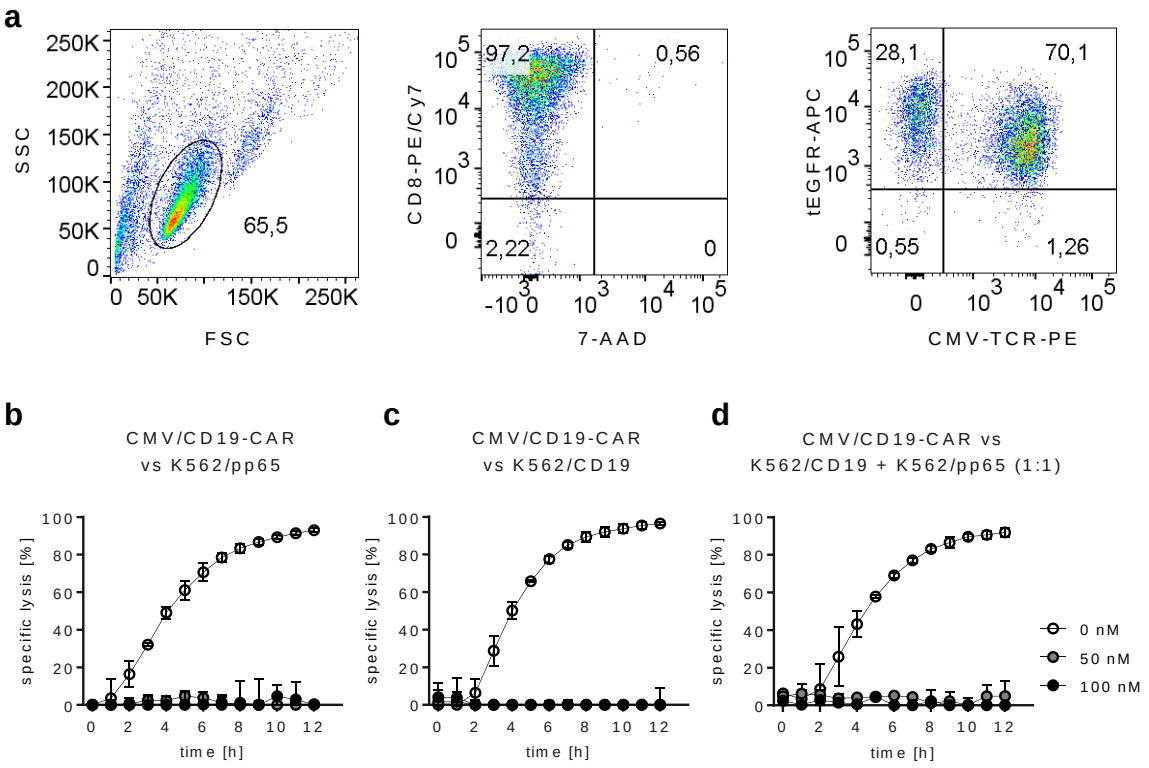


**Figure 9: TCR stimulation does not bypass the function OFF state in dasatinib-treated CAR T-cells.**

(a) Phenotype of CD8+ CMV-specific CAR T-cells. (b-d) The diagrams show lysis of K562/pp65 (b), K562/CD19 (c) and a 1:1 mix of both tumor cell lines (d) by CMV-specific CD19-CAR T-cells (E:T = 5:1) over a 12-hour period. Dasatinib was added at assay set up at the indicated concentrations. Data shown are mean values ± SD obtained in n = 2 independent experiments.

function of CAR T-cells (62.4 % specific lysis of target cells compared to 82 % specific lysis of target cells by untreated CAR T-cells), whereas complete inhibition of cytolytic function was achieved at a concentration of ≥ 100 nM of PP1 in the assay medium (< 3 % specific lysis of target cells compared to 82 % specific lysis of target cells by untreated CAR T-cells).

Bosutinib showed complete inhibition of specific lysis only at a concentration of 1000 nM, and no effects were observed for concentration ≤ 100 nM. In contrast, saracatinib did not show any effect towards the specific lysis by CAR T-cells. Of note, high levels of bosutinib also had direct effects on the survival of K562 cells during the four-hour assay, which was not the case for any of the other tested substances (Figure 10b). In aggregate, these data

show that tyrosine kinase inhibitors other than dasatinib can exert an inhibitory effect to CAR T-cell functions. However, as dasatinib was the only clinically approved substance out of this panel to mitigate efficient control, we focused on dasatinib for the rest of the study.

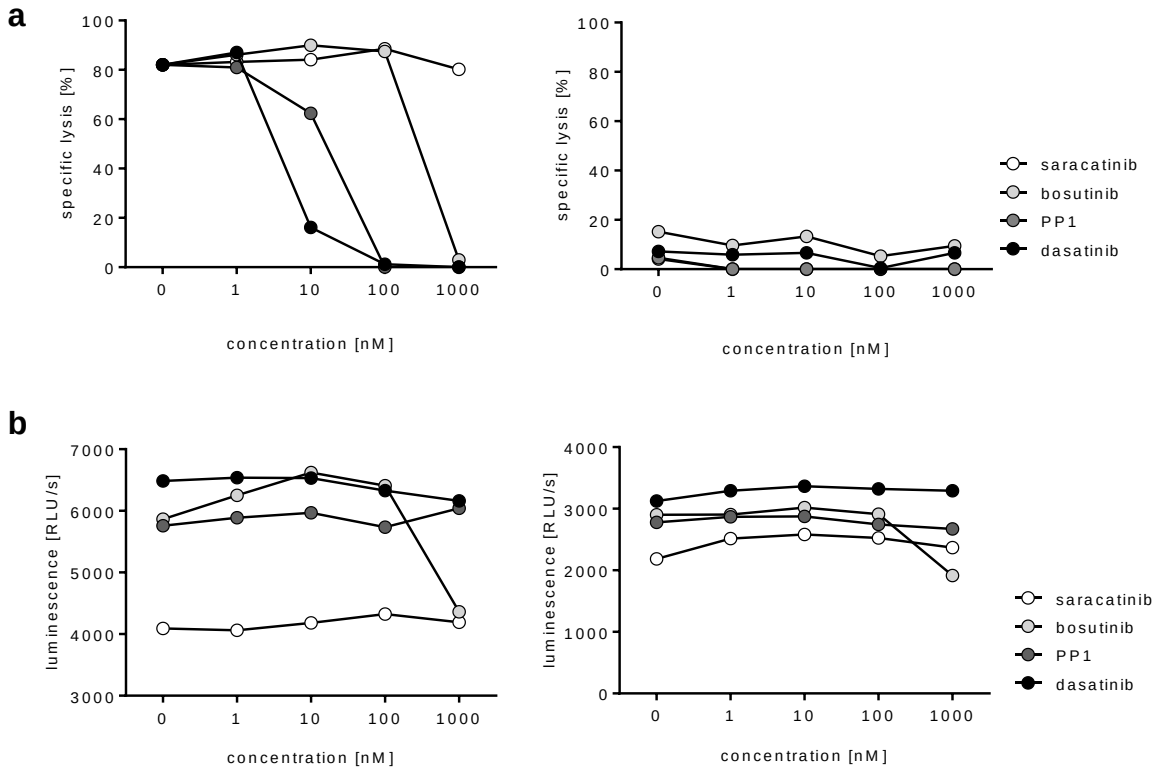


**Figure 10: The effects of a Src kinase inhibitor panel on CAR T-cells.**

(a) cytolytic activity of $CD8^+$ CD19-CAR/4-1BB T-cells in the presence of titrated doses (1 – 1000 nM) of saracatinib, bosutinib, PP1 or dasatinib. The percent specific lysis of antigen-positive target cells (K562/CD19, left diagram) and antigen-negative cells (K562, right diagram) compared to untransduced control T-cells was determined after four hours of co-culture. (b) Survival of K562/CD19 (left diagram) and K562 (right diagram) 4 hours after treatment with titrated amount of TKI in the absence of CAR T-cells.

## 4.2 The effects of CAR-design and T-cell origin on inhibition by dasatinib

Having shown that dasatinib can control execution of effector functions in both resting and activated CD19-CAR/4-1BB T-cells, we sought to determine whether dasatinib can be applied as a general safety tool for CAR T-cells independent of CAR-design. To ensure comparability between CARs, we used a CD19-targeting CAR with CD28 costimulatory domain, and a ROR1 targeting CAR with 4-1BB targeting domain *(54)* of otherwise equal design as the initially used CD19-CAR/4-1BB (Figure 4).

### 4.2.1 Dasatinib-mediated effects are independent of the co-stimulatory domain

First, we evaluated the influence of the co-stimulatory domain used in the CAR towards dasatinib-mediated inhibition. As before, complete inhibition of specific lysis was achieved when co-cultures were treated with 100 nM dasatinib (Figure 11a). However, treatment with 50 nM only led to partial inhibition of cytolysis, and lower amounts did not influence specific lysis. In contrast to that, cytokine secretion by CD19-CAR/CD28 T-cells was equally sensitive towards dasatinib induced blockade as by T-cells expressing CD19-CAR/4-1BB, thus the secretion of IFNγ and IL-2 was significantly blocked in the presence of 50 nM or 100 nM (Figure 11b, c), which correlated with a complete suppression of proliferation (Figure 11d) following stimulation with K562/CD19. We thus conclude that the blockade of T-cell function by dasatinib is similar for CARs comprising 4-1BB or CD28 co-stimulatory moieties.

### 4.2.2 Dasatinib inhibits CAR T-cells targeting ROR1

To evaluate whether the inhibition of CAR T-cell effector functions is a general principle that can be extended to CARs targeting other antigens than CD19, we generated a ROR1-CAR with a 4-1BB costimulatory domain (Figure 4). We then performed dose titration assays in order to study the effects of dasatinib on the function of ROR1-CAR T-cells. Complete inhibition of specific lysis was achieved when co-cultures where treated with concentrations of dasatinib $\geq$ 25 nM (Figure 12a). Treatment with a concentration of 12.5 nM led to partial inhibition as observed by delayed and reduced lysis of target cells when compared to the lysis mediated by untreated CAR T-cells.

ROR1-CAR T-cells treated with concentrations above 50 nM showed completely inhibited secretion of IFNγ and IL-2 when stimulated with K562/ROR1 (Figure 12b). When compared to untreated CAR T-cells, 6.25 to 25 nM dasatinib in the assay medium led to

dose-dependent reduction of cytokines by ROR1-CAR T-cells. These results correlated with the level of proliferation of ROR1-CAR T-cells, which was significantly reduced during treatment with 50 or 100 nM (Figure 12c). These data show that dasatinib similarly blocks the function of CAR T-cells independent of their antigen specificity.

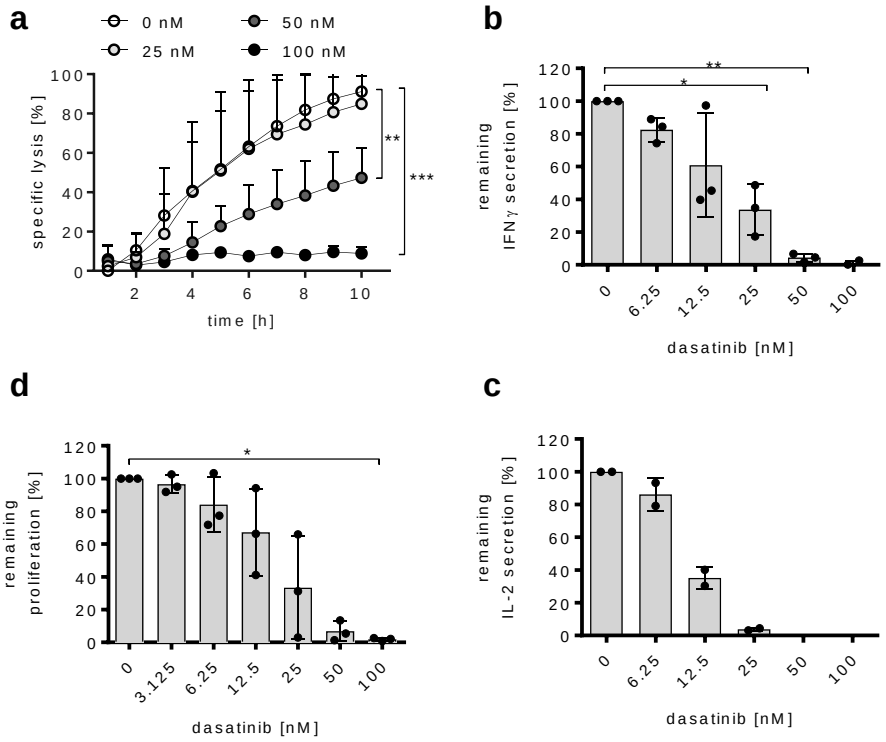


**Figure 11: Dose titration of dasatinib on CD19-CAR/CD28 T-cells.**

$CD8^+$ CAR T-cells were stimulated with K562/CD19 target cells and treated at assay set up with dasatinib at the indicated dose. Data shown are mean values ± SD of n = 3 independent experiments with T-cells of healthy donors unless indicated otherwise. (a) Specific lysis of target cells (E:T 5:1) over time measured in a bioluminescence-based cytotoxicity assay. (b) Secretion of IFNγ (left diagram) and IL-2 (right diagram, n = 2), measured in a standard sandwich ELISA on supernatants obtained after 20 hours of co-culture (E:T 4:1). (c) Proliferation of CD19-CAR/CD28 T-cells 72 hours after stimulation by CFSE dye dilution. The remaining proliferation was calculated based on the cell proliferation index and normalized to untreated T-cells. * $P \leq 0.05$, ** $P \leq 0.005$, *** $P \leq 0.0005$ by standard two-way ANOVA (a) or one-way ANOVA (b, c, Kruskal-Wallis test).

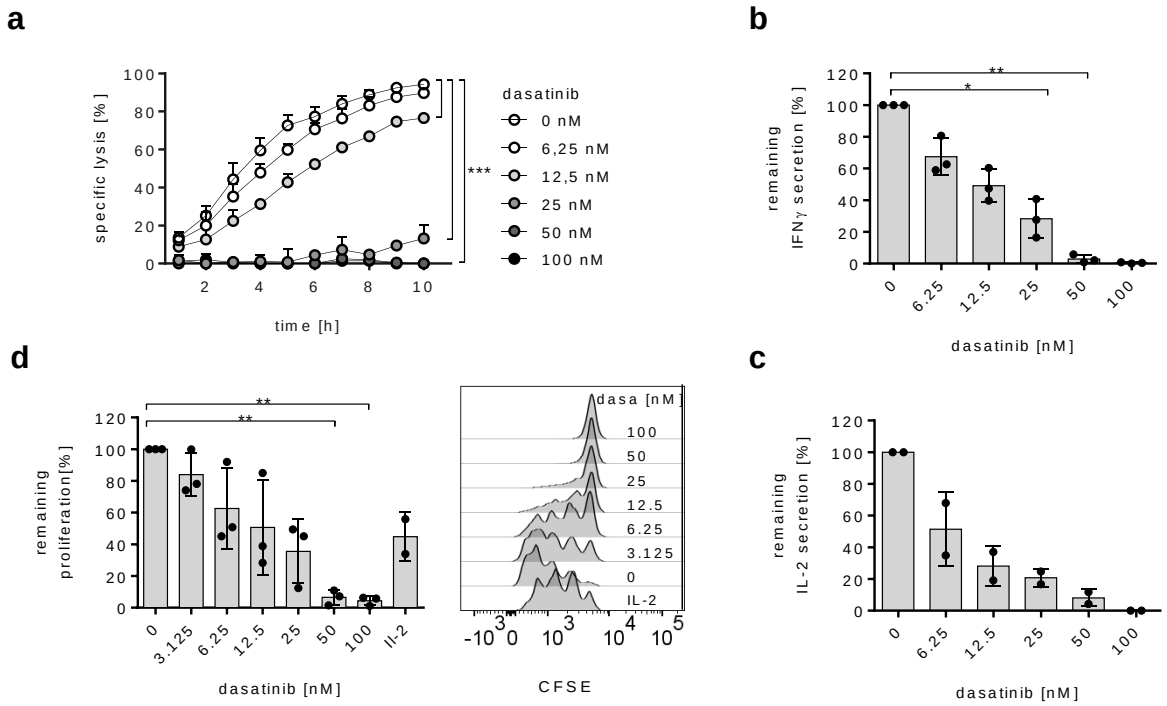


**Figure 12: Dasatinib equally inhibits CAR T-cells targeting ROR1.**

$CD8^+$ CAR T-cells were stimulated with K562/ROR1 target cells. Data shown are mean values ± SD of n = 3 independent experiments with T-cells of healthy donors unless indicated otherwise. (a) Target cell lysis was determined in 1-hour intervals over a period of ten hours at an E:T ratio of 5:1. (b) Secretion of IFNγ (upper diagram) and IL-2 (lower diagram, n = 2) by ELISA was performed on supernatants obtained after 20 hours of co-culture (E:T = 4:1). (c) Proliferation of ROR1-CAR T-cells was evaluated 72 hours after stimulation. The remaining proliferation (bar diagram) was calculated based on the cell proliferation index and normalized to untreated CAR T-cells. Histograms show data from one representative experiment. T-cells treated with titrated amounts of dasatinib were compared to untreated T-cells using standard two-way ANOVA (a) or one-way ANOVA (Kruskal-Wallis test, b, c). * $P \leq 0.05$, ** $P \leq 0.005$, *** $P \leq 0.0005$.

### 4.2.3 Dasatinib instantly blocks the function of $CD4^+$ CAR T-cells

CAR-T-cell products in clinical application almost always contain $CD8^+$ killer and $CD4^+$ helper T-cells. Thus, control over $CD8^+$ and $CD4^+$ CAR T-cells by dasatinib should be achieved with comparable efficacy. The major function of $CD4^+$ CAR T-cells is to support the $CD8^+$ killer cells by the production and secretion of cytokines. We confirmed that dasatinib was also effective with $CD4^+$ CAR T-cells by titrating the amount of dasatinib needed to block the secretion of cytokines by $CD4^+$ CD19/4-1BB CAR T-cells after confirming the $CD4^+$ CAR T-cell phenotype (Figure 13a).

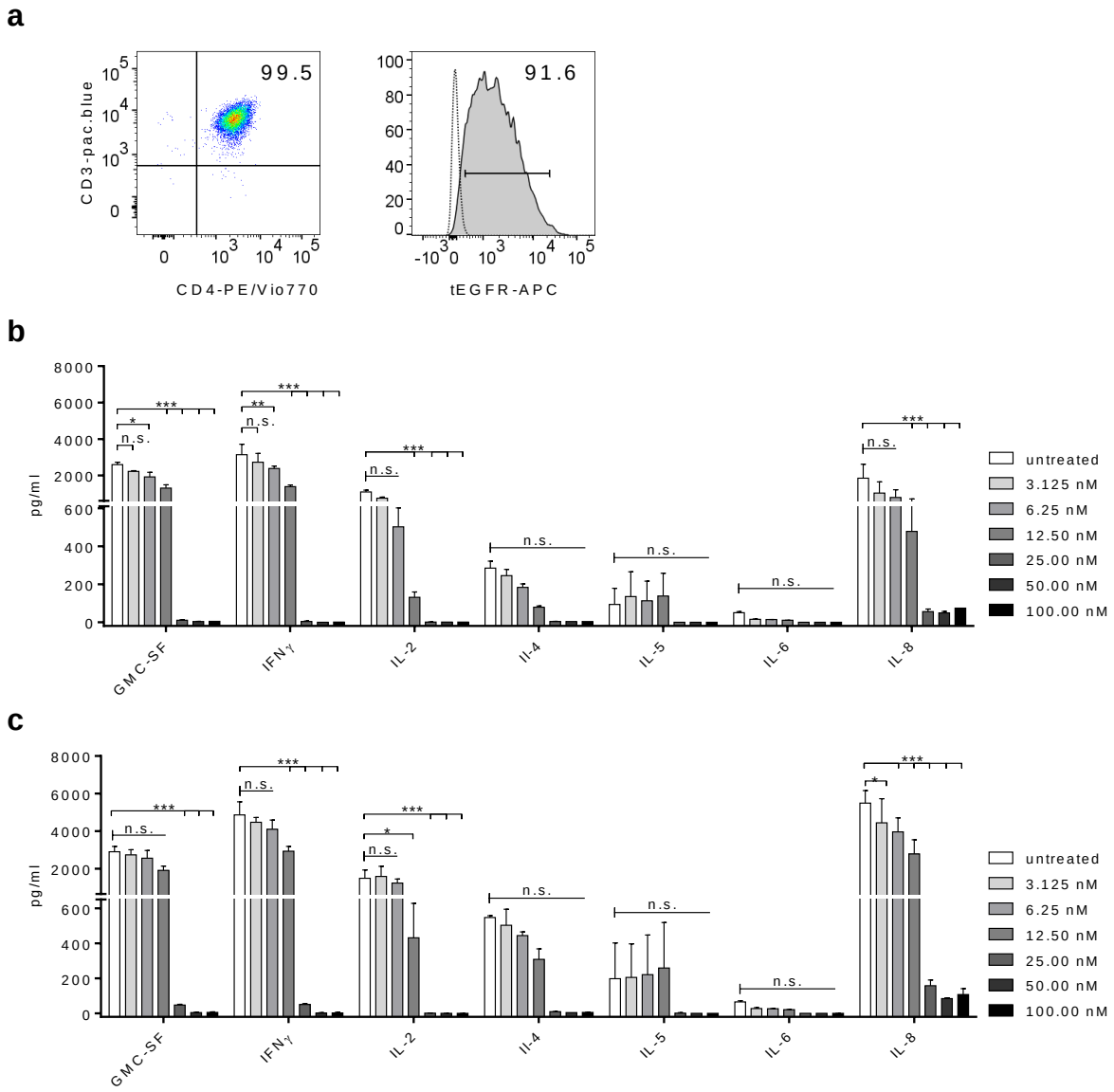


**Figure 13: Dasatinib instantly blocks the function of CD4$^+$ CAR T-cells in a dose dependent manner.**

(a) Phenotype of CD3$^+$/CD4$^+$ bulk T-cells expressing CD19-CAR/4-1BB. tEGFR is the transduction marker encoded with the CAR transgene. Numbers indicate percentages of parental population. (b, c) Multiplex analysis of cytokines after stimulation of (b) CD19-CAR/4-1BB and (c) CD19-CAR/CD28 T-cells with K562/CD19 (E:T = 4:1) in supernatant that was collected after 20 hours of co-culture. The concentration of three cytokines (IL-1, IL-10 and tumor necrosis factor alpha (TNFα)) was below the detection limit and is therefore not displayed. Results were obtained in independent experiments with T-cells from n = 2 healthy donors. T-cells treated with titrated amounts of dasatinib were compared to untreated T-cells using two-way ANOVA (non significant (n.s.) > 0.05, * $P \leq 0.05$, ** $P \leq 0.005$, *** $P \leq 0.0005$,).

We found that ≥ 25 nM dasatinib completely abrogated the production of cytokines including the granulocyte-macrophage colony-stimulating factor (GM-CSF), IFNγ, IL-2 and IL-8 after stimulation with target cells (Figure 13b). Treatment of T-cells below this threshold did not significantly impair the secretion of any of the analyzed cytokines. This trend was confirmed for the secretion of IL-4, IL-5 and IL-6. The amount of IL-1, IL-10 and TNFα was below detection level even in untreated samples; thus the effect of dasatinib on the secretion of these cytokines could not be evaluated. The cytokine levels produced by CD19-CAR/CD28 T-cells were equally influenced by the administration of dasatinib, and were completely blocked in the presence of ≥ 25 nM (Figure 13c).

## 4.3 The genetic consequences of dasatinib-exposure

So far, we demonstrated that dasatinib controls effector functions of resting and activated CAR T-cells independent of specificity, type of co-stimulation and T-cell origin. To further assess transferability, we sought to elucidate the molecular mechanism behind the observed blockade of function. As it is known that similar pathways are involved in the signaling following the activation of the endogenous T-cell receptor and CARs using CD3zeta as the major signaling domain, and because dasatinib can interact with Lck in non-modified T-cells, we initially analyzed the phosphorylation status of key signaling proteins that are directly affected by Lck. In a second step, we analyzed the consequences of dasatinib on a genetic level.

### 4.3.1 Dasatinib prevents the phosphorylation of key kinases in the CAR signaling cascade

We analyzed the phosphorylation state of the CAR-CD3zeta signaling domain and the downstream kinases Zap70 at tyrosine 319 (Y319) and Src family at tyrosine 416 (Y416), which are known key members of the signaling cascade following T-cell activation. We stimulated CAR T-cells with $CD19^+$ RCH-ACV (E:T 5:1) for 30 minutes, and indeed observed phosphorylation of all three kinases in untreated T-cells. In the presence of 100 nM dasatinib, phosphorylation of kinases was inhibited (Figure 14a). Quantitative analysis (Figure 14b) revealed remaining phosphorylation levels of 13 % (CD3zeta), 22 % (Lck) and 12 % (Zap70), respectively, when compared to untreated T-cells.

### 4.3.2 Dasatinib blocks the induction of NFAT

#### 4.3.2.1 Generation of an activation dependent reporter system

To determine whether control of CAR T-cells by dasatinib extends to the prevented induction of the key transcription factor NFAT, we employed a reporter system that enables detecting the activation status of T-cells based on GFP-expression. We designed a gene cassette encoding GFP under the control NFAT-RE (Figure 5). In this reporter, NFAT is transported into the nucleus upon T-cell stimulation and thus can bind to NFAT-RE. Thereby it activates the minimal promotor (minP), which then drives the expression of GFP, enabling an easy readout of activation evaluable by flow cytometry. Her2t was included as a specific transduction marker and for enrichment of transduced T-cells by bead based magnetic sorting. To ensure that this protein would not provide any signals, the signaling domain was truncated, leaving only the

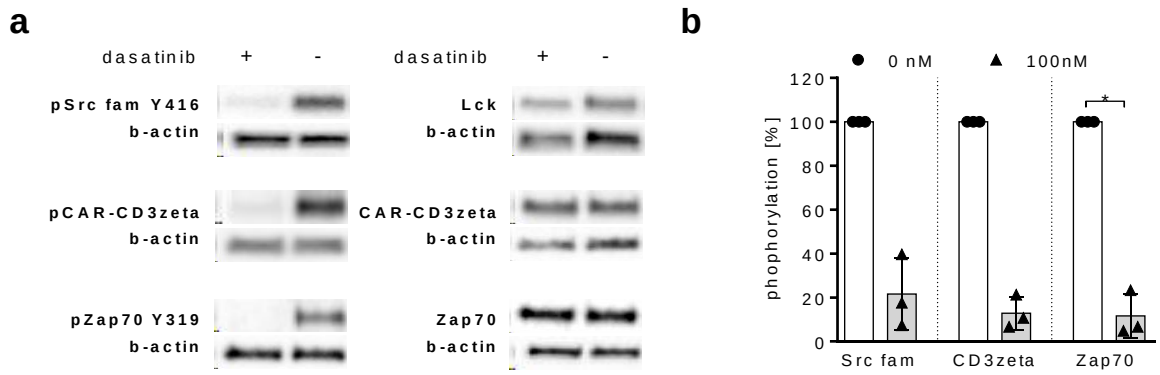


**Figure 14: Dasatinib prevents the phosphorylation of key kinases.**
For western blot analysis, CD19-CAR/4-1BB T-cells were stimulated with $CD19^+$ RCH-ACV and treated with 100 nM dasatinib (+) or not (-). (a) Phosphorylation of CAR-CD3zeta, Lck (Src family) and Zap70; data shown from one representative experiment. (b) Quantitative analysis of western blot data obtained in n = 3 experiments, normalized to total protein expression. Data are mean values + SD analyzed by one-way ANOVA (Kruskal-Wallis test) with * $P \leq 0.05$).

membrane-integrating part and the extracellular domain to be displayed on the cell surface. Her2t was attached to the cassette using a T2A ribosomal skip sequence. Thus, the transduction marker will split from the GFP during translation and will be integrated into the cell membrane as an independent protein.

We tested two variants of GFP for the generation of a reporter system. First, we used a wildtype GFP (GFP(wt)) with an expression half-life of approximately 24 hours. To get a more direct readout of activation, we additionally generated a reporter cassette including a destabilized variant of GFP with an expression half-life of four hours (GFP(d4)). $CD8^+$ and $CD4^+$ T-cells were isolated as described in the methods and transfected with the two different lentiviral constructs at the same time. As the amount of T-cells that successfully incorporated both genes was low (Figure 15), two enrichment steps were performed to generate a T-cell product with at least 50 % of cells expressing both genes, which will further be referred to as ‘double positive’ T-cells (Figure 16).

### 4.3.2.2 Unspecific stimulation of T-cells induces GFP expression

To test if the NFAT/GFP cassette was functional, we stimulated NFAT/GFP containing CAR T-cells with PMA/ionomycin and determined GFP expression level by flow cytometry. With-

out stimulation, expression of GFP was low and comparable to untransduced T-cells. Stimulation

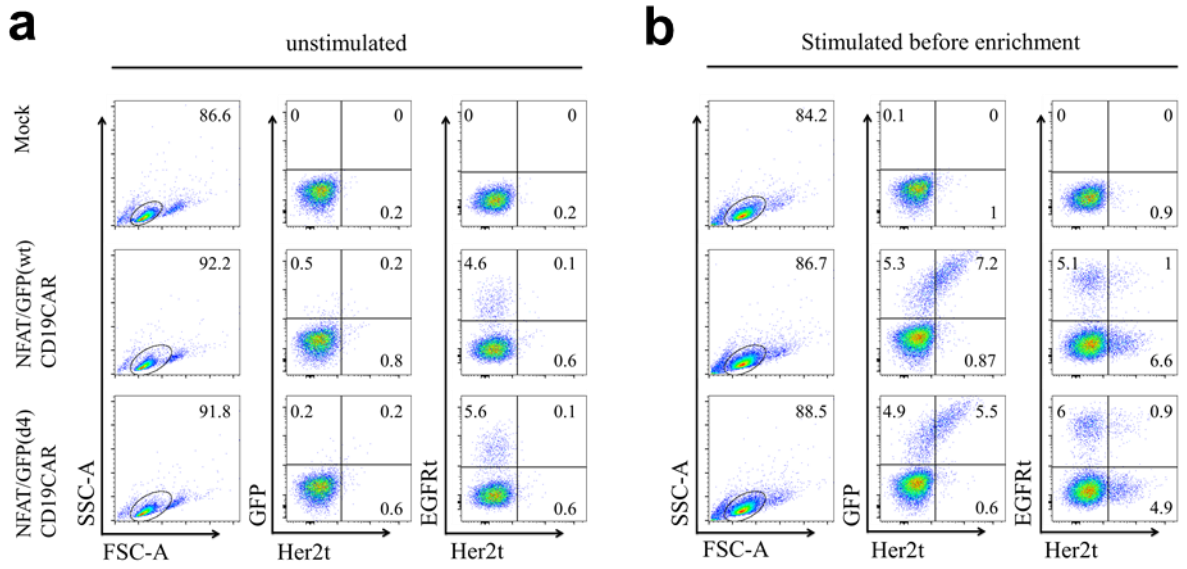


**Figure 15: Transgene expression after double-transduction of T-cells.**

Expression of the reporter gene cassette (GFP, Her2t) and the CAR (tEGFR) in $CD8^+$ T-cells (a) before and (b) after 24 hours of stimulation with PMA/ionomycin. Numbers indicate percentage of parental gate. Transduction efficancy is shown a reporter gene encompassing a GFP with a half-life of approx. 24 hours (NFAT/GFP(wt)) and a variant with half-life of four hours (NFAT/GFP(d4)).

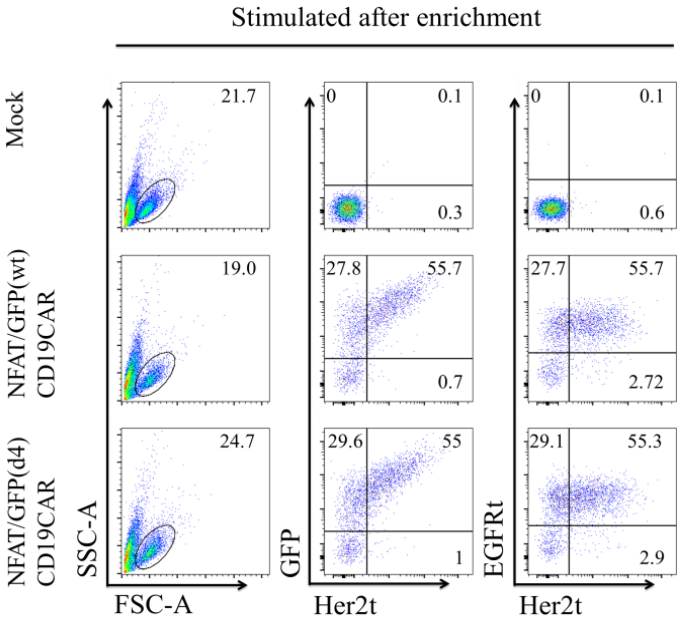


**Figure 16: Transgene expression after enrichment and stimulation of T-cells.**

Expression of the reporter gene cassette (GFP, Her2t) and the CAR (tEGFR) after enrichment for Her2t and EGFRt and expansion. $CD8^+$ T-cells were stimulated with PMA/Ionomycin 24 hours prior to analysis. Numbers indicate percentage of parental gate. Purity is shown for T-cells expressing a

reporter gene encompassing a GFP with a half-life of approximately 24 hours (NFAT/GFP(wt)) and a variant with half-life of four hours (NFAT/GFP(d4)).

of double positive T-cells induced high expression of GFP in both $CD8^+$ **(**Figure 17a) and $CD4^+$ T-cells on day 1 (Figure 17b), that further increased until day 2 after stimulation, when expression was highest, and declined towards day 3. No difference was detected in the GFP expression of GFP(wt) and GFP(d4).

### 4.3.2.3 GFP expression following CAR specific stimulation of T-cells

We went on to characterize the induction and development of GFP expression after antigen dependent stimulation. Thus, irradiated $CD19^+$ Raji or $CD19^-$ K562 (E:T 5:1) were added to T-cells once or every 24 hours, and the GFP expression was measured by flow cytometry once daily. The activation of T-cells was highly antigen-specific, as no GFP-upregulation was observed neither in $CD8^+$ nor $CD4^+$ cells when co-cultures with antigen lacking target cells. Following a single stimulation, $CD8^+$ T-cells with GFP(wt) highly expressed GFP on day 1, and expression subsequently declined (Figure 18a). Repeated stimulation of T-cells led to permanent activation of T-cells, as seen in a stable GFP expression over time, and kinetics were similar in $CD8^+$ and $CD4^+$ T-cells (Figure 18a, b). As there was no difference in the GFP expression of wt and d4 (Figure 18c, d) we decided continue with the destabilized GFP(d4) variant for subsequent experiments.

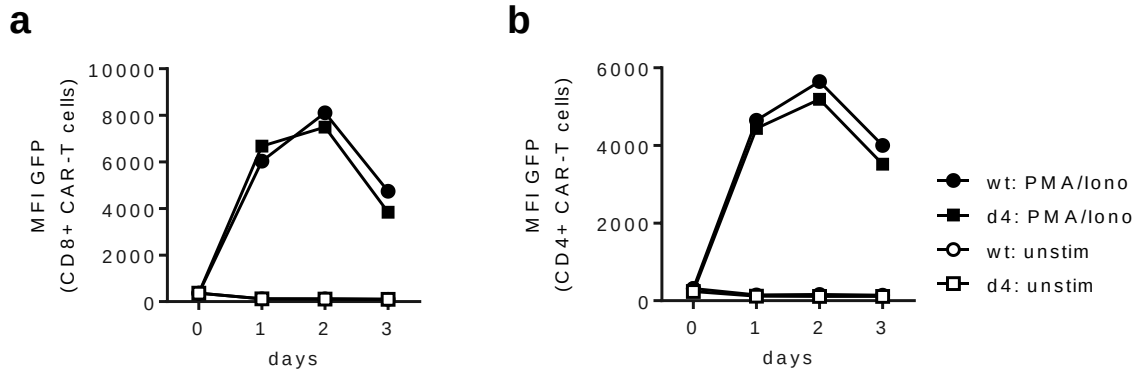


**Figure 17: Antigen independent stimulation of NFAT-reporter CAR T-cells.**

Expression of reporter gene was detected in (a) $CD8^+$ and (b) $CD4^+$ CAR T-cells once per day by flow cytometry and is depicted as mean fluorescence intensity (MFI). MFI is shown for CAR T-cells encompassing a reporter gene with GFP(wt) with a half-life of approximately 24 hours or a variant

with a half-life of four hours (GFP(d4)). Cells were stimulated either with PMA/ionomycin on day 0, or left untreated. Data are mean values obtained in two independent experiments.

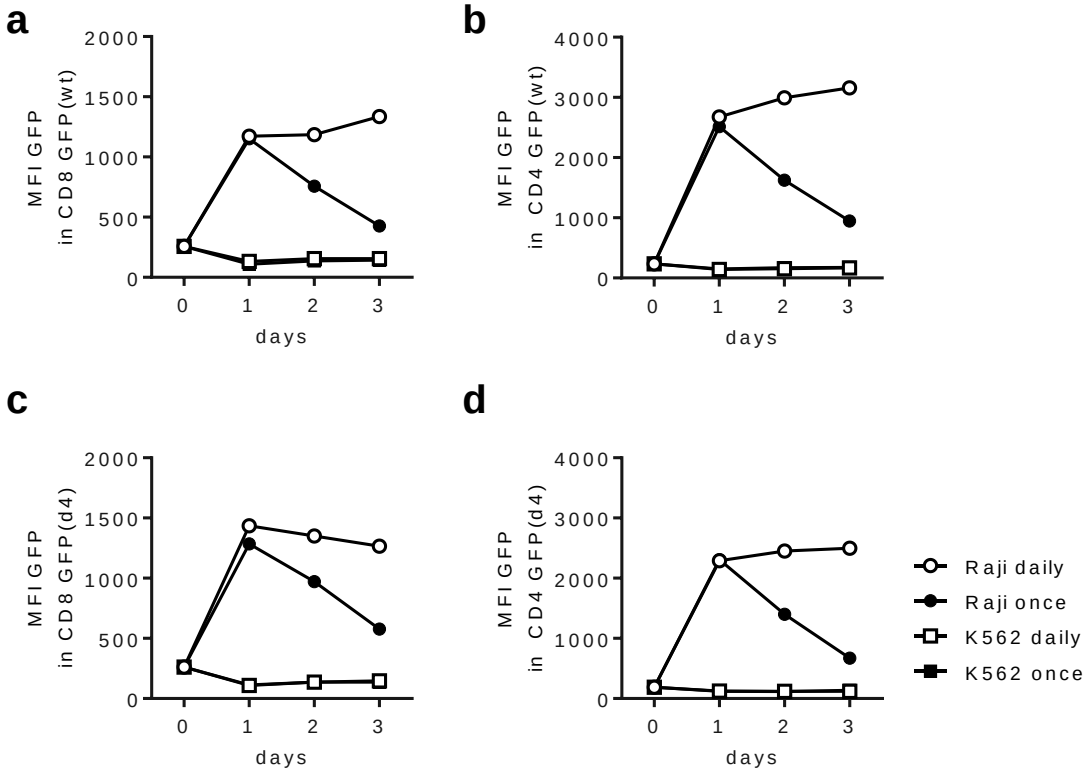


**Figure 18: Antigen dependent induction of GFP-expression in NFAT-reporter CAR T-cells.** Expression of reporter gene was detected in (a, b) $CD8^+$ and (c, d) $CD4^+$ CAR T-cells once per day by flow cytometry and is depicted as mean fluorescence intensity (MFI). MFI is shown for CAR T-cells encompassing a reporter gene with (a, c) GFP(wt) or (b, d) GFP(d4). T-cells were co-cultures with irradiated $CD19^+$ Raji cells or $CD19^-$ K562 once on day 0 or once daily on day 0, 1 and 2. Data are mean values obtained in three independent experiments.

### 4.3.2.4 Blockade of CAR T-cell activation by dasatinib

We sought to monitor T-cell activation in the presence of dasatinib by analyzing GFP expression in NFAT-reporter CAR T-cells. Treatment of $CD8^+$ CAR T-cells with 100 nM dasatinib led to significant inhibition of GFP-expression 24 hours after stimulation with the $CD19^+$ Raji cell line, with a GFP-MFI equal to non-stimulated T-cells and significantly reduced compared to stimulated untreated CAR T-cells (Figure 19a). When dasatinib and stimulation was repeated every 24 hours, the GFP expression remained low (Figure 19b). This block of NFAT signaling could also be observed in $CD4^+$ T-cells (Figure 19c, d). These results suggest that dasatinib blocks the effector functions of CAR T-cells by inhibiting early phosphorylation

events of key signaling kinases, which prevents the induction of transcription factors such as NFAT.

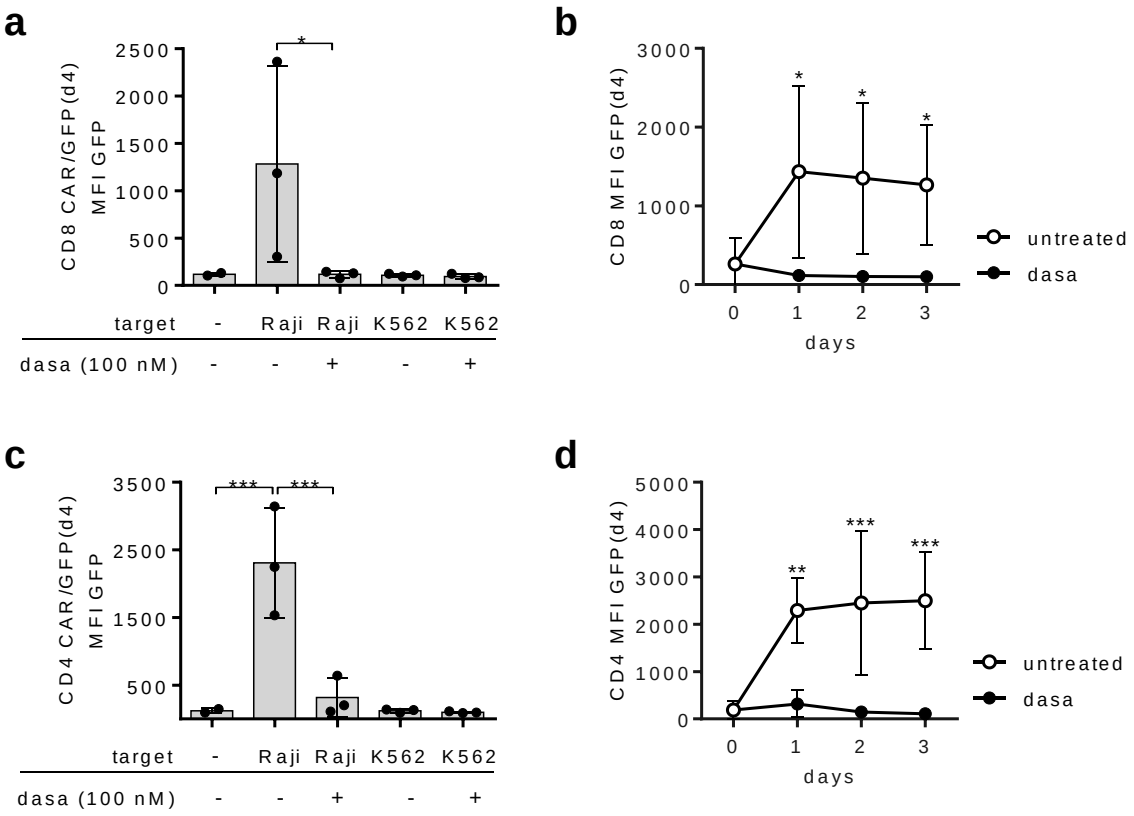


**Figure 19: Dasatinib inhibits NFAT dependent signaling.**

Induction of NFAT displayed by GFP-expression (MFI) in **(a, b)** $CD8^+$ and **(c, d)** $CD4^+$ CAR T-cells during treatment with 100 nM or untreated. T-cells were transduced with an NFAT/GFP(d4) reporter gene and stimulated with $CD19^+$ Raji or $CD19^-$ K562 every 24 hours. (a, c) Reporter gene expression after 24 hours. (b, d) Reporter gene expression over time, analysed once daily. (a-d) Data are mean values ± SD. obtained in three independent experiments analyzed by (a, c) one-way ANOVA (Kruskal-Wallis test) or (b, d) two-way ANOVA with * $P \leq 0.05$, ** $P \leq 0.005$, *** $P \leq 0.0005$)

### 4.3.3 Dasatinib prevents subsequent induction of NFAT in activated T-cells

We employed the NFAT/GFP(d4) reporter system to interrogate the effects of dasatinib on activated CAR T-cells on a signaling level and to evaluate if dasatinib-mediated inhibition could be sustained over time and during sequential antigen encounter. Thus, we co-cultured NFAT-reporter CAR T-cells with Raji cells and treated them with dasatinib one hour after beginning of co-culture. Subsequently, target cells and 100 nM dasatinib were added simultaneously every 24 hours. In this stimulation/inhibition setting, T-cells were slightly activated

on day 1, and GFP levels decrease until day 3, indicating that further antigen specific stimulation was prevented by dasatinib and cells were maintained in a functional OFF state. This observation was confirmed in $CD8^+$ and $CD4^+$ T-cells (Figure 20a, b).

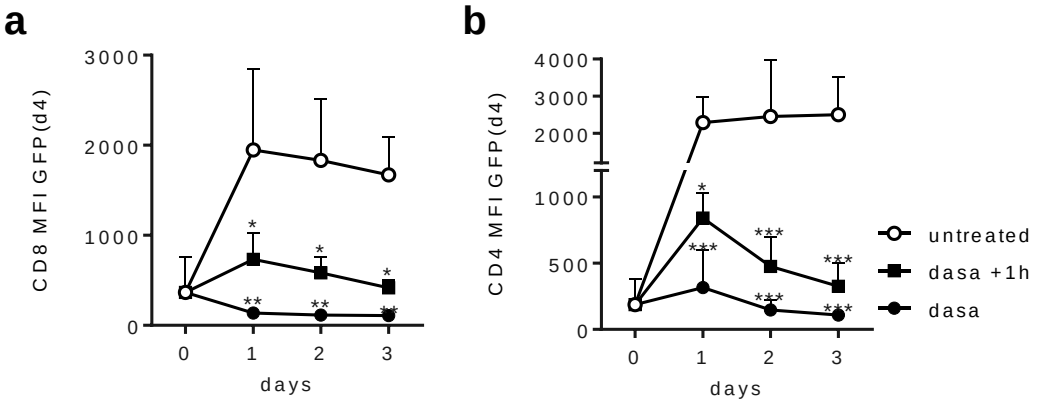


**Figure 20: Sequential stimulation of CAR T-cells in the presence of dasatinib.**
CD19-CAR/4-1BB T-cells expressing an NFAT/GFP(d4) reporter gene were stimulated with $CD19^+$ Raji lymphoma cells every 24 hours. Dasatinib was added either at assay start (black circles) or one hour after assay start (dasa +1h, grey circles), and was then added to the medium every 24 hours. Untreated CAR T-cells are included for comparison. The diagrams show reporter gene expression obtained in (a) $CD8^+$ and (b) $CD4^+$ CAR T-cells. Data shown are mean values + SD obtained in (a) n = 2 and (b) n = 3 experiments with T-cells from different healthy donors. * $P \leq 0.05$, ** $P \leq 0.005$, *** $P \leq 0.0005$ by two-way ANOVA.

## 4.4 Comparison of control exerted by dasatinib and other safety strategies

In order to evaluate how dasatinib would fit into the range of existing safe strategies, we compared the block of function mediated by dasatinib to currently available safety tools. In clinical trials, steroids are used in the treatment of severe side effects caused by CAR T-cells. We therefore investigated the effect of dexamethasone and dasatinib on CAR-T-cell function side-by-side. As in some cases transient inhibition of effector functions might not be sufficient, we analyzed whether dasatinib treated CAR T-cells would still be targetable by eliminating safety tools such as iCasp9.

### 4.4.1 Comparison of dexamethasone and dasatinib on the function of CAR T-cells

Overall, the ability of dexamethasone to inhibit CAR-T-cell function was inferior to dasatinib. Simultaneous treatment with dexamethasone and stimulation of CD19-CAR T-cells with target cells did not show inhibitory effects on specific lysis of target expressing tumor cells (Figure 21a, left diagram). As steroids mostly function on a genomic level, we changed the treatment schedule and analyzed CAR T-cell performance after 24 hours of pretreatment (Figure 21a, right diagram). Significant reduction of specific lysis by CAR T-cells pretreated with 100 µM dexamethasone was observed with a mean lysis of 53 % at t = 12 hours when compared to untreated T-cells; however, complete blockade as detected during the treatment with 100 nM dasatinib could not be achieved in any of the treatment schedules. Neither simultaneous treatment nor pre-treatment of CAR T-cells with dexamethasone showed significant reduction of IFNγ (Figure 21b, left diagram), whereas blockade of IL-2 secretion was observed under all treatment schedules and dosages (Figure 21b, right diagram). This was confirmed by reduced proliferation in contrast to untreated T-cells under all treatment conditions, as shown for one representative experiment (Figure 21c, left diagram) and quantitative analysis of three independent donors (Figure 21c, right diagram), respectively. All in all these data show that administration of dexamethasone to CAR T-cells cannot mediate a complete blockade of CAR T-cell function as observed by treatment of CAR T-cells with dasatinib.

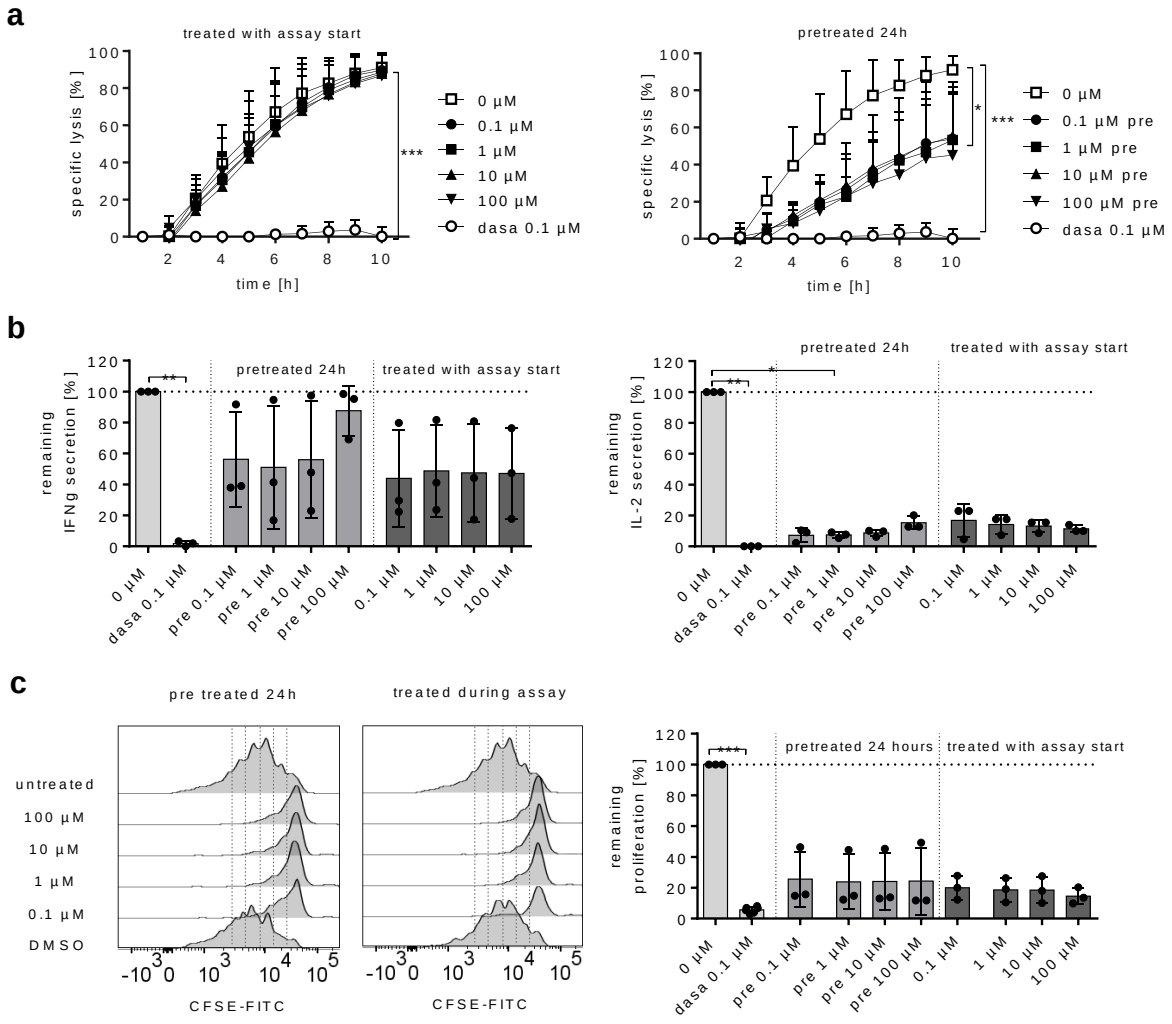


**Figure 21: Dasatinib exerts superior control over CAR T-cells than dexamethasone**.

Dexamethasone was added either at the time of assay start or 24 hours prior to assay start (pretreated). T-cells treated with 100 nM dasatinib at assay start were included for comparison. (a) Specific lysis of K562/CD19 target cells by CD19-CAR T-cells (E:T 5:1) is displayed over time with simultaneous treatment (left diagram) or 24-hour pre-treatment (right diagram). (b) Remaining IFNγ (left diagram) and IL-2 (right diagram) secretion mediated by CAR T-cells upon stimulation (E:T 4:1), normalized to the amount of cytokines released by untreated CAR T-cells. (c) The remaining proliferation, measured in a CFSE dye dilution assay, was calculated based on the proliferation index and normalized to untreated CAR T-cells. Data of one representative experiment (left diagram) and quantification of n = 3 independent experiments (right diagram). (a-c) Shown are the mean values ± SD of n = 3 independent experiments, analyzed by two-way ANOVA (a) or one-way ANOVA (Kruskal-Wallis test, b, c), with * $P \leq 0.05$, ** $P \leq 0.005$, *** $P \leq 0.0005$.

### 4.4.2 Dasatinib-induced control is compatible with iCasp mediated T-cell depletion

In some clinical cases, pausing CAR T-cells may not be sufficient to save a patient, but elimination of CAR T-cells will be necessary. One tool that has been show to efficiently eliminate T-cells *in vivo* is iCasp9 that can be triggered by the administration of an inducing drug *(84)*, however, clinical proof-of-concept is still pending. We therefore generated CAR T-cells co-expressing an iCasp9 suicide gene to evaluate if CAR T-cells that are blocked with dasatinib would still be susceptible to the induction of apoptosis by iCasp9. T-cells were thus double transduced to express an iCasp9 cassette as well as the CAR. These cells were cultured in medium supplemented with 50 U/ml IL-2, either in the absence or in the presence of 100 nM dasatinib, and in the absence or presence of 10 nM AP20187, which is the iCasp9 inducer drug. After 24 hours, cells were labeled with anti-CD3 mAb and analyzed by flow cytometry for the presence of iCasp9$^+$ T-cells. The data show that dasatinib itself does not induce apoptosis in resting CAR T-cells. Additionally, the induction of iCasp9 and following apoptosis of T-cells is not affected by dasatinib (Figure 22).

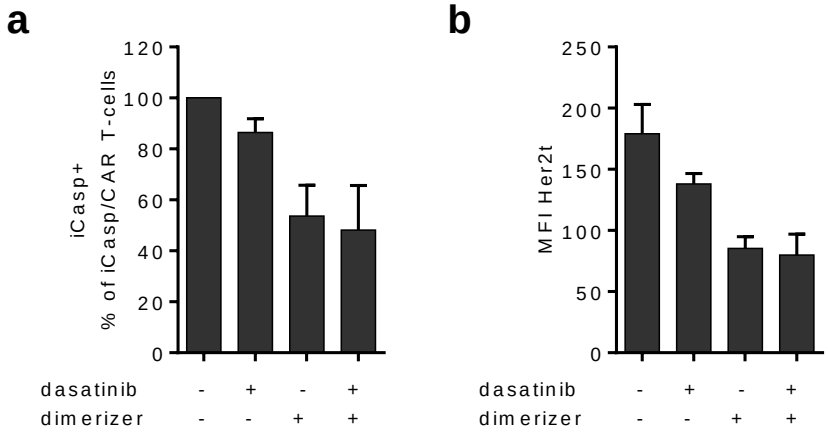


**Figure 22: Induction of iCasp9 in the presence of dasatinib.**

CD8$^+$ CD19-CAR/4-1BB T-cells co-expressing iCasp9 T-cells were cultured in medium supplemented with 50 U/ml IL-2, in the absence (-) or presence (+) of 100 nM dasatinib, and in the absence (-) or presence (+) of iCasp9 dimerizer. After 24 hours, cells were labeled with anti-CD3 mAb and analyzed by flow cytometry for the presence of iCasp$^+$ T-cells. (a) Bar diagram shows surival after treatment normaluted to untreated/uninduced T-cells (-/-). (b) Expression of Her2t, which is the transduction marker encoded with the iCasp9-transgene.

In the presence of dimerizer (dasatinib /dimerizer +), the percentage of iCasp9$^{+}$ cells was reduced to 45 %, which was comparable to the percentage of iCasp9$^{+}$ in the presence of 100 nM dasatinib (36 %) and dimerizer (dasatinib +/dimerizer +). In aggregate, these data show that CAR T-cells that are blocked by dasatinib are susceptible to subsequent elimination with the iCasp9 suicide gene. However, these data also suggest that, independent of treatment with dasatinib, eradication of CAR T-cells by iCasp9 is not sufficient, as residual T-cells remain that cannot be eliminated.

## 4.5 The blockade of CAR T-cell function is reversible

To exclude that the reduced effector functions of resting and activated CAR T-cells were a result of T-cells undergoing apoptosis, we performed 7-AAD/Annexin V staining of co-cultures with target cells (Figure 23). Surprisingly, a high percentage of untreated CAR T-cells entered an early apoptotic state during the first 24 hours of stimulation with K562/CD19, whereas dasatinib treated CAR T-cells showed a lower apoptosis-rate compared to untreated T-cells. However, the rate of apoptosis was still higher in T-cells treated with dasatinib when compared to unstimulated T-cells. We therefore conclude that instead of inducing apoptosis, dasatinib at least partially protects CAR T-cells against the induction of activation induced cell death.

Encouraged by this observation, we sought to evaluate if the observed blockade of T-cell function would be reversible. Thus we assessed the reversibility of CAR T-cell blockade after two hours, 24 hours and seven days of inhibition. After two hours in the presence of dasatinib , thus in a function OFF state, treated CAR T-cells regained functionality within two hours after removing dasatinib and achieved similar specific lysis as previously untreated CAR T-cells four hours after washing (Figure 24a). This reversibility was additionally confirmed for a CAR containing a CD28 costimulatory moiety (Figure 24b).

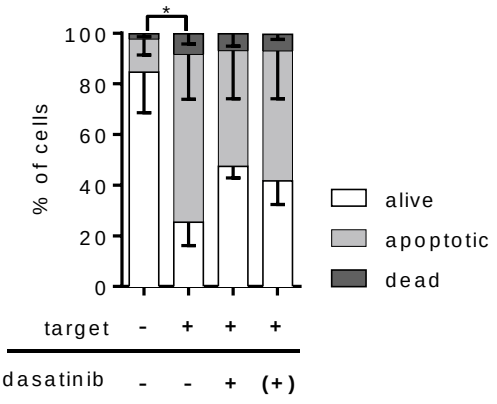


**Figure 23: Dasatinib does not induce apoptosis in stimulated CAR T-cells.**

Viability of $CD3^+$ CAR T-cells with and without stimulation (target -/+), analyzed after 24 hours by staining with 7-AAD/Annexin V. Dasatinib was added at assay set up (+) or one hour after assay set up ((+)). $7\text{-}AAD^-/Annexin\ V^-$ T-cells were considered to be alive; $7\text{-}AAD^-/Annexin\text{-}V^+$ T-cells were considered to be apoptotic; $7\text{-}AAD^+/Annexin\ V^+$ T-cells were considered to be dead. * $P \leq 0.05$, ** $P \leq 0.005$, *** $P \leq 0.000$ by one-way ANOVA (Kruskal Wallis test).

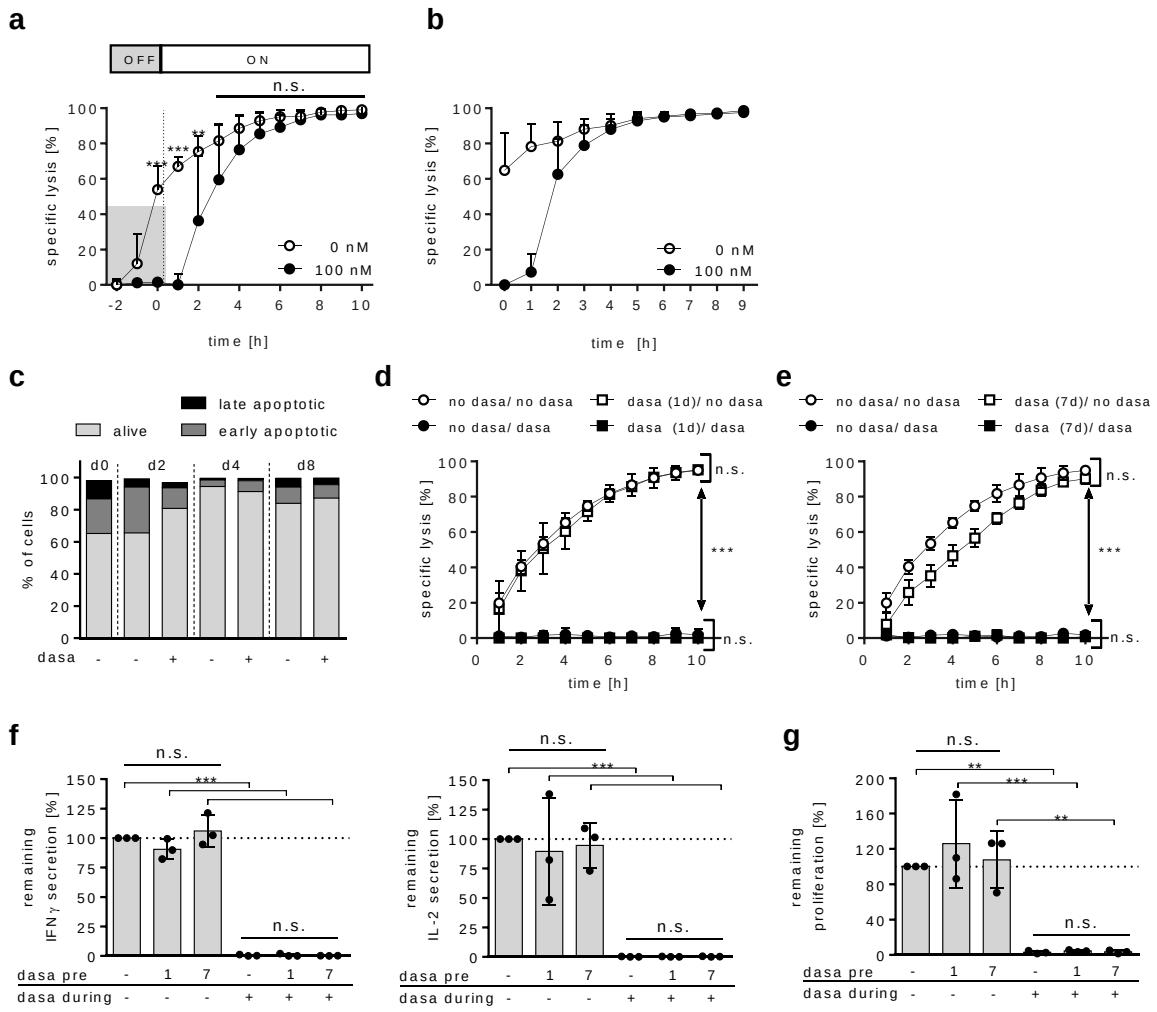


**Figure 24: Removal of dasatinib releases CAR T-cells from OFF to ON upon antigen encounter.** Cytolytic activity of (a) CD19-CAR/4-1BB and (b) CD19-CAR/CD28 T-cells against K562/CD19. Dasatinib (100 nM) was present in the first two hours after assay setup (function OFF), and was removed at t = 0 (function ON). Cytolytic activity without dasatinib (0 nM) is shown for comparison. (c) CD19-CAR/4-1BB T-cells were treated with 100 nM dasatinib once daily over 8 days and were assassed for surival every second day by staining with 7-AAD/Annexin V (n = 1). (d-g) T-cells were treated for one or seven days (fresh dasatinib added once daily) with 100 nM dasatinib. (d, e) Dasatinib was removed and the cytolytic capacity of CAR T-cells was analyzed (dasa/no dasa, i.e. dasatinib pretreatment/no dasatinib in assay). For comparison, lysis by T-cells in the presence of dasatinib (dasa/dasa), without any treatment (no dasa/no dasa) and without dasatinib pretreatment (no dasa/dasa) was evaluated. (d, e) Levels of IFNγ (d) and IL-2 (e) after one or seven days of treatment, normalized to the amount of cytokines produced by untreated T-cells (-). Dasatinib (100 nM) was added at assay setup in the indicated groups (dasa during +). (f) The proliferation was calculated based on the cell proliferation-index and normalized to proliferation of untreated CAR T-cells. Data shown are mean values ± SD obtained in n = 3 experiments with T-cells from independent donors with * $P \leq 0.05$, ** $P \leq 0.005$, *** $P \leq 0.0005$ by two-way (a, d, e) or one-way ANOVA (f, g).

We then examined the effects of short (one day) and long-term (seven days) exposure towards dasatinib on the ability of CAR T-cells to regain their effector functions. Importantly, confirming the observation that dasatinib does not reduce T-cell viability during short exposure, long-term treatment did not induce apoptosis in T-cells (Figure 24c). Even after long-term exposure to dasatinib, CAR-T-cell instantly re-ignited their effector functions after removal of dasatinib and subsequent stimulation, as evidenced by specific high-level cytolytic activity, IFNγ and IL-2 secretion and productive proliferation, which were equivalent to CAR T-cells that had never been exposed to dasatinib (Figure 24d-g). Furthermore, none of the treatment conditions altered the sensitivity of CAR T-cells towards dasatinib, as re-exposure towards dasatinib was equally effective in both treatment conditions (Figure 24d-g). Taken together, the data show that inhibition of CAR T-cells is instantaneously and completely reversible. Seven days of consecutive treatment with dasatinib did not influence subsequent performance of T-cells regarding cytotoxicity, cytokine secretion and proliferation upon target dependent stimulation. Importantly, no desensitization towards dasatinib was observed.

So far, we demonstrated that dasatinib is a suitable candidate as a pharmaceutical safety switch for CAR T-cells *in vitro*. We have shown that by preventing the phosphorylation of key kinases during early signaling events, the induction of transcription factors such as NFAT is hampered and thus, CAR T-cell effector functions are controlled. Moreover, we have described the kinetics of inhibition and re-activation after withdrawal and antigen encounter. Thus, we continued to perform proof-of-concept *in vivo*.

## 4.6 Dasatinib is able to control CAR T-cell activation *in vivo*

### 4.6.1 Switching CAR T-cell function OFF with dasatinib *in vivo*

To obtain proof-of-concept of dasatinib as a reversible, pharmacologic OFF switch for CAR T-cells *in vivo*, we employed a lymphoma xenograft model in immunodeficient NSG mice (Figure 25a). Mice were inoculated with firefly-luciferase_GFP-expressing Raji lymphoma cells on day 0 and received CD19-CAR modified or control T-cells on day 7. All T-cells also expressed the NFAT/GFP reporter gene to allow rapid read-outs of their activation state by flow cytometry. In each cohort, a subgroup of mice received six dosages of each 0.2 mg dasatinib to create a function OFF phase immediately after T-cell transfer between day 7 and day 8. Thereafter, dasatinib administration was discontinued and T-cells were allowed to enter a function ON phase until day 10 (Figure 25a).

Analysis of peripheral blood, bone marrow and spleen on day 8 demonstrated that dasatinib did not compromise CAR T-cell engraftment, as the frequency of T-cells in dasatinib-treated and untreated mice was equivalent (Figure 25b). Repeat analysis on day 10 showed that dasatinib had effectively controlled CAR T-cell proliferation during the OFF phase, as the frequency of CAR T-cells in dasatinib-treated mice was lower compared to untreated mice (Figure 25c). These data are supported by lower levels of NFAT/GFP reporter gene expression in CAR T-cells and control T-cells that were obtained from dasatinib-treated and untreated mice (Figure 25d).

Next, we analyzed lymphoma progression and regression and focused on the treatment group that received CAR T-cells and dasatinib (Figure 25e). During the initial OFF phase, i.e. in the presence of dasatinib between day 7 and day 8 after T-cell transfer (left diagram), there was rapid lymphoma progression. In contrast, we observed rapid lymphoma regression during the ON phase, i.e. once dasatinib had been discontinued (right diagram). Lymphoma progression in this group during the OFF phase was faster compared to mice that received CAR T-cells without dasatinib, indicating that dasatinib inhibited CAR T-cell function *in vivo*. Importantly, once dasatinib had been discontinued, CAR T-cells ignited their function and conferred a potent anti-lymphoma effect, demonstrating that the function OFF phase had been reversed.

### 4.6.2 Switching CAR T-cells OFF after infusion prevents cytokine release

To further characterize dasatinib-mediated control of CAR T-cells *in vivo*, we evalated the serum cytokine levels during OFF and ON phase in mice that had been treated with CAR T-cells. During the OFF phase, treatment with dasatinib prevented the production of cytokines by CAR T-cells. Serum levels of GM-CSF, IFNγ, TNFα, IL-2, IL-5 and IL-6 were significantly lower in mice that had received CAR T-cells and dasatinib compared to mice that had received CAR T-cells alone, and similar to mice that had received control T-cells (Figure 26).

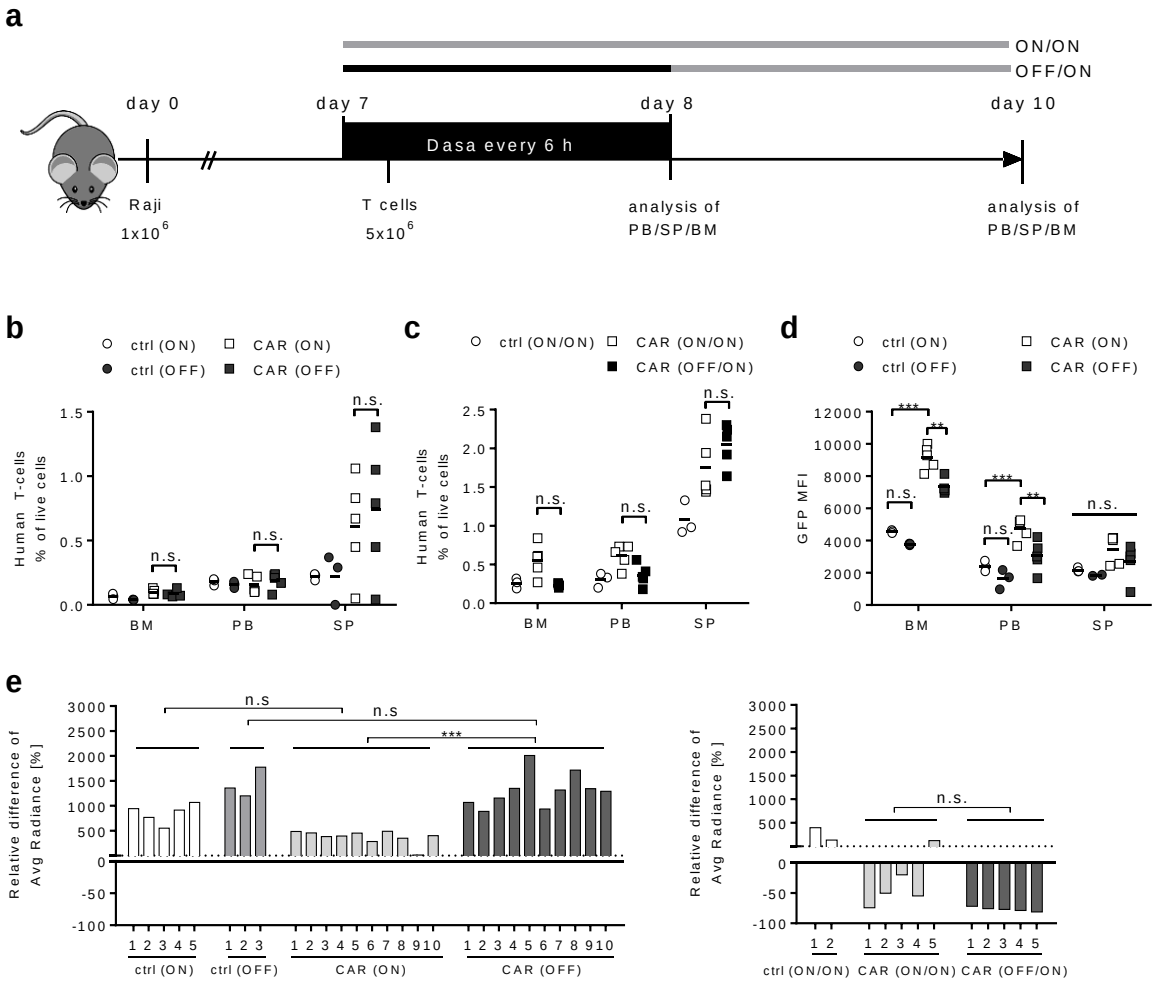


**Figure 25: Dasatinib acts as a reversible OFF switch for CAR T-cells *in vivo*.**

(a) Treatment schedule and experimental setup. NSG mice received either CD19-CAR/4-1BB T-cells or untransduced T-cells (ctrl). Dasatinib was administered to indicated groups from day 7 to day 8 to create a function OFF phase. Afterwards, dasatinib was discontinued to induce a function ON phase. Mice were analyzed for (b) engraftment of T-cells on day 8, and (c) for proliferation of T-cells on day 10. Diagrams show the percentage of human T-cells gated on living cells and defined as $CD19^{-}$, $CD3^{high}$ and $CD45^{high}$. (d) The activation level of CAR T-cells in the function OFF state (day 8) is displayed as the MFI of NFAT dependent GFP expression. (e) Diagrams show lymphoma progression/regression during OFF (day 6 to day 8) and ON phase (day 8 to day 10) in individual mice of each treatment group. The change in tumor burden was calculated from ventral bioluminscence

imaging (BLI) signal. Data shown are mean and individual values analyzed by two-way ANOVA (b-d) or one-way ANOVA (Kruskal-Wallis test) (e) with * $P \leq 0.05$, ** $P \leq 0.005$, *** $P \leq 0.0005$.

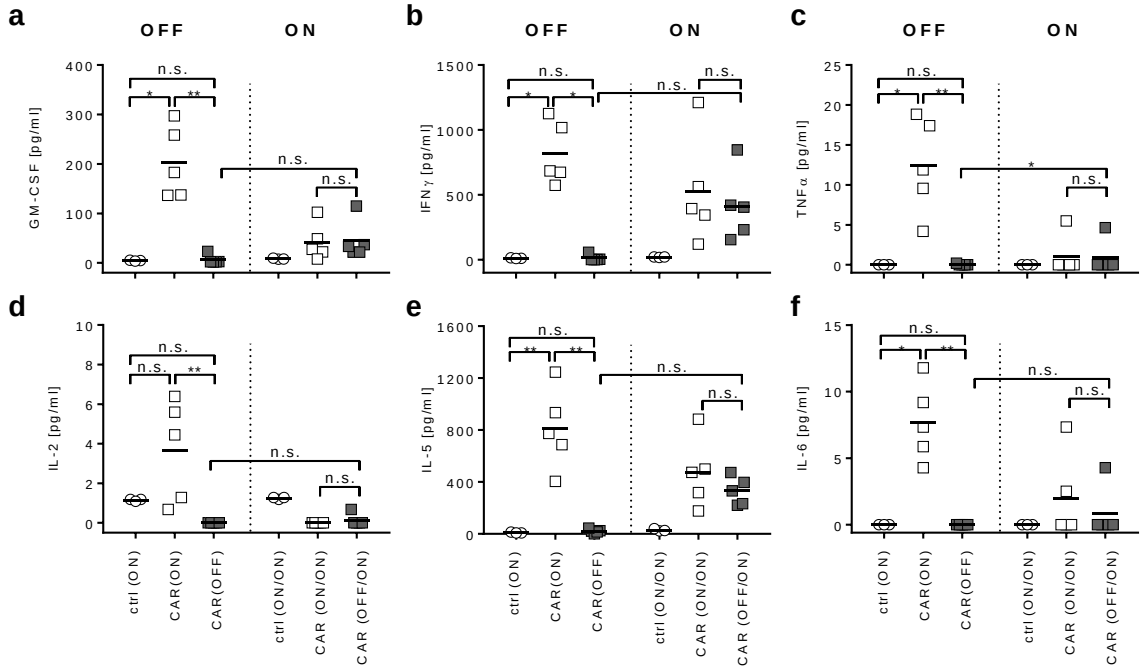


**Figure 26: Placing CAR T-cell function into OFF after infusion prevents cytokine release.**
NSG mice were inoculated with Raji/ffluc_GFP tumor cells. Mice received either CD19-CAR/4-1BB T-cells (CAR) or untransduced T-cells (ctrl). Dasatinib was administered to indicated groups from day 7 to day 8 to create a function OFF phase. Afterwards, dasatinib was discontinued to induce a function ON phase. Diagrams show serum levels of GM-CSF (a), IFNγ (b), TNFα (c), IL-2 (d), IL-5 (e) and IL-6 (f) during the OFF and ON phase. Data shown are mean and individual values analyzed by one-way ANOVA (Kruskal-Wallis test) with * $P \leq 0.05$, ** $P \leq 0.005$.

Consistent with our previous data showing that CAR T-cells re-ignite their function after discontinuation of dasatinib, we detected elevated serum cytokine levels during the ON phase. Notably, the absolute levels of serum cytokines were lower in mice that had gone through an initial OFF phase compared to mice that had not. In summary, our analysis of serum cytokines shows that dasatinib can completely inhibit cytokine secretion from CAR T-cells and suggest that an initial OFF phase immediately after CAR T-cell transfer can lower peak cytokine levels to prevent CRS.

### 4.6.3 Long-term inhibition of CAR T-cells *in vivo*

We evaluated whether dasatinib-mediated inhibition could be maintained over several days. Therefore, we engaged osmotic pumps filled with dasatinib. Due to their special design, these pumps permanently release small amounts of a preloaded drug to the surrounding tissue, which is taken up and distributed to the whole body with the blood flow. In a pre-experiment, we determined the optimal set up and loading of the pump. By filling the pump with 3.75 mg dasatinib dissolved in DMSO/PEG (1:1) mice reached a serum level of 43 µg/L, which equals a concentration of 86 nM. Thus, immunodeficient NSG mice were inoculated with fire-fly-luciferase_GFP-expressing Raji lymphoma cells on day 0 and pumps filled with dasatinib or DMSO/PEG only were implanted on day 7. Taken the priming phase of 20 hours into account, dasatinib was released until day 13, and pumps were explanted on day 14. Mice received $5x10^6$ T-cells composed of $CD8^+$ and $CD4^+$ T-cells at a ratio of 1:1 by i.v. injection on day 8. Imaging was performed regularly to evaluate the development of the tumor burden. Blood was drawn on day 10, 12, 17 and 21 to analyze serum cytokines.

The tumor grew rapidly in mice of the control cohort (ctrl +DMSO), and animals had to be sacrificed due to tumor burden on day 21 (Figure 27a-c). In mice recieving CAR T-cells and control pumps, the tumor increased until day 10, but afterwards started to decrease in three out of four mice and was not detectable by day 21. The fourth mouse showed delayed anti-tumor response starting on day 12, and relapsed after day 21. In mice recieving CAR T-cells and dasatinib filled pumps, the tumor continued to grow until day 14, thus in the presence of dasatinib, in two out of four mice, and was stable in another one. However, tumor growth was decreased in comparison to mice receiving ctrl T-cells. After dasatinib removal, the tumor burden was reduced in all mice of the CAR/dasa cohort, indicating that T-cells had been partially inhibited in the presence of dasatinib, and regained cytolytic function after dasatinib was not longer provided. In two mice of this cohort, no tumor was detectable by day 21, whereas the other two relapsed and needed to be sacrificed on day 28 and 42 respectively (Figure 27a-c).

Additionally, we analyzed the serum cytokine levels by Luminex analysis (Figure **27**d, f). During dasatinib treatment, which was between day 10 and day 12, the levels of IFNγ, IL-2 and IL-5 were reduced. However, the levels of IL-8 and GM-CSF were similar between dasatinib and control treated cohorts. In contrast, the levels of all tested cytokines were higher in mice that had received dasatinib before when compared to mice that had received CAR T-cells and control pumps on day 17, and levels were similar on day 21. In summary, we were able to achieve partial inhibition of T-cell function by the use of osmotic pumps. Block of function was not observed in all animals, and the level of inhibition varied between individu-

als of the treatment cohorts. Additional serum level analysis revealed a highly variable dasatinib serum level in mice despite equal treatment. Thus, we reason that a serum concentration of dasatinib sufficient to completely block all effector functions was not reached in all mice, leading to the described mixed results.

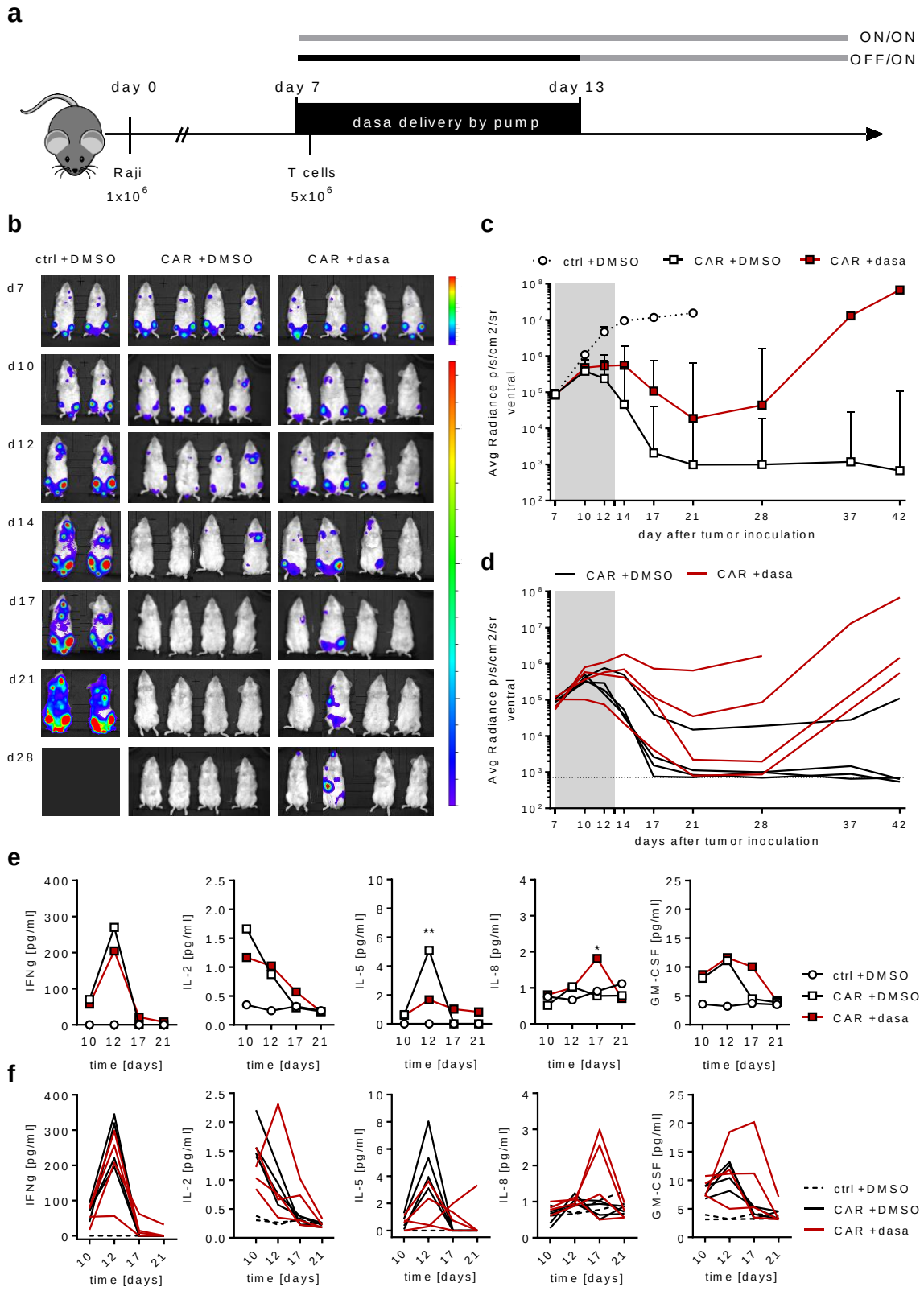

**Figure 27: Long term control of CAR T-cells by dasatinib.**
NSG mice were inoculated with Raji/ffluc_GFP tumor cells on day 0. Mice received either CD19-CAR/4-1BB T-cells (CAR) or untransduced T-cells (ctrl) on day 7. Osmotic pumps containing dasatinib were implanted prior to T-cell administration, releasing dasatinib between day 7 and day 13 to create a function OFF phase. Afterwards, dasatinib was discontinued to induce a function ON phase. **Figure 27** (continued): (a) Luminescence imaging of ffluc Raji tumor cells. Quantification of bioluminescence signal as ventral average radiance, displayed (b) as median of all mice in a referring cohort and (c) signals of individual animals. (d) Serum levels of IFNγ, IL-2, IL-5, IL-8 and GM-CSF were analyzed on indicated days by Luminex analysis. Data shown are mean values analyzed by one-way ANOVA (Kruskal-Wallis test).

### 4.6.4 Dasatinib pauses activated CAR T-cells in a function OFF state *in vivo*

Finally, we wanted to determine whether dasatinib was capable of halting CAR T-cells that were strongly activated and already in the process of conferring their function *in vivo*. In a second set of experiments, we therefore administered dasatinib between day 10 and day 12 after T-cell transfer to create a function ON-OFF-ON sequence (Figure 28a). In the first phase after T-cell transfer (day 7 to day 10), CD19-CAR T-cells commenced exerting their antilymphoma activity and were strongly activated, as demonstrated by BLI (Figure 28b, c) and serum cytokine analysis (function ON) (Figure 28d). In the second phase after T-cell transfer (day 10 to day 12), we administered dasatinib to a subgroup of mice that had received CD19-CAR T-cells. The data show that dasatinib rapidly induced a function OFF state and halted antilymphoma reactivity, as evidenced by increasing BLI signal and decreasing IFNγ in serum from each of the mice in this subgroup. In contrast, the BLI signal did not increase (Figure 28b) and IFNγ remained stable during this phase in mice that had received CD19-CAR T-cells but no dasatinib (Figure 28d). In the third phase (after day 12), administration of dasatinib was discontinued in order to allow CAR T-cells to revert back into their function ON state. Indeed, CAR T-cells rapidly resumed their antilymphoma function as revealed by rapidly decreasing BLI signal and increasing serum IFNγ in each of the mice.

Surprisingly, with longer follow-up, we observed further lymphoma regression and reduction of BLI signal to background levels in the CD19-CAR/dasatinib subgroup that finally achieved a superior response compared to the subgroup of mice that had received CD19-CAR T-cells but no dasatinib (Figure 29a). We thus hypothesized that dasatinib might prevent the induction of exhaustion in T cells. To validate this, we sacrificed the two animals

showing the highest BLI signaling in each group on day 26 (Figure 29b) and analyzed bone marrow for the presence of T-cells and their phenotype.

We observed that in cohorts treated with CAR T-cells only, T-cell presence was inversely correlated with tumor burden, as the mouse with high tumor burden showed lower T-cell counts (Figure 29c). Interestingly, this particular mouse showed only minor response to

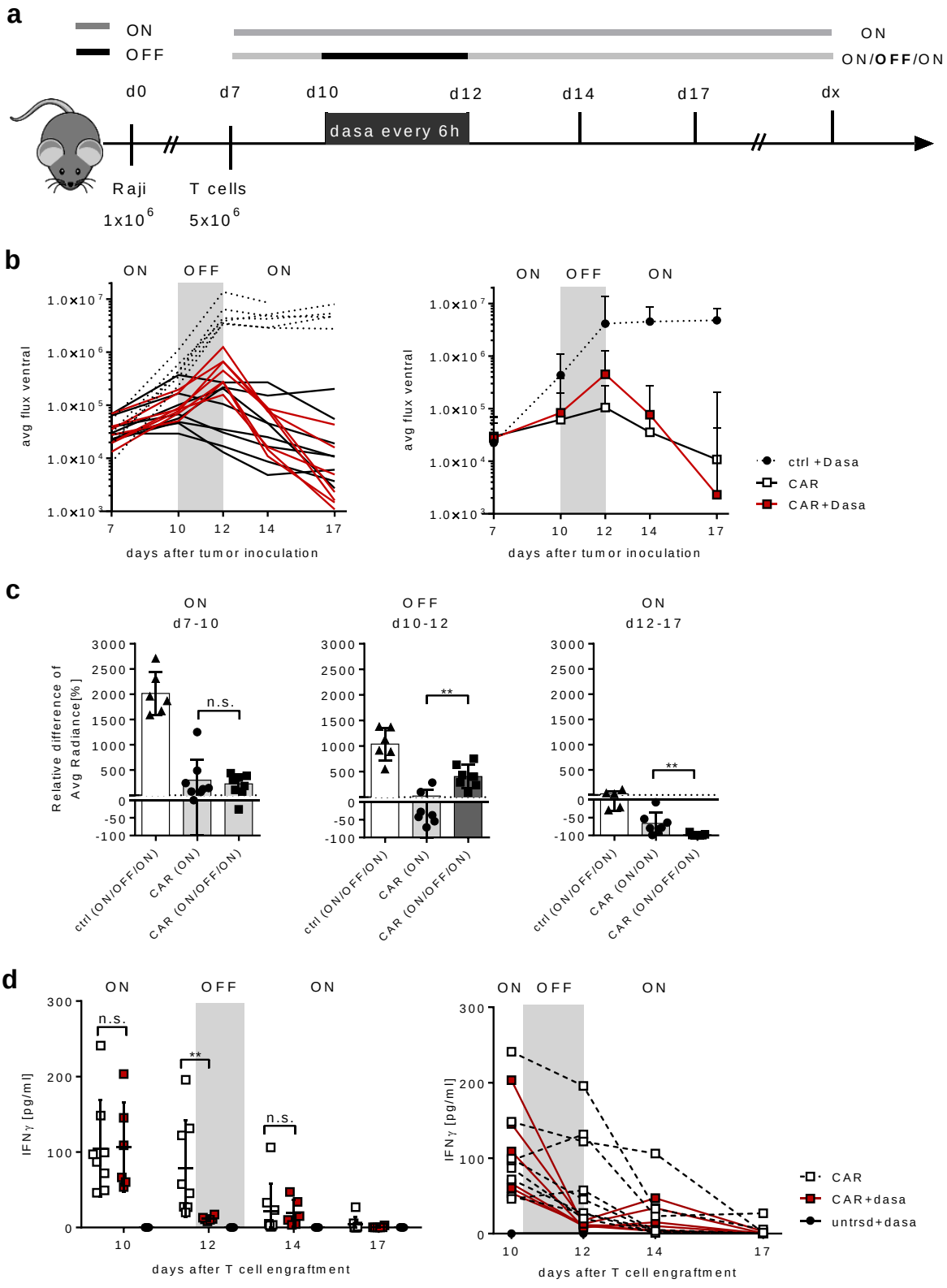


**Figure 28: Dasatinib pauses activated CAR T-cells in a function OFF state *in vivo*.**

(a) Treatment schedule and experimental setup. Mice received either CD19-CAR/4-1BB T-cells or untransduced T-cells (ctrl) on day 7 (function ON phase). Dasatinib was administered to indicated groups from day 10 to day 12 to create a function OFF phase. Afterwards, dasatinib was discontinued (function ON phase).

**Figure 28** (continued): (b) Diagrams show tumor burden in each treatment group in the function ON-OFF-ON sequence for individual mice (left diagram) an median BLI signal (right diagram). (c) Bar diagrams show lymphoma progression/regression during ON (day 7-10), OFF (day 10-12) and ON phase (day 12-17) in individual mice of each treatment group. (d) IFNγ serum level during ON (day 10, day 14, day 17) and OFF phases (day 12). Data shown are mean and individual values. Statistical analysis was performed between CAR (ON) and CAR (ON/OFF/ON) by two-way ANOVA (b, d) or Mann-Whitney-U-test (c) with * $P \leq 0.05$, ** $P \leq 0.005$, *** $P \leq 0.0005$.

CAR-treatment in the beginning, resulting in rapid tumor progression at time of analysis. PD-1 was upregulated on human CAR T-cells isolated from this mouse (Figure 29d), suggesting that high tumor burden induced exhaustion in CAR T-cells that fail to proliferate and thus to eradicate the tumor.

Regarding the presence of T-cells, there was no difference between mice of comparable tumor burden in CAR- and ctrl treated cohorts with and without dasatinib. As expected, the ratio of $CD8^+$ and $CD4^+$ cells was not altered by dasatinib in CAR-treated animals (Figure 29e). However, in ctrl T-cell treated mice, remaining T-cells were mostly of $CD8^+$ origin, whereas the level of $CD4^+$ T-cells was low. PD-1 was highly expressed on the surface of ctrl T-cells, which was probably due their failure to reduce tumor burden, and was comparable between CAR T-cell treated mice with low burden.

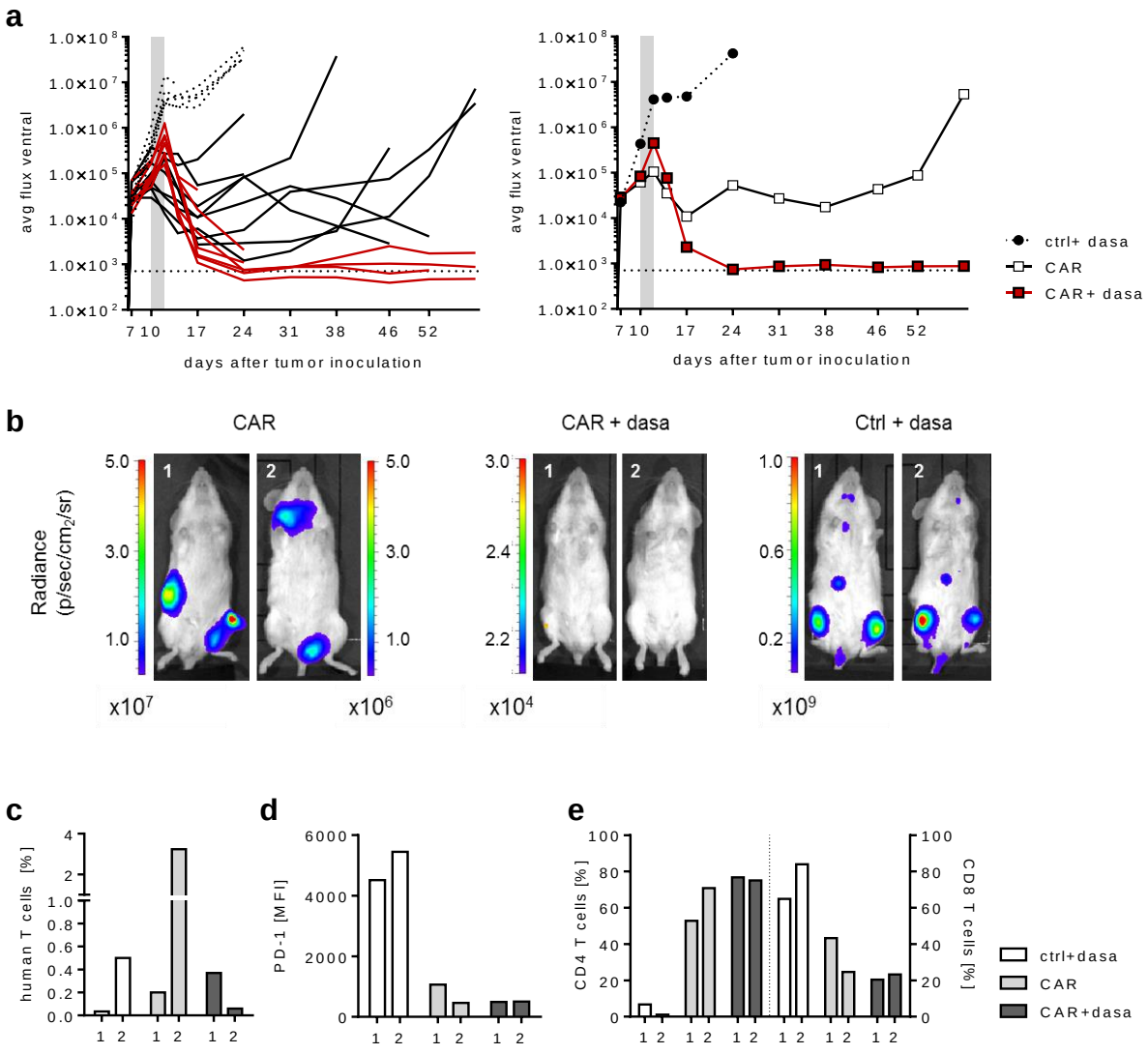


**Figure 29: Long term effects of switching CAR T-cells OFF *in vivo*.**

Mice received either CD19-CAR/4-1BB T-cells (CAR) or untransduced T-cells (ctrl) on day 7. Dasatinib was administered to indicated groups from day 10 to day 12 to create a transient function OFF phase (CAR+dasa, ctrl+dasa). Afterwards, dasatinib was discontinued (function ON phase). (a) Diagrams show development of tumor burden in each treatment group over 52 days for individual mice (left diagram) and median BLI signal (right diagram). (b) Diagram shows bioluminescence of each two mice per cohort with highest tumor burden measured on day 24, that were sacrificed on day 26. (c) Bar diagram shows presence of human T-cells in bone marrow as percentage of living events in mice sacrificed on day 26. Samples are stained with 7-AAD to discriminate dead cells, and human T-cells are defined as $CD3^+$ $CD45^+$. (d) PD-1 expression on human T-cells and (e) distribution of $CD4^+$ (left axis) and $CD8^+$ T-cells (right axis), pregated on living human T-cells, out of bone marrow samples of mice sacrificed on day 26.

## 4.7 Intermittent treatment with dasatinib enhances T-cell performance

The previous data suggested that switching CAR T-cells OFF for two days improves the outcome by preventing T-cell exhaustion. We thus sought to study whether we could prevent exhaustion in T-cells while avoiding a complete shutdown of T-cell function. We therefore employed a xenograft model in immunodeficient mice (NSG/Raji) to analyze if CAR T-cells efficacy could benefit from intermittent exposure to dasatinib. Thus, cohorts of n≥ 2 mice were inoculated with $1x10^6$ firefly-luciferase_GFP-transduced Raji tumor cells on day 0. CAR T-cells (i.e. $CD8^+$ and $CD4^+$ CD19-CAR/4-1BB T-cells, total dose: $5x10^6$; CD8:CD4 ratio = 1:1) or untransduced control T-cells were administered on day 7 by tail vein injection. 5 mg/kg dasatinib were administered by i.p. injection every 24 hours from day 7 until day 11 followed by i.p. injection every 36 hours on day 12 and day 14 (total seven doses) (Figure 30a).

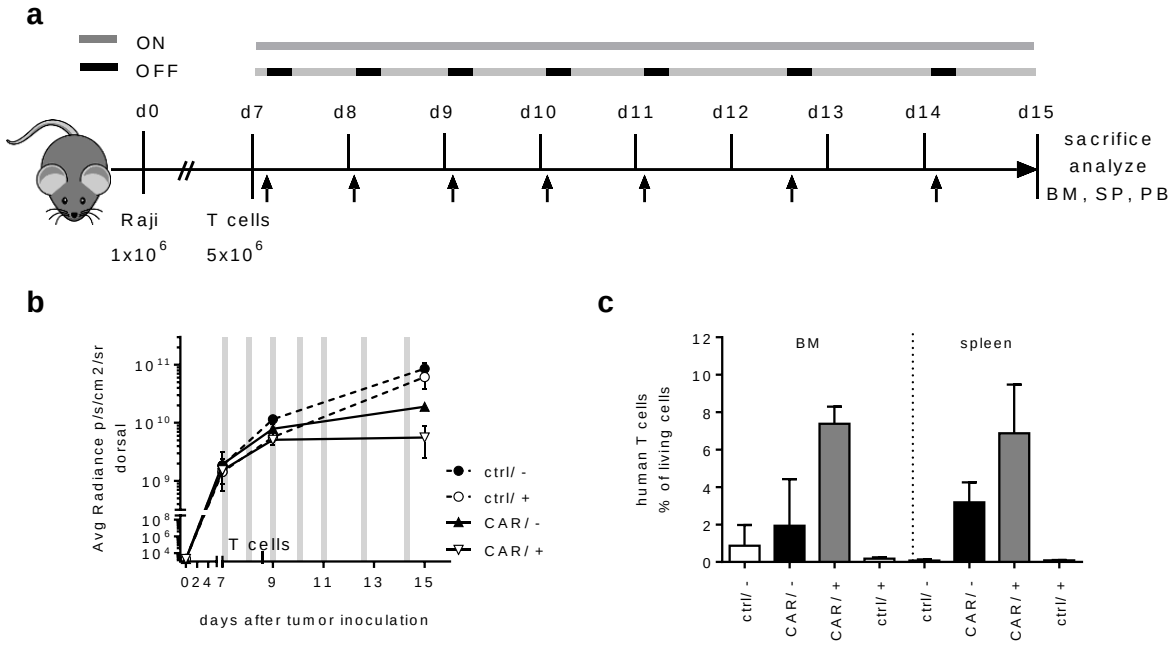


**Figure 30: Improved function of CAR T-cells after intermittent administration of dasatinib.**
(a) Mice received either CD19-CAR/4-1BB T-cells (CAR) or untransduced T-cells (ctrl) on day 7. Dasatinib was administered once daily to indicated groups from day 7 to day 14, as indicated by arrows. (b) Dorsal BLI signal is displayed as average radiance in $p/s/cm^2/sr$ obtained from regions of interest encompassing the entire dorsal body of each mouse in the respective treatment cohort. (c) The frequency of CAR-modified and control untransduced T-cells (identified as $CD3^+$ $CD45^+$) as percentage of live ($7\text{-}AAD^-$) cells. Each cohort consists of two animals. Key to legend: ctrl/- : mice had received untransduced control T cells and received no dasatinib; ctrl/+ : mice had received

untransduced control T cells and received dasatinib; CAR/- : mice had received CD19-CAR T cells and received no dasatinib; CAR/+ : mice had received CD19-CAR T cells and had received dasatinib.
Based on the known pharmacokinetic and -dynamic of dasatinib in mice *(85)*, this provided a window of approximately six hours after each injection when dasatinib was present in mouse serum at a concentration of > 50 nM, which should lead to a temporary blockade of CAR T-cell function as shown in the previous chapters. During the following 21 hours (until the next injection), dasatinib should be below the inhibitory threshold of 50 nM and therefore should not have inhibitory effects on CAR T-cell function. On day 15, mice were sacrificed and bone marrow (BM) and spleen (SP) were analyzed for the presence of human CAR T-cells by flow cytometry.

Mice that had received CAR T-cells and dasatinib showed superior tumor control and slower tumor progression compared to mice that had received CAR T-cells without dasatinib (Figure 30b). On day 15, the average bioluminescence signal in mice that had received CAR T-cells without dasatinib was 1.9e10 p/s/cm*2/sr, whereas in mice that received CAR T-cells and intermittent treatment with dasatinib the average bioluminescence signal was only 5.6e9 p/s/cm*2/sr. On day 15, there was no difference in bioluminescence signal between mice that had received untransduced control T-cells with or without dasatinib. Additionally, the percentage of human CAR T-cells in bone marrow and spleen was higher in animals that had been treated with intermittent dasatinib (BM: 7.3 %; SP: 6.9 %) when compared to animals that had received CAR T-cells but no intermittent dasatinib (BM: 1.9 %, SP: 3.2 %). This improved proliferation and persistence seems to be antigen-specific, as control T-cells did not show higher percentages in cohorts that additionally received dasatinib (Figure 30c).

When the experiment was repeated, the treatment schedule was slightly altered (Figure 31a). As before, T-cells showed improved performance when dasatinib was injected once daily, and lowered the tumor burden (Figure 31b). However, the percentages of human T-cells in all analyzed tissues were similar between dasatinib- and control-treated animals (Figure 31c). We thus analyzed the surface expression of PD-1 on human CAR T-cells in bone marrow, peripheral blood and spleen by flow cytometry to evaluate if dasatinib could influence the T-cell phenotype with regard to exhaustion. The data show that intermittent exposure of dasatinib significantly reduces PD-1 expression in CAR T-cells in bone marrow and peripheral blood compared to CAR T-cells in corresponding organs of mice that were not exposed to intermittent dasatinib (Figure 31d). In bone marrow, the MFI obtained after staining CAR T-cells with an anti-PD1 mAb was 9461 (4318 in SP, 4110 in PB, respectively) in mice that

had not been exposed to dasatinib (CAR/-), and was 7025 (3652 in SP, 2775 in PB, respectively) in mice that had been intermittently treated with dasatinib (CAR/+).

In aggregate, these data show that intermittent exposure to dasatinib augments the antitumor function of CAR T-cells *in vivo*. This could be explained by increased T-cell numbers, which are more efficient in the eradication of tumor, and by downregulation of PD-1 which might result in more efficient tumor killing, even when numbers of T-cells are not altered.

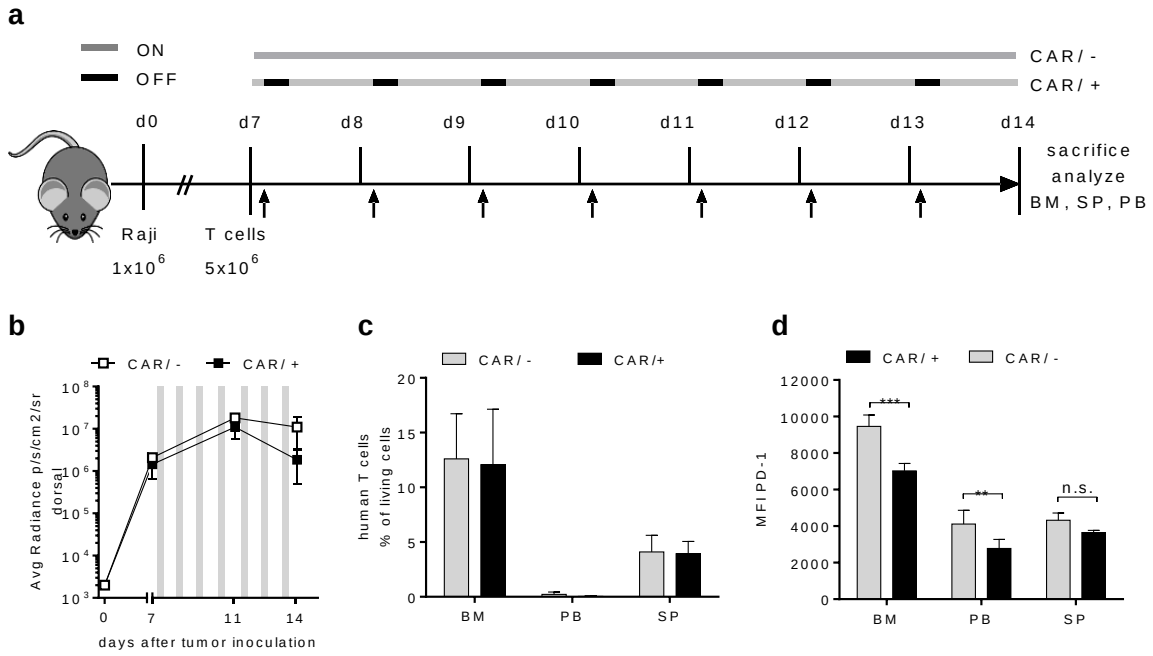


**Figure 31: Intermittent treatment with dasatinib reduces PD-1 expression in CAR T-cells**

(a) Mice received either CD19-CAR/4-1BB T-cells (CAR) or untransduced T-cells (ctrl) on day 7. Dasatinib was administered once daily to indicated groups from day 7 to day 13. (b) Tumor burden was assessed by bioluminescence imaging. Dorsal bioluminescence signal is displayed as average radiance in p/s/cm$^2$/sr obtained from regions of interest encompassing the entire dorsal body of each mouse in the respective treatment cohort. (c) The frequency of CAR-modified and control untransduced T-cells (identified as human CD3$^+$ / human CD45$^+$) as percentage of live (7-AAD$^-$) cells. (d) PD-1 expression on CD19-CAR/4-1BB T-cells as mean fluorescence intensity (MFI) obtained after staining with anti-PD1 mAb. Each cohort consists of 4 animals. ** $P \leq 0.005$, *** $P \leq 0.0005$. Key to legend: CAR/- : mice had received CD19-CAR T-cells and received no dasatinib (black bars); CAR/+ : mice had received CD19-CAR T-cells and had received dasatinib (grey bars).

## 4.8 Conclusion

CAR T-cells are ‘living’ anticancer drugs that are essentially ‘out of control’ after administration to the patient. Because of their tremendous potency and detrimental ability to induce life-threatening toxicity, there is an unmet desire for technologies that provide control over CAR T-cells and their effector functions in real-time during the course of adoptive immunotherapy. We hypothesized that the use of kinase inhibitors would provide an excellent option for a tailor-made control of CAR T-cells. Indeed, we demonstrate that the TKI dasatinib can be used as a reversible, pharmacologic OFF switch for CAR T-cells. Our data show that dasatinib confers titratable, partial to complete control over cytolytic and cytotoxic activity, cytokine secretion and proliferation in $CD8^+$ and $CD4^+$ CAR T-cells. We show that treatment with dasatinib retains resting CAR T-cells in an inactive function OFF state; and pauses CAR T-cells that are captured early during their activation phase. Intriguingly, dasatinib treatment does not affect the viability of CAR T-cells, and after discontinuation of dasatinib, the function OFF state is rapidly and completely reversed. Additionally, we show that other TKIs including clinically approved Bosutinib and experimentally tested PP1 influence the effector functions of CAR T-cells.

Based on these data, we accept the hypothesis that the TKI dasatinib provides an elegant option to exert control over CAR T-cell activation and effector functions by interfering with the phosphorylation of key kinases involved in CAR signaling. Having shown that dasatinib cuts off the signaling cascade and thus the activation of CAR T-cells we additionally discovered that intermittent application of dasatinib can mitigate exhaustion in CAR T-cells *in vivo*.

# 5 Discussion

## 5.1 Dasatinib - a universally applicable safety tool for CAR T-cell therapy

### 5.1.1 Controlling CAR T-cells with dasatinib

For the presented study, we had hypothesized that kinase inhibitors could be a tool to steer CAR T-cell effector functions in anti-cancer therapy. Dasatinib was identified as the lead candidate by screening a panel of TKI and Src kinase inhibitors, including imatinib and nilotinib, where it was the only substance to modulate CAR T-cell effector functions at feasible dose *(86)*. So far, dasatinib is clinically approved for the treatment of $Ph^+$ leukemia, and functions by inhibiting the BCR-ABL fusion protein that is caused by a translocation of chromosome 9 and 22.

In the presented study, we show for the first time that dasatinib also blocks the activation and execution of effector functions of CAR modified T-cells. The literature describes that besides BCR-ABL, dasatinib also interferes with a variety of other kinases including Lck, which is part of the T-cell signaling cascade. After TCR engagement, Lck undergoes auto-phosphorylation, and confers phosphorylation of CD3zeta and Zap70, leading to activation of primary T-cells. Thereby, Lck is known as the key mediator that is essential for TCR induced activation *(87)*. By western blot analysis, we show that dasatinib prevents activation-induced phosphorylation of Lck and its downstream kinases in resting CAR T-cells. Similar to its role in signaling of the endogenous TCR, Lck is one of the key molecules in the CAR mediated signaling after antigen-recognition. By inhibiting Lck, dasatinib consecutively prevents the induction of transcription factor NFAT, and CAR T-cells are retained in a function OFF state in the presence of dasatinib. Previous studies have shown that by acting as a competitive binder, dasatinib blocks the ATP binding site of Lck, and thus prevents the activation of unmodified T-cells *(73)*. To achieve complete blockade of T-cell function it therefore seems to be necessary to block all available Lck molecules are blocked by dasatinib. Thus, when dasatinib is administered at a level not sufficient to suppress ATP binding to Lck, T-cells might get partially activated and exert a reduced level of effector functions.

When added simultaneously or shortly after beginning of the co-culture, dasatinib completely blocked all effector functions. Thus, our data suggest that dasatinib pauses activated CAR T-cells in a function OFF when applied before phosphorylation of Lck is completed. As dasatinib does not affect the late signaling events that are related to gene expression, it does not prevent the execution of effector functions once the signaling has passed beyond the phosphorylation of Lck, which can be defined as a ‘point of no return’. However, our data al-

so show that late administration of dasatinib prevents the subsequent activation of CAR T-cells when encountering antigen in a second stimulation, and demonstrate that once inhibition is established, it can be perpetuated as long as dasatinib is provided at a concentration of > 50 nM.

When comparing the sensitivity of T-cells expressing different CARs towards dasatinib, we observed that changing the costimulatory domain slightly altered the sensitivity of CAR T-cells towards dasatinib-mediated inhibition. CARs containing a 4-1BB costimulatory domain were more sensitive towards dasatinib induced blockade of function when compared to a CAR with CD28 co-stimulation and otherwise equal design. This might be caused by differences in the signaling cascade evoked by both costimulatory domains *(88)*. In non-modified T-cells, engagement of 4-1BB enhances phosphorylation of Lck *(89)*, whereas CD28 directly binds Lck and thus mediates recruitment of Lck to the immune synapse *(90)*. As this study focused on receptors containing CD28 or 4-1BB as costimulatory moieties, it needs to be evaluated how dasatinib affects CARs containing other co-stimulatory domains, e.g. inducible T-cell costimulator (ICOS) and tumor necrosis factor receptor superfamily, member 4 (OX40). However, due to the mechanism of action revealed in this study, we expect the steering features of dasatinib over CAR T-cell activation to apply for any CAR using CD3zeta as the major signaling domain, or any receptor relying on Lck mediated signaling.

Furthermore, we have shown that dasatinib-induced inhibition of T-cell function is largely independent of CAR-specificity. We observed only minor differences in the sensitivity of CD19- and ROR1-targeting CAR T-cells towards dasatinib-mediated. These differences could be target specific and related to antigen density, but could also be caused by CAR affinity for their respective epitope. The antigen binding fragment of an antibody (Fab) used to generate the scFvs of the CARs used in this study have different affinities of 0.42 nM (CD19, FMC63) and 0.56 nM (ROR1, R12), respectively *(91, 92)*. In our study, the ROR1-CAR (thus the CAR with lower affinity) was slightly more susceptible towards dasatinib-mediated inhibition, as a lower concentration of dasatinib was sufficient to mediate a total block of function in ROR1 targeting CAR T-cells when compared to the CARs targeting CD19. From the fact that all tested CARs in this study where susceptible to dasatinib-mediated inhibition in general, we conclude that dasatinib can be used as a universally applicable tool to steer CAR T-cell function, even though the amount of dasatinib needed to achieve full control might need to be adjusted depending on the CAR itself.

Additionally, we have demonstrated that dasatinib not only confers complete blockade of CAR T-cell function, but also can be titrated to induce a gradual reduction of effector func-

tions. In our study, concentrations between 3.25 nM and 25 nM conferred dose dependent reduction of effector functions. Based on the underlying mechanism, we conclude that low levels of dasatinib do not induce saturation of ATP binding sites at the Lck molecule, and T-cells can get partially activated. Using an NFAT-based reporter system *(93)*, we confirmed that reduced CAR T-cell function is caused by lower activation on a single cell level.

Our experiments focused mainly on the effects of dasatinib towards $CD8^+$ central memory T-cells. However, recent studies suggest that there are advantages of using naïve $CD8^+$ T-cells for immunotherapy, as these can differentiate into both long lasting memory and short lived effector T-cells with high cytolytic potential and can be generated at higher numbers *(20, 94)*. It has been shown in non-modified T-cells that naïve T-cell subsets are equally affected by dasatinib, and only minor differences have been described with regard to the concentration needed for full inhibition of non-modified naïve and memory T-cells *(76)*. Therefore, we anticipate that dasatinib will be equally effective in naïve and memory T cells. As CAR T-cell products contain a combination of $CD8^+$ and $CD4^+$ T-cells, we confirmed our observations in $CD4^+$ bulk T-cells. In these cells, the sensitivity towards dasatinib-mediated inhibition was only marginally changed when compared to $CD8^+$ central memory derived T-cells, which is in line with published literature regarding unmodified T-cells *(76)*. As the early signaling events after CAR engagement are similar in $CD4^+$ and $CD8^+$ CAR T-cells, the kinetics and sensitivity of dasatinib-mediated inhibition are similar in $CD4^+$ and $CD8^+$ derived T-cell subsets.

### 5.1.2 Regaining effector functions after CAR T-cell inhibition

During our study, neither the prevention nor the abrogation of CAR T-cell activation with dasatinib induced apoptosis. Instead, we observed high levels of early apoptotic T-cells following antigen specific activation in the absence of dasatinib. Apoptosis only occurred in CAR T-cells in the presence of antigen expressing target cells, and remaining T-cells recovered original numbers by proliferation in two to three days. We explain this observation by activation induced cell death (AICD), which is in line with current literature describing AICD in CARs tuned to elicit the highest magnitude of T-cell function *(95)*. In our study, apoptosis was reduced in the presence of dasatinib, indicating that dasatinib can prevent activation induced cell death and thus can improve the viability of CAR T-cells.

The fact that dasatinib itself is not toxic towards CAR T-cells highlights its potential use as a reversible safety switch, which is an advantage of dasatinib over safety tools that function by T-cell elimination. Indeed, inhibition was instantly reversible independent of

treatment duration. Structural analyses suggest that the interaction between dasatinib and Lck is based on hydrogen bounds, mediating a rapidly reversible interaction *(73)*. When the concentration of dasatinib is reduced, e.g. by washing (*in vitro*) or due to clearance *in vivo*, dasatinib dissociates from Lck. Subsequently, ATP can enter its designated pockets, leading to auto-phosphorylation of Lck and activation of CAR T-cells. Accordingly, we found that the blockade of CAR T-cell function was rapidly reversible after removal of dasatinib in our *in vitro* assays, and discontinuation of dasatinib administration in our *in vivo* model. The data also suggest that dasatinib does not change the genomic expression of the CAR or kinases involved in CAR signaling, but interacts with the phosphorylation of Lck, Zap70 and CD3zeta. Thus, the achieved blockade of CAR T-cell activation and also the subsequent regain of function enable a highly flexible use of dasatinib to steer CAR T-cell effector function *in vitro* and *in vivo*. Confirmed by our data, reversibility of inhibition equally applies for short-term inhibition of a few hours, but also for long-term inhibition of up to seven days. We therefore conclude that, considering CAR T-cell fitness and reversibility of inhibition, switching T-cells OFF for at least seven days is highly feasible. Using dasatinib to control CAR T-cells for approximately one week also seems to be a relevant therapeutic window for the treatment of adverse events in patients, considering that many side effects including CRS requiring control are acute toxicities that need to be managed immediately, but normally resolve within a few days. However, due to the instant reversibility of dasatinib-mediated T-cell blockade, (partial) elimination of CAR T-cells might be appropriate and should be considered when long-term regulation is required.

### 5.1.3 Pharmacokinetic of dasatinib in mice and human

So far, dasatinib is available as an orally administered pill, which might be sufficient in humans to achieve CAR T-cell control. As controlled oral application is difficult in mice, and because dasatinib has a serum half-life of less than one hour in mice *(85)* we administered dasatinib to mice by regular i.p. injections in order to keep the serum level above the threshold required for complete CAR T-cell inhibition. Indeed, using this model, we could demonstrate that a full blockade of T-cell functions including proliferation, specific lysis and the secretion of cytokines could be achieved in resting and activated CAR T-cells.

The intended time frame for the clinical use of dasatinib as a reversible CAR T-cell OFF switch is in the order of one to several consecutive days. We thus aimed to demonstrate the concept of dasatinib as an OFF switch over longer time. As multiple daily injections over a time of up to one week was neither applicable for mice nor researchers, we performed a pi-

lot study in mice and implanted osmotic pumps with a drug delivery span of seven days. Unfortunately, release of dasatinib from the pump was perpetuated by the low solubility of dasatinib in aqueous surrounding, leading to highly variable serum levels in mice treated with dasatinib. Consequential, the activity of T-cells ranged from completely blocked to fully functional. However, issues associated with solubility and fast elimination might not arise in the treatment of human patients, as administration routes are different in human than in mice. Analyses of dasatinib's pharmacokinetic in humans have shown that serum levels of 100 nM can be achieved by single administration of today's standard dose of 100 mg to 180 mg per day. However, due to the elimination half-life of four hours after oral administration in humans, multiple dosages per day might be needed to maintain the desired serum level that enables complete suppression of CAR T-cell activation *(96)*. This assumption is supported by the fact that most patients receiving dasatinib once daily at a dose of 100 mg to 180 mg for the treatment of CML or ALL do not show signs of immunosuppression. If dasatinib proves to be appropriate for the treatment of CAR related toxicities, the development of other formulations including i.v. infusions could be considered. In summary, neither the poor solubility nor the relatively short elimination half-life should be a reason to not pursue the use of dasatinib as a pharmaceutical CAR control.

Accordingly, we analyzed the capability of other clinically approved TKIs with longer elimination half-life to effectively control CAR T-cell function. Saracatinib is an experimental drug originally developed for the treatment of cancer patients, but its development was further pursued for other applications including Alzheimer's disease. Additionally, we included bosutinib in our study, which is approved since 2012 for the second line treatment of CML. Both TKIs were chosen for evaluation in our study because of their similar inhibition pattern compared to dasatinib, as they selectively block the phosphorylation of BCR-ABL and SRC family kinases. In contrast to dasatinib, saracatinib and bosutinib show a prolonged elimination half-life of 40 hours and 20 hours, respectively, in patients. In the tested dose range, only bosutinib was able to mediate T-cell inhibition, and high levels (> 100 nM) were needed to observe inhibitory effects. From pharmacological studies it is known that levels up to ~200 nM can be achieved in patients following single oral administration of 500 mg, a dosing that is accompanied by acceptable side effects *(97)*. Therefore, bosutinib might display an interesting alternative to dasatinib that could be used to steer CAR T-cell function while offering a longer half-life than dasatinib. In our study, saracatinib did not show inhibitory effects towards CAR T-cells; however, it cannot be excluded that higher levels of saracatinib are needed to induce T-cell inhibition. Of note, the maximum oral dose of saracatinib is 175 mg once daily, leading

to a serum concentration of ~275 nM *(98)*, which was not sufficient to induce immunomodulatory effects in our study. During phase I clinical trial, higher dosing was associated with non-tolerable toxicities *(98)*; therefore saracatinib seems not to be suitable as a pharmaceutical safety switch for CAR T-cells.

We hypothesized that TKIs targeting Lck should in general be able to influence (CAR) T-cell functions, with the level of inhibition being a matter of dosage. To support this notion, we show that PP1, which is a highly specific inhibitor targeting Src family kinases, can prevent the specific lysis of target cells at a similar dosing scheme as dasatinib. Unfortunately, PP1 is not clinically tested nor approved, and its elimination half-life is unknown. In conclusion, it might be interesting to further investigate the inhibitory potential of selective Src family inhibitors.

### 5.1.4 Clinical application and feasibility

The concept underlying a dasatinib-based pharmacologic OFF switch is that in the absence of the drug, CAR T-cells are able to exert their antitumor function (ON) and are prevented to do so in the presence of the drug (function OFF). When using dasatinib as a modulator of T-cell function, we aim at the key mediators of signaling. By blocking Lck, the phosphorylation of CD3zeta is complete abrogated, a fact that makes this concept compatible with all CARs depending on CD3zeta as their major signaling domain. This is the case for all CAR constructs that are currently being evaluated in clinical trials (or are already clinically approved), making dasatinib an immediately clinically applicable safety switch. Our data show that dasatinib can exert temporary control over CAR T-cell function with rapid onset upon exposure, and rapid release upon removal to the drug. In our experiments we have retained CAR T-cells in a function OFF state between two hours and seven days. Also after seven days, the inhibitory effect of dasatinib on CAR T-cell function did not diminish, and CAR T-cells re-ignited their antitumor function immediately after withdrawal of the drug. These data suggest that dasatinib can indeed be used as a pharmacologic OFF switch to steer CAR T-cells in real-time. After more than decade-long experience with dasatinib in hematology, no severe side effects are known to be caused by dasatinib itself, supporting its role as a CAR-safety drug. Dasatinib-associated side effects commonly arise after several months of treatment, and can include fever, skin rash, diarrhea and headache, with the strongest described adverse events being cytopenia occurring during the first two months of treatment *(99)*, pleural effusion starting after three months of treatment *(100)*, and cardiotoxicity *(101)*. Due to the intended time of application, which is in the range of days, we don’t anticipate significant dasatinib related se-

vere toxicity towards T-cells or other tissues within this period of treatment. Furthermore, eventually upcoming minor effects can be neglected in comparison to the benefit that is achieved by treating CAR related toxicities with dasatinib. Thus, the evaluation of dasatinib as a new safety and OFF control drug in CAR T-cell immunotherapy should be feasible and straightforward.

As all clinically approved CAR T-cell products maintain their respective endogenous TCR, we confirmed that inhibition of the CAR could not be bypassed by the engagement of the TCR. Following the literature, 25 to 100 nM dasatinib are sufficient to completely prevent the activation of non-modified T-cells after engagement of their endogenous TCR, dependent on the TCR specificity *(75–77, 102)*. In our study, TCR and CAR mediated effector functions were completely blocked in the presence of ≥ 50 nM dasatinib, even when both receptors were stimulated simultaneously. In the complete absence of signals triggering survival, T-cells might enter a contraction phase and become apoptotic. Of note, T-cells seemed to respond to IL-2 that was present in the culture medium, indicating that dasatinib prevents CAR and TCR mediated stimulation, but leaves T-cells susceptible to cytokine dependent signaling pathways. This has already been described in the literature for non-modified T-cells *(102)* and needs to be taken into account especially in a clinical scenario when control over CAR T-cells is required. During CRS, where pro-inflammatory cytokines are highly expressed, these may still induce responses in CAR T-cells despite the presence of dasatinib, and additional treatment including eradication of CAR T-cells as last option may need to be considered.

### 5.1.5 Dasatinib in the spectrum of existing safety strategies in CAR T-cell immunotherapy

In the presented study, we show that dasatinib rapidly induces a reversible function OFF state in CAR T-cells. This feature is unique and distinguishes this pharmacologic OFF switch from conventional safety switches that have been developed with the intention to terminate CAR T-cells in case of severe toxicity. Indeed, depletion markers like EGFRt or CD20t can be employed to remove CAR T-cells through administration of the cognate mAb; and suicide genes like iCasp9 or HSV-TK can be triggered to remove CAR T-cells within several hours or days. Undesirably, these conventional safety switches can only be triggered once and terminate the antitumor effect. As a consequence, physicians and patients have been reluctant to use these safety switches, even when side effects of CAR T-cells were severe. There are multiple clinical scenarios where CAR T-cell induced toxicity is of transient nature, e.g. in patients that experience tumor lysis syndrome, CRS or CRES after CD19-CAR T-cell therapy. In these set-

tings, it might be sufficient to place CAR T-cells into a temporary function OFF phase, and to re-ignite their function once the adverse reaction is over. In the current clinical situation, corticosteroids are one of the main tools used to deal with CAR T-cell related side effects. Therefore, we compared dasatinib to dexamethasone, which is clinically used in an attempt to mitigate CAR T-cell induced toxicity. Our data show that dexamethasone exerts inferior control over CAR T-cell function and acts much slower than dasatinib. This is consistent with dexamethasone's mode of action which is not direct interference with CAR (or TCR) signaling, but impairment of NFκB induction at the transcriptional level *(103)*. The pattern and extent of functional inhibition by dexamethasone in our study is comparable with prior work in non-CAR modified T-cells *(104)*.

Other investigators have proposed alternative ON/OFF switches requiring specific CAR designs. In the "ON-switch CAR" approach, targeting moiety and signaling module are separated into two distinct proteins such that CAR T-cells idle in a function OFF state in the absence of a dimerizing control drug. With these designs, CAR T-cell function is only ignited when targeting compound or control drug are administered to the patient (function ON) *(71)*. In the SUPRA CAR, the signaling moiety is inactive and can only be activated after binding the antigen-binding domain, which connects to the signaling domain by leucine zippers, and the subsequent recognition of antigen *(72)*. These concepts are reciprocal to our approach, but limited in their applicability as they can only be used with specific CAR designs. Clinical proof-of-concept for the safety and efficacy of programmable CAR constructs and split CAR designs has not yet been demonstrated.

In summary, the existing spectrum of safety strategies in CAR T-cell immunotherapy comprises symptomatic treatment like neutralization of cytokines during CRS; attempts of gaining control over CAR T-cells through glucocorticoids, which is ineffective; triggering depletion markers and suicide genes that are included in some CAR T products but also terminates the desired antitumor effect, and structural changes of the CAR that require alternative CAR-designs. In this spectrum, our concept of dasatinib-mediated reversible control over CAR T-cell function represents a missing link providing effective and complete control over CAR T-cells as they are currently clinically used, while conserving their therapeutic potential.

## 5.2 Enhancing the outcome of CAR T-cell therapy with dasatinib

During our studies in mice, we observed development of liver metastasis that could not be controlled despite CD19-CAR T-cells being present in the tumor. Analyses by flow cytometry revealed a high expression of PD-1 on tumor infiltrating CAR T-cells (data not shown). It is

known that upregulation of PD-1 expression is a marker of T-cell exhaustion, which normally occurs in chronic infections when the source of antigen cannot be eliminated. Hallmarks of exhaustion include the upregulation of inhibitory receptors following activation, including PD-1. Subsequently, T-cells enter a dysfunctional state, which is characterized by a sequential loss of function and finally leads to apoptosis. Exhaustion can be reversed by blocking PD-1, e.g. by PD-1 blocking antibodies, if T-cells are treated at an early dysfunctional state *(105)*. Evidence is accumulating that exhaustion of T-cells can contribute to T-cell failure during CAR T-cell therapy *(106, 107)*, which is supported by our observations. In our study, we show that short periods of treatment with low doses of dasatinib can not only decrease PD-1 expression in CAR T-cells, but also improve the eradication of tumor in an environment of permanent stimulation. In this treatment schedule, dasatinib does not permanently block CAR T-cell signaling, but inhibits CAR T-cells intermittently (e.g. approximately six hours of inhibition followed by 18 hours of activation), and thus is likely able to prevent exhaustion. As PD-1 is also a marker for activation, one could argue that a reduced expression of PD-1 is a consequence of lower activation in the presence of dasatinib. In contrast, we observed improved T-cell proliferation and enhanced tumor lysis in mice that had been intermittently treated with dasatinib. This is in line with published literature. showing that temporary cessation of TCR phosphorylation with a small molecule induced rejuvenation in exhausted cells, with improved outcome even when compared to checkpoint inhibitors such as PD-1 blocking antibodies *(108)*. In fact, this resembles the mode of action that we demonstrated to cause dasatinib-mediated inhibition of CAR T-cells.

## 5.3 Outlook on feature research and clinical perspective

Until now, physicians (and patients) essentially lose control over CAR T-cells once they are being administered. Our data demonstrate that through the use of dasatinib, it is now possible to steer the function of CAR T-cells in real-time, and thus have the potential to set a landmark in CAR T-cell immunotherapy. Our data show that dasatinib blocks cytokine production by CAR T-cells and prevents the systemic release of cytokines in an *in vivo* model. We are therefore proposing the use of dasatinib as a control drug to steer CAR T-cell function and to prevent or mitigate toxicity. However, the development of mouse models displaying clinical adverse events including CRS has been challenging, as the transfer of CAR T-cells alone into tumor bearing, immuno-deficient mice is not sufficient to induce CRS. Recently, the first mouse models imitating CRS after CAR T-cell transfer has been reported *(50, 51)*. Both studies show that tumor infiltrating monocytes and macrophages getting activated by CAR T-cells

are the major source of IL-1 and IL-6 which are the main cytokines driving CRS. It has been described that dasatinib can control the activation of these cells by inhibiting FMS receptor at similar doses as needed to exert T-cell control *(109)*. Thus, it would be a logical next step to test whether dasatinib is able to mitigate CRS in one of these or a similar model, before transferring our results into the clinic.

The majority of CAR T-cell products that are currently employed in clinical trials, and also the two FDA-approved CD19-CAR T-cell products Kymriah® and Yescarta®, are not equipped with a control switch. As a consequence, the use of systemic immunosuppression with steroids is at present the only available option for physicians in an attempt to exert control over CAR T-cells *in vivo*. In our study, we have compared dasatinib and dexamethasone side by side and demonstrate that dexamethasone is largely ineffective in controlling CAR T-cells. Having shown that interference with key signaling kinases by small inhibitors can mediate control over CAR T-cell activation, there is a high probability that other potent inhibitors can be identified from the broad range of small molecule inhibitors. By selecting single agents, only a small fraction of substances can be analyzed. We therefore suggest the use of a high throughput screening platform to identify additional suitable candidate substances out of drug libraries, e.g. by using a recently published reporter system that enables easy readout of drug mediated effects by FACS detectable expression of activation dependent markers *(93)*. From the small panel we screened, only dasatinib was capable of completely controlling CAR T-cell activation and function. However, TKI may influence CAR T-cells in many ways, including inhibition of specific effector functions while leaving others untouched, and may also enhance particular functions. Therefore, further investigation is indicated that may yield combinations where specific CAR T-cell functions are affected. Due to the decade-long experience with dasatinib in hematology, the clinical investigation and implementation of dasatinib as a CAR T-cell control and safety drug is realistic and feasible.

# References

1. M. K. Juric, S. Ghimire, J. Ogonek, E. M. Weissinger, E. Holler, J. J. van Rood, M. Oudshoorn, A. Dickinson, H. T. Greinix, Milestones of Hematopoietic Stem Cell Transplantation - From First Human Studies to Current Developments., *Front. Immunol.* **7**, 470 (2016).

2. M. Boyiadzis, K. A. Foon, Approved monoclonal antibodies for cancer therapy, *Expert Opin. Biol. Ther.* **8**, 1151–1158 (2008).

3. C. H. June, Adoptive T cell therapy for cancer in the clinic., *J. Clin. Invest.* **117**, 1466–76 (2007).

4. G. Gross, T. Waks, Z. Eshhar, Expression of immunoglobulin-T-cell receptor chimeric molecules as functional receptors with antibody-type specificity., *Proc. Natl. Acad. Sci. U. S. A.* **86**, 10024–8 (1989).

5. Z. Eshhar, T. Waks, G. Gross, D. G. Schindler, Specific activation and targeting of cytotoxic lymphocytes through chimeric single chains consisting of antibody-binding domains and the gamma or zeta subunits of the immunoglobulin and T-cell receptors., *Proc. Natl. Acad. Sci.* **90**, 720–724 (1993).

6. J. Maher, R. J. Brentjens, G. Gunset, I. Rivière, M. Sadelain, Human T-lymphocyte cytotoxicity and proliferation directed by a single chimeric TCRζ /CD28 receptor, *Nat. Biotechnol.* **20**, 70–75 (2002).

7. C. Imai, K. Mihara, M. Andreansky, I. C. Nicholson, C.-H. Pui, T. L. Geiger, D. Campana, Chimeric receptors with 4-1BB signaling capacity provoke potent cytotoxicity against acute lymphoblastic leukemia, *Leukemia* **18**, 676–684 (2004).

8. J. N. Kochenderfer, W. H. Wilson, J. E. Janik, M. E. Dudley, M. Stetler-Stevenson, S. A. Feldman, I. Maric, M. Raffeld, D.-A. N. Nathan, B. J. Lanier, R. A. Morgan, S. A. Rosenberg, Eradication of B-lineage cells and regression of lymphoma in a patient treated with autologous T cells genetically engineered to recognize CD19, *Blood* **116**, 4099–4102 (2010).

9. M. Kalos, B. L. Levine, D. L. Porter, S. Katz, S. A. Grupp, A. Bagg, C. H. June, T cells with chimeric antigen receptors have potent antitumor effects and can establish memory in patients with advanced leukemia., *Sci. Transl. Med.* **3**, 95ra73 (2011).

10. R. J. Brentjens, I. Rivière, J. H. Park, M. L. Davila, X. Wang, J. Stefanski, C. Taylor, R. Yeh, S. Bartido, O. Borquez-Ojeda, M. Olszewska, Y. Bernal, H. Pegram, M. Przybylowski, D. Hollyman, Y. Usachenko, D. Pirraglia, J. Hosey, E. Santos, E. Halton, P. Maslak, D. Scheinberg, J. Jurcic, M. Heaney, G. Heller, M. Frattini, M. Sadelain, R. J. Brentjens, Safety and persistence of adoptively transferred autologous CD19-targeted T cells in patients with relapsed or chemotherapy refractory B-cell leukemias., *Blood* **118**, 4817–28 (2011).

11. J. Calmes-Miller, FDA Approves Second CAR T-cell Therapy*Cancer Discov.* **8**, 5–6 (2018).

12. X. Wang, A. Naranjo, C. E. Brown, C. Bautista, C. W. Wong, W.-C. Chang, B. Aguilar, J. R. Ostberg, S. R. Riddell, S. J. Forman, M. C. Jensen, Phenotypic and Functional Attributes of Lentivirus-modified CD19-specific Human CD8+ Central Memory T Cells Manufactured at Clinical Scale, *J. Immunother.* **35**, 689–701 (2012).

13. R. Monjezi, C. Miskey, T. Gogishvili, M. Schleef, M. Schmeer, H. Einsele, Z. Ivics, M. Hudecek, Enhanced CAR T-cell engineering using non-viral Sleeping Beauty transposition from minicircle vectors, *Leukemia* **31**, 186–194 (2017).

14. S. A. Ali, V. Shi, I. Maric, M. Wang, D. F. Stroncek, J. J. Rose, J. N. Brudno, M. Stetler-Stevenson, S. A. Feldman, B. G. Hansen, V. S. Fellowes, F. T. Hakim, R. E. Gress, J. N. Kochenderfer, T cells expressing an anti-B-cell maturation antigen chimeric antigen receptor cause remissions of multiple myeloma., *Blood* **128**, 1688–700 (2016).

15. S. A. Ali, V. Shi, I. Maric, M. Wang, D. F. Stroncek, J. J. Rose, J. N. Brudno, M. Stetler-Stevenson, S. A. Feldman, B. G. Hansen, V. S. Fellowes, F. T. Hakim, R. E. Gress, J. N. Kochenderfer, T cells expressing an anti-B-cell maturation antigen chimeric antigen receptor cause remissions of multiple myeloma, *Blood* **128**, 1688–1700 (2016).

16. J. H. Park, I. Rivière, M. Gonen, X. Wang, B. Sénéchal, K. J. Curran, C. Sauter, Y. Wang, B. Santomasso, E. Mead, M. Roshal, P. Maslak, M. Davila, R. J. Brentjens, M. Sadelain, Long-Term Follow-up of CD19 CAR Therapy in Acute Lymphoblastic Leukemia., *N. Engl. J. Med.* **378**, 449–459 (2018).

17. S. L. Maude, T. W. Laetsch, J. Buechner, S. Rives, M. Boyer, H. Bittencourt, P. Bader, M. R. Verneris, H. E. Stefanski, G. D. Myers, M. Qayed, B. De Moerloose, H. Hiramatsu, K. Schlis, K. L. Davis, P. L. Martin, E. R. Nemecek, G. A. Yanik, C. Peters, A. Baruchel, N.

Boissel, F. Mechinaud, A. Balduzzi, J. Krueger, C. H. June, B. L. Levine, P. Wood, T. Taran, M. Leung, K. T. Mueller, Y. Zhang, K. Sen, D. Lebwohl, M. A. Pulsipher, S. A. Grupp, Tisagenlecleucel in Children and Young Adults with B-Cell Lymphoblastic Leukemia., *N. Engl. J. Med.* **378**, 439–448 (2018).

18. C. J. Turtle, K. A. Hay, L.-A. Hanafi, D. Li, S. Cherian, X. Chen, B. Wood, A. Lozanski, J. C. Byrd, S. Heimfeld, S. R. Riddell, D. G. Maloney, Durable Molecular Remissions in Chronic Lymphocytic Leukemia Treated With CD19-Specific Chimeric Antigen Receptor-Modified T Cells After Failure of Ibrutinib., *J. Clin. Oncol.* **35**, 3010–3020 (2017).

19. D. L. Porter, W.-T. Hwang, N. V. Frey, S. F. Lacey, P. A. Shaw, A. W. Loren, A. Bagg, K. T. Marcucci, A. Shen, V. Gonzalez, D. Ambrose, S. A. Grupp, A. Chew, Z. Zheng, M. C. Milone, B. L. Levine, J. J. Melenhorst, C. H. June, Chimeric antigen receptor T cells persist and induce sustained remissions in relapsed refractory chronic lymphocytic leukemia, *Sci. Transl. Med.* **7**, 303ra139-303ra139 (2015).

20. C. J. Turtle, L.-A. Hanafi, C. Berger, M. Hudecek, B. Pender, E. Robinson, R. Hawkins, C. Chaney, S. Cherian, X. Chen, L. Soma, B. Wood, D. Li, S. Heimfeld, S. R. Riddell, D. G. Maloney, Immunotherapy of non-Hodgkin's lymphoma with a defined ratio of CD8+ and CD4+ CD19-specific chimeric antigen receptor-modified T cells., *Sci. Transl. Med.* **8**, 355ra116 (2016).

21. S. S. Neelapu, F. L. Locke, N. L. Bartlett, L. J. Lekakis, D. B. Miklos, C. A. Jacobson, I. Braunschweig, O. O. Oluwole, T. Siddiqi, Y. Lin, J. M. Timmerman, P. J. Stiff, J. W. Friedberg, I. W. Flinn, A. Goy, B. T. Hill, M. R. Smith, A. Deol, U. Farooq, P. McSweeney, J. Munoz, I. Avivi, J. E. Castro, J. R. Westin, J. C. Chavez, A. Ghobadi, K. V. Komanduri, R. Levy, E. D. Jacobsen, T. E. Witzig, P. Reagan, A. Bot, J. Rossi, L. Navale, Y. Jiang, J. Aycock, M. Elias, D. Chang, J. Wiezorek, W. Y. Go, Axicabtagene Ciloleucel CAR T-Cell Therapy in Refractory Large B-Cell Lymphoma., *N. Engl. J. Med.* **377**, 2531–2544 (2017).

22. E. Medicines Agency, *First two CAR-T cell medinices recommended for approval in the European Union* (2018; www.ema.europa.eu).

23. D. Pettitt, Z. Arshad, J. Smith, T. Stanic, G. Holländer, D. Brindley, CAR-T Cells: A Systematic Review and Mixed Methods Analysis of the Clinical Trial Landscape, *Mol. Ther.* **26**, 342–353 (2018).

24. J. Scholler, T. L. Brady, G. Binder-Scholl, W.-T. Hwang, G. Plesa, K. M. Hege, A. N. Vogel, M. Kalos, J. L. Riley, S. G. Deeks, R. T. Mitsuyasu, W. B. Bernstein, N. E. Aronson, B. L. Levine, F. D. Bushman, C. H. June, Decade-long safety and function of retroviral-modified chimeric antigen receptor T cells., *Sci. Transl. Med.* **4**, 132ra53 (2012).

25. A. P. Rapoport, E. A. Stadtmauer, G. K. Binder-Scholl, O. Goloubeva, D. T. Vogl, S. F. Lacey, A. Z. Badros, A. Garfall, B. Weiss, J. Finklestein, I. Kulikovskaya, S. K. Sinha, S. Kronsberg, M. Gupta, S. Bond, L. Melchiori, J. E. Brewer, A. D. Bennett, A. B. Gerry, N. J. Pumphrey, D. Williams, H. K. Tayton- Martin, L. Ribeiro, T. Holdich, S. Yanovich, N. Hardy, J. Yared, N. Kerr, S. Philip, S. Westphal, D. L. Siegel, B. L. Levine, B. K. Jakobsen, M. Kalos, C. H. June, NY-ESO-1–specific TCR–engineered T cells mediate sustained antigen-specific antitumor effects in myeloma, *Nat. Med.* **21**, 914–921 (2015).

26. C. J. Turtle, L.-A. Hanafi, C. Berger, T. A. Gooley, S. Cherian, M. Hudecek, D. Sommermeyer, K. Melville, B. Pender, T. M. Budiarto, E. Robinson, N. N. Steevens, C. Chaney, L. Soma, X. Chen, C. Yeung, B. Wood, D. Li, J. Cao, S. Heimfeld, M. C. Jensen, S. R. Riddell, D. G. Maloney, CD19 CAR-T cells of defined CD4+:CD8+ composition in adult B cell ALL patients., *J. Clin. Invest.* **126**, 2123–38 (2016).

27. S. A. Grupp, M. Kalos, D. Barrett, R. Aplenc, D. L. Porter, S. R. Rheingold, D. T. Teachey, A. Chew, B. Hauck, J. F. Wright, M. C. Milone, B. L. Levine, C. H. June, Chimeric Antigen Receptor–Modified T Cells for Acute Lymphoid Leukemia, *N. Engl. J. Med.* **368**, 1509–1518 (2013).

28. S. L. Maude, N. Frey, P. A. Shaw, R. Aplenc, D. M. Barrett, N. J. Bunin, A. Chew, V. E. Gonzalez, Z. Zheng, S. F. Lacey, Y. D. Mahnke, J. J. Melenhorst, S. R. Rheingold, A. Shen, D. T. Teachey, B. L. Levine, C. H. June, D. L. Porter, S. A. Grupp, Chimeric Antigen Receptor T Cells for Sustained Remissions in Leukemia, *N. Engl. J. Med.* **371**, 1507–1517 (2014).

29. D. L. Porter, N. V. Frey, J. J. Melenhorst, W.-T. Hwang, S. F. Lacey, P. Shaw, A. Chew, S. A. Grupp, J. Capobianchi, J. Gilmore, M. Kalos, M. Litchman, L. Lledo, A. W. Loren, Y. Mahnke, K. T. Marcucci, H. McConville, A. Shen, P. A. Wood, Z. Zheng, B. L. Levine, C. H. June, Randomized Phase II Dose Optimization Study of Chimeric Antigen Receptor Modified T Cells Directed Against CD19 (CTL019) in Patients with Relapsed, Refractory CLL, *Blood* **124** (2014).

30. J. N. Kochenderfer, R. P. T. Somerville, T. Lu, V. Shi, A. Bot, J. Rossi, A. Xue, S. L. Goff, J. C. Yang, R. M. Sherry, C. A. Klebanoff, U. S. Kammula, M. Sherman, A. Perez, C. M. Yuan, T. Feldman, J. W. Friedberg, M. J. Roschewski, S. A. Feldman, L. McIntyre, M. A. Toomey, S. A. Rosenberg, Lymphoma Remissions Caused by Anti-CD19 Chimeric Antigen Receptor T Cells Are Associated With High Serum Interleukin-15 Levels, *J. Clin. Oncol.* **35**, 1803–1813 (2017).

31. J. A. Fraietta, C. L. Nobles, M. A. Sammons, S. Lundh, S. A. Carty, T. J. Reich, A. P. Cogdill, J. J. D. Morrissette, J. E. DeNizio, S. Reddy, Y. Hwang, M. Gohil, I. Kulikovskaya, F. Nazimuddin, M. Gupta, F. Chen, J. K. Everett, K. A. Alexander, E. Lin-Shiao, M. H. Gee, X. Liu, R. M. Young, D. Ambrose, Y. Wang, J. Xu, M. S. Jordan, K. T. Marcucci, B. L. Levine, K. C. Garcia, Y. Zhao, M. Kalos, D. L. Porter, R. M. Kohli, S. F. Lacey, S. L. Berger, F. D. Bushman, C. H. June, J. J. Melenhorst, Disruption of TET2 promotes the therapeutic efficacy of CD19-targeted T cells, *Nature* **558**, 307–312 (2018).

32. M. L. Davila, I. Riviere, X. Wang, S. Bartido, J. Park, K. Curran, S. S. Chung, J. Stefanski, O. Borquez-Ojeda, M. Olszewska, J. Qu, T. Wasielewska, Q. He, M. Fink, H. Shinglot, M. Youssif, M. Satter, Y. Wang, J. Hosey, H. Quintanilla, E. Halton, Y. Bernal, D. C. G. Bouhassira, M. E. Arcila, M. Gonen, G. J. Roboz, P. Maslak, D. Douer, M. G. Frattini, S. Giralt, M. Sadelain, R. Brentjens, Efficacy and Toxicity Management of 19-28z CAR T Cell Therapy in B Cell Acute Lymphoblastic Leukemia, *Sci. Transl. Med.* **6**, 224ra25-224ra25 (2014).

33. Y. Xu, M. Zhang, C. A. Ramos, A. Durett, E. Liu, O. Dakhova, H. Liu, C. J. Creighton, A. P. Gee, H. E. Heslop, C. M. Rooney, B. Savoldo, G. Dotti, Closely related T-memory stem cells correlate with in vivo expansion of CAR.CD19-T cells and are preserved by IL-7 and IL-15., *Blood* **123**, 3750–9 (2014).

34. H. Dai, W. Zhang, X. Li, Q. Han, Y. Guo, Y. Zhang, Y. Wang, C. Wang, F. Shi, Y. Zhang, M. Chen, K. Feng, Q. Wang, H. Zhu, X. Fu, S. Li, W. Han, Tolerance and efficacy of autologous or donor-derived T cells expressing CD19 chimeric antigen receptors in adult B-ALL with extramedullary leukemia., *Oncoimmunology* **4**, e1027469 (2015).

35. R. J. Brentjens, M. L. Davila, I. Riviere, J. Park, X. Wang, L. G. Cowell, S. Bartido, J. Stefanski, C. Taylor, M. Olszewska, O. Borquez-Ojeda, J. Qu, T. Wasielewska, Q. He, Y. Bernal, I. V. Rijo, C. Hedvat, R. Kobos, K. Curran, P. Steinherz, J. Jurcic, T. Rosenblat, P.

Maslak, M. Frattini, M. Sadelain, CD19-Targeted T Cells Rapidly Induce Molecular Remissions in Adults with Chemotherapy-Refractory Acute Lymphoblastic Leukemia, *Sci. Transl. Med.* , sc (2013).

36. C. A. Ramos, B. Savoldo, V. Torrano, B. Ballard, H. Zhang, O. Dakhova, E. Liu, G. Carrum, R. T. Kamble, A. P. Gee, Z. Mei, M.-F. Wu, H. Liu, B. Grilley, C. M. Rooney, M. K. Brenner, H. E. Heslop, G. Dotti, Clinical responses with T lymphocytes targeting malignancy-associated κ light chains., *J. Clin. Invest.* **126**, 2588–96 (2016).

37. J. Hartmann, M. Schüßler-Lenz, A. Bondanza, C. J. Buchholz, Clinical development of CAR T cells—challenges and opportunities in translating innovative treatment concepts, *EMBO Mol Med* **9**, 1183–1197 (2017).

38. J. Gust, K. A. Hay, L.-A. Hanafi, D. Li, D. Myerson, L. F. Gonzalez-Cuyar, C. Yeung, W. C. Liles, M. Wurfel, J. A. Lopez, J. Chen, D. Chung, S. Harju-Baker, T. Özpolat, K. R. Fink, S. R. Riddell, D. G. Maloney, C. J. Turtle, Endothelial Activation and Blood-Brain Barrier Disruption in Neurotoxicity after Adoptive Immunotherapy with CD19 CAR-T Cells., *Cancer Discov.* **7**, 1404–1419 (2017).

39. K. Ishii, H. Shalabi, B. Yates, C. Delbrook, C. L. Mackall, T. J. Fry, N. N. Shah, Tocilizumab-Refractory Cytokine Release Syndrome (CRS) Triggered By Chimeric Antigen Receptor (CAR)-Transduced T Cells May Have Distinct Cytokine Profiles Compared to Typical CRS, *Blood* **128**, 3358 (2016).

40. N. V Frey, B. L. Levine, S. F. Lacey, S. A. Grupp, S. L. Maude, S. J. Schuster, P. Shaw, W.-T. Hwang, M. A. Wasik, A. Obstfeld, M. Leung, A. Shen, S. G. Ericson, J. J. Melenhorst, C. H. June, D. Porter, Refractory Cytokine Release Syndrome in Recipients of Chimeric Antigen Receptor (CAR) T Cells, *Blood* **124**, 2296 (2014).

41. S. S. Neelapu, S. Tummala, P. Kebriaei, W. Wierda, C. Gutierrez, F. L. Locke, K. V. Komanduri, Y. Lin, N. Jain, N. Daver, J. Westin, A. M. Gulbis, M. E. Loghin, J. F. de Groot, S. Adkins, S. E. Davis, K. Rezvani, P. Hwu, E. J. Shpall, Chimeric antigen receptor T-cell therapy - assessment and management of toxicities., *Nat. Rev. Clin. Oncol.* **15**, 47–62 (2018).

42. D. W. Lee, R. Gardner, D. L. Porter, C. U. Louis, N. Ahmed, M. Jensen, S. A. Grupp, C. L. Mackall, Current concepts in the diagnosis and management of cytokine release syndrome., *Blood* **124**, 188–95 (2014).

43. Z. Wang, W. Han, Biomarkers of cytokine release syndrome and neurotoxicity related to CAR-T cell therapy., *Biomark. Res.* **6**, 4 (2018).

44. D. W. Lee, J. N. Kochenderfer, M. Stetler-Stevenson, Y. K. Cui, C. Delbrook, S. A. Feldman, T. J. Fry, R. Orentas, M. Sabatino, N. N. Shah, S. M. Steinberg, D. Stroncek, N. Tschernia, C. Yuan, H. Zhang, L. Zhang, S. A. Rosenberg, A. S. Wayne, C. L. Mackall, T cells expressing CD19 chimeric antigen receptors for acute lymphoblastic leukaemia in children and young adults: a phase 1 dose-escalation trial, *Lancet* **385**, 517–528 (2015).

45. D. T. Teachey, S. F. Lacey, P. A. Shaw, J. J. Melenhorst, S. L. Maude, N. Frey, E. Pequignot, V. E. Gonzalez, F. Chen, J. Finklestein, D. M. Barrett, S. L. Weiss, J. C. Fitzgerald, R. A. Berg, R. Aplenc, C. Callahan, S. R. Rheingold, Z. Zheng, S. Rose-John, J. C. White, F. Nazimuddin, G. Wertheim, B. L. Levine, C. H. June, D. L. Porter, S. A. Grupp, Identification of Predictive Biomarkers for Cytokine Release Syndrome after Chimeric Antigen Receptor T-cell Therapy for Acute Lymphoblastic Leukemia, *Cancer Discov.* **6**, 664–679 (2016).

46. M. V Maus, S. A. Grupp, D. L. Porter, C. H. June, Antibody-modified T cells: CARs take the front seat for hematologic malignancies., *Blood* **123**, 2625–35 (2014).

47. R. A. Morgan, J. C. Yang, M. Kitano, M. E. Dudley, C. M. Laurencot, S. A. Rosenberg, Case Report of a Serious Adverse Event Following the Administration of T Cells Transduced With a Chimeric Antigen Receptor Recognizing ERBB2, *Mol. Ther.* **18**, 843–851 (2010).

48. F. Chen, D. T. Teachey, E. Pequignot, N. Frey, D. Porter, S. L. Maude, S. A. Grupp, C. H. June, J. J. Melenhorst, S. F. Lacey, Measuring IL-6 and sIL-6R in serum from patients treated with tocilizumab and/or siltuximab following CAR T cell therapy, *J. Immunol. Methods* **434**, 1–8 (2016).

49. D. M. Barrett, N. Singh, T. J. Hofmann, Z. Gershenson, S. A. Grupp, Interleukin 6 Is Not Made By Chimeric Antigen Receptor T Cells and Does Not Impact Their Function, *Blood* **128** (2016).

50. M. Norelli, B. Camisa, G. Barbiera, L. Falcone, A. Purevdorj, M. Genua, F. Sanvito, M. Ponzoni, C. Doglioni, P. Cristofori, C. Traversari, C. Bordignon, F. Ciceri, R. Ostuni, C. Bonini, M. Casucci, A. Bondanza, Monocyte-derived IL-1 and IL-6 are differentially required for cytokine-release syndrome and neurotoxicity due to CAR T cells, *Nat. Med.* **24**, 1–10

(2018).

51. T. Giavridis, S. J. C. van der Stegen, J. Eyquem, M. Hamieh, A. Piersigilli, M. Sadelain, CAR T cell–induced cytokine release syndrome is mediated by macrophages and abated by IL-1 blockade, *Nat. Med.* **24**, 731–738 (2018).

52. F. Van Laethem, E. Baus, L. A. Smyth, F. Andris, F. Bex, J. Urbain, D. Kioussis, O. Leo, Glucocorticoids attenuate T cell receptor signaling., *J. Exp. Med.* **193**, 803–14 (2001).

53. I. Kite Pharma, *Yescarta package insert.* (2017; www.fda.gov/medwatch.).

54. M. Hudecek, D. Sommermeyer, P. L. Kosasih, A. Silva-Benedict, L. Liu, C. Rader, M. C. Jensen, S. R. Riddell, The Nonsignaling Extracellular Spacer Domain of Chimeric Antigen Receptors Is Decisive for In Vivo Antitumor Activity, *Cancer Immunol. Res.* **3**, 125–135 (2015).

55. S. Terakura, T. N. Yamamoto, R. A. Gardner, C. J. Turtle, M. C. Jensen, S. R. Riddell, Generation of CD19-chimeric antigen receptor modified CD8+ T cells derived from virus-specific central memory T cells., *Blood* **119**, 72–82 (2012).

56. H. Karlsson, E. Svensson, C. Gigg, M. Jarvius, U. Olsson-Strömberg, B. Savoldo, G. Dotti, A. Loskog, Evaluation of Intracellular Signaling Downstream Chimeric Antigen Receptors., *PLoS One* **10**, e0144787 (2015).

57. B. G. Till, M. C. Jensen, J. Wang, E. Y. Chen, B. L. Wood, H. A. Greisman, X. Qian, S. E. James, A. Raubitschek, S. J. Forman, A. K. Gopal, J. M. Pagel, C. G. Lindgren, P. D. Greenberg, S. R. Riddell, O. W. Press, Adoptive immunotherapy for indolent non-Hodgkin lymphoma and mantle cell lymphoma using genetically modified autologous CD20-specific T cells., *Blood* **112**, 2261–71 (2008).

58. M. C. Jensen, L. Popplewell, L. J. Cooper, D. DiGiusto, M. Kalos, J. R. Ostberg, S. J. Forman, Antitransgene rejection responses contribute to attenuated persistence of adoptively transferred CD20/CD19-specific chimeric antigen receptor redirected T cells in humans., *Biol. Blood Marrow Transplant.* **16**, 1245–56 (2010).

59. O. U. Kawalekar, R. S. O'Connor, J. A. Fraietta, L. Guo, S. E. McGettigan, A. D. Posey, P. R. Patel, S. Guedan, J. Scholler, B. Keith, N. W. Snyder, I. A. Blair, M. C. Milone, C. H. June, R. S. O'Connor, J. A. Fraietta, L. Guo, S. E. McGettigan, A. D. Posey, P. R. Patel, S.

Guedan, J. Scholler, B. Keith, N. W. Snyder, I. A. Blair, M. C. Milone, C. H. June, Distinct Signaling of Coreceptors Regulates Specific Metabolism Pathways and Impacts Memory Development in CAR T Cells, *Immunity* **44**, 380–390 (2016).

60. H. Abken, Costimulation Engages the Gear in Driving CARs, *Immunity* **44**, 214–216 (2016).

61. Z. Zhao, M. Condomines, S. J. C. Van Der Stegen, F. Perna, C. C. Kloss, G. Gunset, J. Plotkin, M. Sadelain, Structural Design of Engineered Costimulation Determines Tumor Rejection Kinetics and Persistence of CAR T Cells, *Cancer Cell* **28**, 415–428 (2015).

62. X. Wang, W.-C. Chang, C. W. Wong, D. Colcher, M. Sherman, J. R. Ostberg, S. J. Forman, S. R. Riddell, M. C. Jensen, A transgene-encoded cell surface polypeptide for selection, in vivo tracking, and ablation of engineered cells., *Blood* **118**, 1255–63 (2011).

63. P. J. Paszkiewicz, S. P. Fräßle, S. Srivastava, D. Sommermeyer, M. Hudecek, I. Drexler, M. Sadelain, L. Liu, M. C. Jensen, S. R. Riddell, D. H. Busch, Targeted antibody-mediated depletion of murine CD19 CAR T cells permanently reverses B cell aplasia., *J. Clin. Invest.* **126**, 4262–4272 (2016).

64. M. Serafini, M. Manganini, G. Borleri, M. Bonamino, L. Imberti, A. Biondi, J. Golay, A. Rambaldi, M. Introna, Characterization of CD20-Transduced T Lymphocytes as an Alternative Suicide Gene Therapy Approach for the Treatment of Graft-Versus-Host Disease, **15**, 63–76 (2004).

65. K. C. Straathof, M. A. Pulè, P. Yotnda, G. Dotti, E. F. Vanin, M. K. Brenner, H. E. Heslop, D. M. Spencer, C. M. Rooney, An inducible caspase 9 safety switch for T-cell therapy., *Blood* **105**, 4247–54 (2005).

66. A. Di Stasi, S.-K. Tey, G. Dotti, Y. Fujita, A. Kennedy-Nasser, C. Martinez, K. Straathof, E. Liu, A. G. Durett, B. Grilley, R. Ph, H. Liu, C. R. Cruz, B. Savoldo, A. P. Gee, J. Schindler, R. A. Krance, H. E. Heslop, D. M. Spencer, C. M. Rooney, M. K. Brenner, Inducible Apoptosis as a Safety Switch for Adoptive Cell Therapy, *N Engl J Med* **18365**, 1673–83 (2011).

67. C. Bonini, G. Ferrari, S. Verzeletti, P. Servida, E. Zappone, L. Ruggieri, M. Ponzoni, S. Rossini, F. Mavilio, C. Traversari, C. Bordignon, HSV-TK gene transfer into donor lymphocytes for control of allogeneic graft-versus-leukemia., *Science* **276**, 1719–24 (1997).

68. R. Greco, G. Oliveira, M. T. L. Stanghellini, L. Vago, A. Bondanza, J. Peccatori, N. Cieri, S. Marktel, S. Mastaglio, C. Bordignon, C. Bonini, F. Ciceri, Improving the safety of cell therapy with the TK-suicide gene., *Front. Pharmacol.* **6**, 95 (2015).

69. I. Diaconu, B. Ballard, M. Zhang, Y. Chen, J. West, G. Dotti, B. Savoldo, Inducible Caspase-9 Selectively Modulates the Toxicities of CD19-Specific Chimeric Antigen Receptor-Modified T Cells, *Mol. Ther.* **25**, 580–592 (2017).

70. C. Berger, M. E. Flowers, E. H. Warren, S. R. Riddell, Analysis of transgene-specific immune responses that limit the in vivo persistence of adoptively transferred HSV-TK-modified donor T cells after allogeneic hematopoietic cell transplantation, *Blood* **107**, 2294–2302 (2006).

71. C.-Y. Wu, K. T. Roybal, E. M. Puchner, J. Onuffer, W. A. Lim, Remote control of therapeutic T cells through a small molecule-gated chimeric receptor., *Science* **350**, aab4077 (2015).

72. J. H. Cho, J. J. Collins, W. W. Wong, Universal Chimeric Antigen Receptors for Multiplexed and Logical Control of T Cell Responses, *Cell* **173**, 1426–1438.e11 (2018).

73. J. S. Tokarski, J. A. Newitt, C. Y. J. Chang, J. D. Cheng, M. Wittekind, S. E. Kiefer, K. Kish, F. Y. F. Lee, R. Borzillerri, L. J. Lombardo, D. Xie, Y. Zhang, H. E. Klei, The structure of Dasatinib (BMS-354825) bound to activated ABL kinase domain elucidates its inhibitory activity against imatinib-resistant ABL mutants., *Cancer Res.* **66**, 5790–7 (2006).

74. P. C. Nowell, D. A. Hungerford, Chromosome studies on normal and leukemic human leukocytes., *J. Natl. Cancer Inst.* **25**, 85–109 (1960).

75. S. Blake, T. P. Hughes, G. Mayrhofer, A. B. Lyons, The Src/ABL kinase inhibitor dasatinib (BMS-354825) inhibits function of normal human T-lymphocytes in vitro, *Clin. Immunol.* **127**, 330–339 (2008).

76. R. Weichsel, C. Dix, L. Wooldridge, M. Clement, A. Fenton-May, A. K. Sewell, J. Zezula, E. Greiner, E. Gostick, D. A. Price, H. Einsele, R. Seggewiss, Profound Inhibition of Antigen-Specific T-Cell Effector Functions by Dasatinib, *Clin. Cancer Res.* **14**, 2484–2491 (2008).

77. F. Fei, Y. Yu, A. Schmitt, M. T. Rojewski, B. Chen, J. Greiner, M. Götz, P. Guillaume, H.

Döhner, D. Bunjes, M. Schmitt, Dasatinib exerts an immunosuppressive effect on CD8+ T cells specific for viral and leukemia antigens, *Exp. Hematol.* **36**, 1297–1308 (2008).

78. M. Wölfl, F. Langhammer, V. Wiegering, M. Eyrich, P. G. Schlegel, Dasatinib medication causing profound immunosuppression in a patient after haploidentical SCT: functional assays from whole blood as diagnostic clues, *Bone Marrow Transplant.* **48**, 875–877 (2013).

79. C. Sillaber, H. Herrmann, K. Bennett, U. Rix, C. Baumgartner, A. Böhm, S. Herndlhofer, E. Tschachler, G. Superti-Furga, U. Jäger, P. Valent, Immunosuppression and atypical infections in CML patients treated with dasatinib at 140 mg daily, *Eur. J. Clin. Invest.* **39**, 1098–1109 (2009).

80. J. S. Abramson, M. L. Palomba, L. I. Gordon, M. A. Lunning, J. E. Arnason, A. Forero-Torres, M. Wang, T. M. Albertson, T. Allen, C. Sutherland, B. Xie, J. Garcia, T. Siddiqi, CR rates in relapsed/refractory (R/R) aggressive B-NHL treated with the CD19-directed CAR T-cell product JCAR017 (TRANSCEND NHL 001)., *J. Clin. Oncol.* **35**, 7513–7513 (2017).

81. M. Hudecek, M.-T. Lupo-Stanghellini, P. L. Kosasih, D. Sommermeyer, M. C. Jensen, C. Rader, S. R. Riddell, Receptor Affinity and Extracellular Domain Modifications Affect Tumor Recognition by ROR1-Specific Chimeric Antigen Receptor T Cells, *Clin. Cancer Res.* **19**, 3153–3164 (2013).

82. X. Wang, C. Berger, C. W. Wong, S. J. Forman, S. R. Riddell, M. C. Jensen, Engraftment of human central memory-derived effector CD8+ T cells in immunodeficient mice., *Blood* **117**, 1888–98 (2011).

83. S. R. Riddell, P. D. Greenberg, The use of anti-CD3 and anti-CD28 monoclonal antibodies to clone and expand human antigen-specific T cells, *J. Immunol. Methods* **128**, 189–201 (1990).

84. T. Gargett, M. P. Brown, The inducible caspase-9 suicide gene system as a safety switch to limit on-target, off-tumor toxicities of chimeric antigen receptor T cells, *Front. Pharmacol.* **5** (2014), doi:10.3389/fphar.2014.00235.

85. F. R. Luo, Z. Yang, A. Camuso, R. Smykla, K. McGlinchey, K. Fager, C. Flefleh, S. Castaneda, I. Inigo, D. Kan, M.-L. Wen, R. Kramer, A. Blackwood-Chirchir, F. Y. Lee, Dasatinib (BMS-354825) Pharmacokinetics and Pharmacodynamic Biomarkers in Animal

Models Predict Optimal Clinical Exposure, *Clin. Cancer Res.* **12**, 7180–7186 (2006).

86. K. Mestermann, The influence of tyrosine kinase inhibitors on tumor recognition by chimeric antigen receptor- modified T cells, *Masterthesis* (2014).

87. M. Huse, The T-cell-receptor signaling network., *J. Cell Sci.* **122**, 1269–73 (2009).

88. O. U. Kawalekar, R. S. O'Connor, J. A. Fraietta, L. Guo, S. E. McGettigan, A. D. Posey, P. R. Patel, S. Guedan, J. Scholler, B. Keith, N. W. Snyder, I. A. Blair, M. C. Milone, C. H. June, Distinct Signaling of Coreceptors Regulates Specific Metabolism Pathways and Impacts Memory Development in CAR T Cells, *Immunity* **44**, 380–390 (2016).

89. K.-O. Nam, H. Kang, S.-M. Shin, K.-H. Cho, B. Kwon, B. S. Kwon, S.-J. Kim, H.-W. Lee, Cross-linking of 4-1BB activates TCR-signaling pathways in CD8+ T lymphocytes., *J. Immunol.* **174**, 1898–905 (2005).

90. R. Tavano, G. Gri, B. Molon, B. Marinari, C. E. Rudd, L. Tuosto, A. Viola, CD28 and lipid rafts coordinate recruitment of Lck to the immunological synapse of human T lymphocytes., *J. Immunol.* **173**, 5392–7 (2004).

91. I. C. Nicholson, K. A. Lenton, D. J. Little, T. Decorso, F. T. Lee, A. M. Scott, H. Zola, A. W. Hohmann, Construction and characterisation of a functional CD19 specific single chain Fv fragment for immunotherapy of B lineage leukaemia and lymphoma, *Mol. Immunol.* **34**, 1157–1165 (1997).

92. J. Yang, S. Baskar, K. Y. Kwong, M. G. Kennedy, A. Wiestner, C. Rader, C. Bunce, Ed. Therapeutic Potential and Challenges of Targeting Receptor Tyrosine Kinase ROR1 with Monoclonal Antibodies in B-Cell Malignancies, *PLoS One* **6**, e21018 (2011).

93. S. Rosskopf, J. Leitner, W. Paster, L. T. Morton, R. S. Hagedoorn, P. Steinberger, M. H. M. Heemskerk, A Jurkat 76 based triple parameter reporter system to evaluate TCR functions and adoptive T cell strategies., *Oncotarget* **9**, 17608–17619 (2018).

94. D. Sommermeyer, M. Hudecek, P. L. Kosasih, T. Gogishvili, D. G. Maloney, C. J. Turtle, S. R. Riddell, Chimeric antigen receptor-modified T cells derived from defined CD8 + and CD4 + subsets confer superior antitumor reactivity in vivo HHS Public Access, *Leukemia* **30**, 492–500 (2016).

95. A. Künkele, A. J. Johnson, L. S. Rolczynski, C. A. Chang, V. Hoglund, K. S. Kelly-

Spratt, M. C. Jensen, Functional Tuning of CARs Reveals Signaling Threshold above Which CD8+ CTL Antitumor Potency Is Attenuated due to Cell Fas-FasL-Dependent AICD., *Cancer Immunol. Res.* **3**, 368–79 (2015).

96. L. J. Christopher, D. Cui, C. Wu, R. Luo, J. A. Manning, S. J. Bonacorsi, M. Lago, A. Allentoff, F. Y. F. Lee, B. McCann, S. Galbraith, D. P. Reitberg, K. He, A. Barros, A. Blackwood-Chirchir, W. G. Humphreys, R. A. Iyer, Metabolism and Disposition of Dasatinib after Oral Administration to Humans, *Drug Metab. Dispos.* **36**, 1357–1364 (2008).

97. D. A. Solimando, J. Aubrey Waddell, A. Waddell, Cancer Chemotherapy Update Drug Monographs: Bosutinib and Regorafenib, *Hosp Pharm* **48**, 190–194 (2013).

98. J. Baselga, A. Cervantes, E. Martinelli, I. Chirivella, K. Hoekman, H. I. Hurwitz, D. I. Jodrell, P. Hamberg, E. Casado, P. Elvin, A. Swaisland, R. Iacona, J. Tabernero, Phase I safety, pharmacokinetics, and inhibition of SRC activity study of saracatinib in patients with solid tumors., *Clin. Cancer Res.* **16**, 4876–83 (2010).

99. M. Conchon, C. M. B. de M. Freitas, M. A. do C. Rego, J. W. R. Braga Junior, Dasatinib - clinical trials and management of adverse events in imatinib resistant/intolerant chronic myeloid leukemia., *Rev. Bras. Hematol. Hemoter.* **33**, 131–9 (2011).

100. A. G. Brixey, R. W. Light, Pleural effusions due to dasatinib, *Curr. Opin. Pulm. Med.* **16**, 351–356 (2010).

101. Z. Xu, S. Cang, T. Yang, D. Liu, Cardiotoxicity of tyrosine kinase inhibitors in chronic myelogenous leukemia therapy, *Hematol. Rep.* **1**, 4 (2009).

102. A. E. Schade, G. L. Schieven, R. Townsend, A. M. Jankowska, V. Susulic, R. Zhang, H. Szpurka, J. P. Maciejewski, Dasatinib, a small-molecule protein tyrosine kinase inhibitor, inhibits T-cell activation and proliferation, *Blood* **111**, 1366–1377 (2007).

103. C. Brandl, C. Haas, S. D'Argouges, T. Fisch, P. Kufer, K. Brischwein, N. Prang, R. Bargou, J. Suzich, P. A. Baeuerle, R. Hofmeister, The effect of dexamethasone on polyclonal T cell activation and redirected target cell lysis as induced by a CD19/CD3-bispecific single-chain antibody construct., *Cancer Immunol. Immunother.* **56**, 1551–63 (2007).

104. T. Nerreter, E. Distler, C. Köchel, H. Einsele, W. Herr, R. Seggewiss-Bernhardt, Combining dasatinib with dexamethasone long-term leads to maintenance of antiviral and

antileukemia specific cytotoxic T cell responses in vitro, *Exp. Hematol.* **41**, 604–614.e4 (2013).

105. A. Schietinger, M. Philip, V. E. Krisnawan, E. Y. Chiu, J. J. Delrow, R. S. Basom, P. Lauer, D. G. Brockstedt, S. E. Knoblaugh, G. J. Hämmerling, T. D. Schell, N. Garbi, P. D. Greenberg, Tumor-Specific T Cell Dysfunction Is a Dynamic Antigen-Driven Differentiation Program Initiated Early during Tumorigenesis, *Immunity* **45**, 389–401 (2016).

106. J. A. Fraietta, S. F. Lacey, E. J. Orlando, I. Pruteanu-Malinici, M. Gohil, S. Lundh, A. C. Boesteanu, Y. Wang, R. S. O'Connor, W.-T. Hwang, E. Pequignot, D. E. Ambrose, C. Zhang, N. Wilcox, F. Bedoya, C. Dorfmeier, F. Chen, L. Tian, H. Parakandi, M. Gupta, R. M. Young, F. B. Johnson, I. Kulikovskaya, L. Liu, J. Xu, S. H. Kassim, M. M. Davis, B. L. Levine, N. V. Frey, D. L. Siegel, A. C. Huang, E. J. Wherry, H. Bitter, J. L. Brogdon, D. L. Porter, C. H. June, J. J. Melenhorst, Determinants of response and resistance to CD19 chimeric antigen receptor (CAR) T cell therapy of chronic lymphocytic leukemia, *Nat. Med.* **24**, 563–571 (2018).

107. E. A. Chong, J. J. Melenhorst, S. F. Lacey, D. E. Ambrose, V. Gonzalez, B. L. Levine, C. H. June, S. J. Schuster, PD-1 blockade modulates chimeric antigen receptor (CAR)-modified T cells: refueling the CAR., *Blood* **129**, 1039–1041 (2017).

108. C. L. Mackall, Enhancing the Efficacy of CAR T Cells, *Blood* **130** (2017).

109. N. Brownlow, C. Mol, C. Hayford, S. Ghaem-Maghami, N. J. Dibb, Dasatinib is a potent inhibitor of tumour-associated macrophages, osteoclasts and the FMS receptor, *Leukemia* **23**, 590–594 (2009).

# List of figures

# List of abbreviations

| | |
|---|---|
| 7-AAD | 7-Aminoactinomycin D |
| ADCC | antibody-dependent cell-mediated cytotoxicity |
| ALL | Acute lymphoblastic leukemia |
| APC | Allophycocyanin |
| ATP | Adenosine tri-phosphate |
| BCMA | Breast cancer maturation antigen |
| BCR-ABL | Breakpoint cluster region - Abelson murine leukemia viral oncogene homolog 1 |
| BSA | Bovine serum albumin |
| CAR | Chimeric antigen receptor |
| CD | Cluster of differentiation |
| CDC | Cell dependent cytotoxicity |
| CFSE | Carboxyfluorescein succinimidyl ester |
| CLL | Chronic lymphocytic leukemia |
| CML | Chronic myeloid leukemia |
| CMV | Cytomegalovirus |
| CRS | Cytokine release syndrome |
| DMEM | Dulbecco’s minimal essential medium |
| DMSO | Dimethyl sulfoxide |
| DMSZ | Deutsche Sammlung von Mikroorganismen und Zellkulturen |
| DPBS | Dulbeccos phosphate buffered saline |
| ECL | Enhanced Chemiluminescence |
| EDTA | Ethylene-diamine-tetra-acetic acid |
| EGFP | Enhanced green fluorescent protein |
| EGFR | epidermal growth factor receptor |
| EGFRt | Truncated epidermal growth factor receptor |
| epHIV | Enhanced plasmid of Human Immunodeficiency Virus |
| FACS | Fluorescence-activated cell sorting |
| FCS | Fetal calf serum |
| FDA | Food and drug administration |
| ffluc | Firefly luciferase |
| FITC | Fluorescein isothiocyanate |
| GFP | Green fluorescent protein |

| | |
|---|---|
| GM-CSF | Granulocyte-macrophage colony-stimulating factor |
| GR | Glucocorticoid receptor |
| HBS | Hepes buffered saline |
| HEPES | 4-(2-hydroxyethyl)-1-piperazineethanesulfonic acid |
| Her2 | Human epidermal growth factor receptor 2 |
| HLA | Human leukocyte antigen |
| HLH | Hemophagocytic lymphohistocytosis |
| HRP | Horseradish Peroxidase |
| HSV-TK | Herpes Simplex Virus-1 Thymidine Kinase |
| i.p | Intra peritoneal |
| i.v. | Intra venous |
| iCASP9 | Inducible caspase 9 |
| ICU | Intensive care unit |
| IFN | Interferon |
| IgG | Immunoglobulin G |
| IL | Interleukin |
| IL | Illinois |
| Lck | Lymphocyte-specific protein tyrosine kinase |
| MA | Massachusetts |
| mAB | Monoclonal antibody |
| MAS | Macrophage activation syndrom |
| MFI | Mean fluorescence intensity |
| minP | Minimal promotor |
| MIP-1 | Macrophage inflammatory protein 1 |
| MO | Missouri |
| MOI | Multiplicity of infection |
| mRNA | Messenger Ribonucleic acid |
| NE | Neurotoxic event |
| NFAT | Nuclear factor of activated T-cells |
| NF-κB | Nuclear factor kappa-light-chain-enhancer of activated B cells |
| NHL | Non-Hodgkin lymphoma |
| NKG2D | Natural-killer group 2, member D |
| NOD | Non-obsese diabetic |
| NSG mice | NOD scid gamma mice |

| | |
|---|---|
| NT | Neurotoxicity |
| OR | Oregon |
| PBMC | Peripheral blood mononuclear cells |
| PBS | Phosphate buffered saline |
| PD1 | Programmed cell death protein 1 |
| PD1-L | Programmed cell death protein 1-Ligand |
| PE | Phycoerythrin |
| PEG | Poly ethylene glycol |
| Ph+ | Philadelphia chromosome positive |
| PMA | Phorbol 12-myristate 13-acetate |
| RE | Responsive element |
| RIPA | Radio-immunoprecipitation assay buffer |
| ROR1 | Receptor tyrosine kinase-like orphan receptor 1 |
| RPMI | Roswell Park Memorial Institute medium |
| SBP | Systolic blood pressure |
| scFv | Single chain variable Fragment |
| SDS | Sodium dodecyl sulfate |
| SP | Signaling peptide |
| TAE buffer | Buffer containing Tris base, acetic acid and EDTA |
| TBS-T | Tris-buffered saline – Tween20 |
| $T_{CM}$ | central memory T-cells |
| TCR | T-cell receptor |
| TEMED | Tetramethylethylenediamine |
| TKI | Tyrosine kinase inhibitor |
| TRIS | Tris(hydroxymethyl)aminomethane |
| TU | Titer unit |
| UKW | Universitätsklinikum Würzburg |
| wt | Wildtype |
| ZAP70 | Zeta-chain-associated protein kinase 70 |

# Affidavit

I hereby confirm that my thesis entitled “Pharmacologic control of chimeric antigen receptor T-cells by the tyrosine kinase inhibitor dasatinib“ is the result of my own work. I did not receive any help or support from commercial consultants. All sources and / or materials applied are listed and specified in the thesis.

Furthermore, I confirm that this thesis has not yet been submitted as part of another examination process neither in identical nor in similar form.

Place, Date Signature

# Eidesstattliche Erklärung

Hiermit erkläre ich an Eides statt, die Dissertation „Pharmakologische Kontrolle chimärer Antigenrezeptor T-Zellen durch den Tyrosinkinase Inhibitor Dasatinib“ eigenständig, d.h. insbesondere selbständig und ohne Hilfe eines kommerziellen Promotionsberaters, angefertigt und keine anderen als die von mir angegebenen Quellen und Hilfsmittel verwendet zu haben.

Ich erkläre außerdem, dass die Dissertation weder in gleicher noch in ähnlicher Form bereits in einem anderen Prüfungsverfahren vorgelegen hat.

Ort, Datum Unterschrift

# Danksagung

Zunächst einmal möchte ich mich bei Dr. Michael Hudecek bedanken, der mir in seiner Arbeitsgruppe die finanziellen Mittel und die wissenschaftliche Unterstützung geleistet hat, um mein Doktorarbeit anzufertigen. Danke an meine Co-Supervisors PD. Dr. Friederike Berberich-Siebelt und Prof. Thomas Hermann für den offenen Austausch in persönlichen und wissenschaftlichen Fragen, und Prof. Hermann Einsele für die übergeordnete Betreuung meiner Arbeit.

Ein besonderer Dank gebührt Dr. Christoph Rader, für die herzliche Aufnahme und Betreuung in Florida. Diese Zeit hat mich vor allem persönlich, aber natürlich auch wissenschaftlich und nicht zuletzt sprachlich einen großen Schritt voran gebracht.

Der größte Dank gebührt Dr. Dirk Pühringer. Danke, für deine Unterstützung in den letzten Jahren, für deine Motivation, dein Verständnis, für dein Korrekturlesen, deine Meinung. Du warst mir die wichtigste Stütze in dieser Zeit.

Danke an Lars und Julian, ihr seid die besten Bürokollegen! Danke für die Ablenkungen vom Alltag! Danke an Vasco. A german saying goes: „geteiltes Leid ist halbes Leid“. It is a pleasure to know you, you always make me laugh. Danke an Markus, für die Kaffeepausen, den geteilten Kuchen und deine Schulter zum Ausweinen. Danke an Sabrina, für die liebevolle Versorgung mit Zucker und Koffein, und für deine moralische Unterstützung. Danke an Silke, für die Nachtschichten, deine Geduld und deine ruhige Hand. Ohne deine Hilfe wären die Mausexperimente in meiner Arbeit nicht möglich gewesen.

Danke an das ganze Team: Hardik, Razieh, Justus, Julia, Stefan, Philip, Felix, Franzi, Christine, Thomas, Miriam, Estefania, Elke. Jeder von euch hat seinen Teil dazu beigetragen, mir die Arbeit angenehmer, leichter und abwechslungsreicher zu machen. Danke – für eure Kritik, eure Inspiration, die Diskussionen, und für eure Sicht auf die Welt.

Danke an meinen Familie: Dafür dass ihr versucht zu verstehen, was ich tue, auch wenn es nicht immer gelingt. Dafür dass ich weiß, dass ich immer nach Hause kommen kann, wenn ich eine Auszeit brauche, oder auch nur einfach so. Dass ihr mich immer ermutigt habt, einen Schritt weiter zugehen. Danke an Jasmin. Dein schwesterliches Ohr musste so manche Schimpftirade ertragen. Danke für deine Hilfe – immer, und auf den letzten Metern.

# Curriculum vitae